

Correlators, Probabilities and Topologies in $\mathcal{N} = 4$ SYM

T. Brown¹, R. de Mello Koch², S. Ramgoolam¹, N. Toumbas³

¹Department of Physics
Queen Mary, University of London
Mile End Road
London E1 4NS UK

² Department of Physics
University of Witwatersrand
Wits, 2050
South Africa

³ Department of Physics
University of Cyprus
Nicosia 1678, Cyprus

Abstract

We calculate transition probabilities for various processes involving giant gravitons and small gravitons in AdS space, using the dual $\mathcal{N} = 4$ SYM theory. The normalization factors for these probabilities involve, in general, correlators for manifolds of non-trivial topology which are obtained by gluing simpler four-manifolds. This follows from the factorization properties which relate CFT correlators for different topologies. These points are illustrated, in the first instance, in the simpler example of a two dimensional Matrix CFT. We give the bulk five dimensional interpretation, involving neighborhoods of Witten graphs, of these gluing properties of the four dimensional boundary CFT. As a corollary we give a simple description, based on Witten graphs, of a multiplicity of bulk topologies corresponding to a fixed boundary topology. We also propose to interpret the correlators as topology-changing transition amplitudes between LLM geometries.

t.w.brown@qmul.ac.uk, robert@neo.phys.wits.ac.za, s.ramgoolam@qmul.ac.uk, nick@ucy.ac.cy

Contents

1	Introduction	4
2	Transitions from giants to KK gravitons: a puzzle	5
2.1	1/2 BPS states in the AdS/CFT correspondence: a brief review	5
2.2	Statement of the puzzle	7
3	From factorization to probability interpretation of correlators	9
3.1	Factorization on S^4 and probabilities	9
3.2	Higher topology and multi-particle normalization	10
4	Factorization and gluing amplitudes in two dimensions	12
4.1	Matrix Model CFT	12
4.2	An inner product on the states	13
4.3	Sphere factorization	14
4.4	Geometrical gluing and factorization of higher genus correlators	16
4.4.1	The torus gluing	16
4.4.2	Factorization of torus correlators	17
4.4.3	Reflection Positivity	21
4.5	Probabilities and Inequalities in 2D	22
4.5.1	The metric on the Schur Polynomials	22
4.5.2	Three point function calculations	23
4.5.3	The torus two point function	24
4.5.4	The inequality	25
4.5.5	Probability interpretation in the large L, N limits	27
4.6	Miscellaneous comments	28
4.6.1	Zero coupling gauge theory v/s unconstrained free fields	28
4.6.2	Windings from torus factorization sums	29
5	Factorization in the 4D CFT	29
5.1	Introduction	29
5.2	Metric	30
5.3	The genus zero factorization in four dimensions	30
5.4	The genus one factorization in four dimensions	31
5.5	The genus one factorization and inequality	31
5.6	The correlator on $S^3 \times S^1$	32
5.6.1	The Inequality	35
5.7	Probability interpretation in the large T limit	37

6	Results for probabilities	37
6.1	$G = 0$ factorization	38
6.2	$G = 1$ factorization	39
6.3	Higher genus factorization	41
7	Bulk interpretation of the gluing properties of correlators	41
7.1	Bulk geometries for $S^3 \times S^1$ boundary from Witten graphs	43
7.1.1	Further topologies with $S^3 \times S^1$ boundary	45
7.2	Gluing to higher genus 4-manifolds and corresponding bulk topologies . . .	46
7.2.1	Handlebody decompositions	46
7.2.2	Gluing for the complements of connected Witten graphs	47
7.2.3	Gluing for the complements of disconnected graphs	48
7.2.4	Homology groups	49
7.3	Holographic topology change	51
7.4	Towards holographic topological gravity theory	53
7.5	Operator-Wavefunctional correspondence in quantum gravity	53
8	Summary and Outlook	54
A	Appendix	56
A.1	Multiparticle-normalized transitions of S and AdS-giants	56
A.2	Overlap normalizations : general formulas	58
A.3	Overlap normalization for $(\text{tr } \Phi)^M$	58
A.4	Overlap normalization for $(\text{tr } (\Phi^2))^M$	59
A.4.1	Overlap normalization for $(\text{tr } \Phi^2)^M$ from Casimir diagrammatics . . .	60
A.4.2	The recursion method for $ (\text{tr } (\Phi^2))^M $	64
A.5	$J = L, L/2$ for both normalizations	65
A.6	General formula for $ (\text{tr } \Phi)^{M_1} (\text{tr } \Phi^2)^{M_2} ^2$	66
A.7	More general results	68
B	Conditional probabilities	69
C	The Metric, Euclidean time reversal and Orientation	70
D	Sphere Factorization	71
E	The Weierstrass elliptic function	73
E.1	Limits of the Weierstrass elliptic function	73
E.2	The method of images and the Weierstrass function	74
F	Windings from torus factorization sums	75
G	Some results with correct normalizations	76
G.1	Sphere factorization	76
G.2	$G = 1$ factorization	77
G.2.1	Giants to KK gravitons	77

G.3	Higher genus factorization	79
H	Topology for 5D bulk and 4D boundary	80
H.1	Complements of graph neighborhoods in B^5 and wedge sum of spheres . . .	80
H.2	Cell complexes	81
H.3	Cell decomposition and homology for the complement of a connected graph .	81
H.4	Cell decomposition and homology for the complement of a disconnected graph	83
H.5	Cell decomposition and homology for $\Sigma_4(G)$	84
H.6	Handlebody decompositions	85
H.6.1	Handlebody decomposition for the complement of a connected graph	85
H.6.2	Handlebody decomposition for the complement of a disconnected graph	86
I	Topology for gluings in general dimensions	87
I.1	Cell decomposition and homology for the complement of a connected graph .	87
I.2	Cell decomposition and homology for the complement of a disconnected graph	87
I.3	General genus boundaries	88
I.4	Handlebody decompositions	88
I.4.1	Handlebody decomposition for the complement of a connected graph	88
I.4.2	Handlebody decomposition for the complement of a disconnected graph	89
J	Identities, notation and conventions	89

1 Introduction

AdS/CFT duality [1][2][3] provides a framework to study hard questions of quantum gravity, using tractable calculations in gauge theory. The discovery of giant gravitons [4][5][6] and the identification of their dual gauge theory operators [7][8] open the way to exploring transitions among these brane-like objects, as well as transitions from giant gravitons into small, ordinary gravitons. From the point of view of the bulk gravity theory, these processes are non-perturbative in nature and difficult to analyze quantitatively.

In this paper, we explain how to calculate the corresponding transition probabilities. These can be obtained by appropriately normalizing the relevant gauge theory correlators describing the bulk interactions. We show that, in general, the normalization factors involve correlators on manifolds of non-trivial topologies. The result is a direct consequence of CFT factorization equations, which relate correlators on manifolds of different topologies. Factorization is expected to be a generic property of conformal field theories, which follows from the operator/state correspondence and sewing properties of path integrals. Here, we explore some of its implications for the case of the four dimensional $\mathcal{N} = 4$ Super Yang Mills theory. We prove explicit inequalities that follow after we discard some intermediate states from four dimensional factorization equations. As we shall demonstrate with specific examples, factorization relations among correlators on spaces of different topologies constrain the relative growth of the correlators as the number of colors is increased, in a manner consistent with the probability interpretation. These probabilities are the generic observables of string theory in asymptotically *AdS* backgrounds.

This paper is organized as follows. In Section 2, we consider two normalization prescriptions, one which we call the overlap-of-states normalization, and the other which we call the multi-particle normalization, and use them to compute transition probabilities. Both normalization schemes have been used in various contexts in the literature [7, 8, 9]. We find that there is a problem with the use of the multi-particle normalization prescription. We give several examples for which “multi-particle normalized” amplitudes grow with N , and so they do not yield well defined probabilities. The resolution of this puzzle is the first main result of this paper. In general, to get well defined probabilities, we need to divide by correlators on manifolds of more complicated topologies, as implied by factorization. The main ideas relating factorization and probabilities are explained in Section 3.

In Section 4, we review the main aspects of factorization and apply them to derive inequalities and probabilities in a simpler two dimensional model involving free complex matrix fields. In Section 5, we extend the discussion to the more relevant case of the four dimensional $\mathcal{N} = 4$ Super Yang Mills theory. In Section 6, we summarize results of explicit transition probability computations for processes involving giant and small gravitons in AdS space.

Motivated by the need for the gluing properties of the boundary CFT in the correct formulation of probabilities for bulk spacetime processes, we investigate how to lift the geometrical boundary gluing properties to the bulk five dimensional Euclidean space. The results are presented in Section 7. Witten graphs, i.e. graphs with end points corresponding to CFT operator insertions on the boundary of AdS and vertices in the bulk, and their neighborhoods, are found to provide a simple framework for the bulk lifting of the boundary gluings. Finally, we propose to interpret CFT correlators involving operators of large R charge as topology-changing transition amplitudes between LLM geometries [10]. Section 7 may be read independently of the rest of the paper. Technical computations are described in the Appendices. A summary of notation used is given in Appendix J.

2 Transitions from giants to KK gravitons: a puzzle

2.1 1/2 BPS states in the AdS/CFT correspondence: a brief review

We are interested in various interactions among particles and branes in the $AdS_5 \times S^5$ geometry, and for cases in which the interacting states have non-zero angular momentum on S^5 . These interactions can be studied in the context of the AdS/CFT correspondence by making use of the dictionary relating bulk states with conformal field theory operators. We focus on 1/2 BPS states characterized by a single angular momentum charge J under a $U(1)$ subgroup of the $SO(6)$ rotation group, and for which exact, non-perturbative results can be obtained. Such states correspond to chiral primary operators of conformal weight $\Delta = |J|$ in the dual $U(N)$ $\mathcal{N} = 4$ Super Yang Mills theory.

For small angular momentum, $J \ll N$, the states describe Kaluza-Klein (KK) bulk gravitons. Single particle KK states correspond to single trace operators of the form $\text{tr}(\Phi^J)$ in the boundary conformal field theory [2][3]. Here Φ is a complex field in the adjoint representation of $U(N)$, and this field has unit charge under the particular $U(1)$ R -symmetry

subgroup we are considering. Perturbative supergravity interactions among KK graviton states have been studied in [11][12], and the results have been matched with boundary conformal field theory computations.

When we increase the angular momentum so that $J \sim \sqrt{N}$, the states describe strings in plane wave backgrounds [13]. More precisely, the operator $\text{tr}(\Phi^J)$ for $J \sim \sqrt{N}$ can be associated to the ground state of the string in light-cone gauge. Excited string states can be obtained by replacing some of the Φ 's in the trace with other transverse scalars. These states are nearly BPS and their interactions have been studied in [14][15][16] from the gauge theory and the bulk point of view.

When the angular momentum is a finite fraction of N , $J \sim N$, some of the states describe large spherical $D3$ branes inside the S^5 component or spherical branes inside the AdS_5 component of the bulk geometry, the so called giant gravitons [4][5][6]. To describe giant graviton states in the boundary Super Yang Mills theory, we use a basis for the space of 1/2 BPS operators that consists of Schur polynomials of the matrix Φ . The space of Schur polynomials is in one-to-one correspondence with the set of Young diagrams characterizing irreducible representations of $U(N)$. Thus we denote the Schur polynomials by $\chi_R(\Phi)$, with R denoting the corresponding $U(N)$ representation. Now if the Young diagram corresponding to the $U(N)$ representation R has n boxes, then it also characterizes an irreducible representation of the symmetric group S_n . Explicitly $\chi_R(\Phi)$ is given by

$$\chi_R(\Phi) = \frac{1}{n!} \sum_{\sigma \in S_n} \chi_R(\sigma) \text{tr}(\sigma \Phi) = \frac{1}{n!} \sum_{\sigma \in S_n} \chi_R(\sigma) \left[\sum_{i_1, i_2, \dots, i_n} \Phi_{i_{\sigma(1)}}^{i_1} \Phi_{i_{\sigma(2)}}^{i_2} \dots \Phi_{i_{\sigma(n)}}^{i_n} \right] \quad (1)$$

Using the dictionary developed in [8][17] (see also [7]), the Schur operator corresponding to an AdS giant with L units of angular momentum on S^5 is given by $\chi_{[L]}(\Phi)$, where we denote by $[L]$ a Young diagram with a single row of length L . This Young diagram describes a symmetric representation of $U(N)$. Similarly, the operator corresponding to a sphere giant is given by $\chi_{[1^L]}(\Phi)$, where $[1^L]$ denotes a Young diagram with a single column of length L describing an antisymmetric representation¹. Operators describing open string excitations on giant gravitons have been discussed in [19][20].

At even larger values for the angular momentum, $J \sim N^2$, one finds bulk geometries [10]. These geometries have an $SO(4) \times SO(4) \times R$ isometry group and preserve 16 of the original 32 supersymmetries. In the boundary theory, they are described by free fermion droplets in the two dimensional phase space occupied by the fermions. These fermions are the eigenvalues of the matrix Φ [21].

Interactions involving small KK gravitons, giant gravitons and LLM geometries should be encoded in the correlation functions of the corresponding dual CFT operators². Our basic remarks on normalizations and probabilities are general, valid for any coupling in the gauge theory, but our explicit computations are done in the free gauge theory limit.

¹Kaluza-Klein gravitons can also be described in the Schur polynomial basis: for small angular momenta, the single trace operators $\text{tr}(\Phi^J)$ can be expressed in terms of combinations of Schur polynomials corresponding to small Young diagrams. The choice of the single trace basis allows one to match directly the Fourier modes of the operators with the particle creation and annihilation operators of perturbative bulk supergravity [18]

²For some discussions of such gauge theory correlators see [22, 23, 24, 9, 25].

When they involve the special class of correlators called extremal, the explicit results are valid for any coupling. These are correlators in which the spacetime coordinates of all anti-holomorphic operators involving Φ^\dagger coincide while the positions of holomorphic operators are arbitrary (and vice versa). Non-renormalization theorems protect extremal correlators of 1/2-BPS chiral primaries so that the weak coupling computation of the correlators can be extrapolated to strong coupling without change [12, 26, 27, 28].

Some extremal correlators describe transitions from a giant graviton state into multi-particle KK graviton states. For example, the correlator

$$\langle \chi_{[N]}(\Phi^\dagger)(y) \text{tr}(\Phi^{J_1})(x_1) \text{tr}(\Phi^{J_2})(x_2) \dots \text{tr}(\Phi^{J_n})(x_n) \rangle \quad (2)$$

such that $\sum_i^n J_i = N$ and $J_i \ll N$, encodes information about the transition from an *AdS* giant with N units of angular momentum into several KK gravitons. Note that these processes involve “in” and “out” states that are half-BPS and stable. Their existence does not indicate an instability of the initial state, since the survival probability does not fall off exponentially with time. We may view the transitions in terms of a choice of detectors. In the above case for example, the detectors are chosen to detect KK gravitons. The strong dependence of transition probabilities on the choice of measurement was emphasized in [29][30]. The reverse process, where several KK gravitons give rise to a giant graviton is also of interest. We wish to calculate the probabilities for such transitions to occur. Most of these probabilities will be exponentially suppressed in $N \sim 1/g_s$ indicating the non-perturbative nature of such transitions.

2.2 Statement of the puzzle

We want to work out the normalized amplitudes for the transition from *AdS* and sphere giant graviton states either into other giant gravitons or into many Kaluza-Klein gravitons. We make use of two different normalizations: the multi-particle normalization and the overlap-of-states normalization. For the multi-particle normalization we divide the correlator by the norms of each of the products separately; for the overlap-of-states normalization we divide by the norm of all the outgoing states together. In this section, we ignore the spatial structure of the correlators and only consider the matrix-index structure. In our exact treatment later we cannot ignore the spatial dependencies of the correlators.

The multi-particle-normalized transition from an *AdS* giant graviton state with angular momentum N into several Kaluza-Klein gravitons, all of which have angular momentum J , is given by

$$\frac{|\langle \chi_{[N]}(\Phi^\dagger)(\text{tr}(\Phi^J))^{N/J} \rangle|^2}{\langle \chi_{[N]}(\Phi^\dagger) \chi_{[N]}(\Phi) \rangle \langle \text{tr}(\Phi^{J_1}) \text{tr}(\Phi^{J_2}) \dots \text{tr}(\Phi^{J_n}) \rangle^{N/J}} \quad (3)$$

and the overlap-of-states-normalized *S* giant transition is given by

$$\frac{|\langle \chi_{[1^N]}(\Phi^\dagger)(\text{tr}(\Phi^J))^{N/J} \rangle|^2}{\langle \chi_{[1^N]}(\Phi^\dagger) \chi_{[1^N]}(\Phi) \rangle \langle (\text{tr}(\Phi^{J_1}))^{N/J} (\text{tr}(\Phi^{J_2}))^{N/J} \dots (\text{tr}(\Phi^{J_n}))^{N/J} \rangle} \quad (4)$$

The first part of the puzzle is that, in general, the multi-particle normalization does not yield well-defined probabilities. For example if we calculate the *AdS* giant graviton process

(3) for $J = N/2$, we get the answer

$$\frac{\left| \langle \chi_{[N]}(\Phi^\dagger) \text{tr}(\Phi^{\frac{N}{2}}) \text{tr}(\Phi^{\frac{N}{2}}) \rangle \right|^2}{\langle \chi_{[N]}(\Phi^\dagger) \chi_{[N]}(\Phi) \rangle \langle \text{tr}(\Phi^{\frac{N}{2}}) \text{tr}(\Phi^{\frac{N}{2}}) \rangle \langle \text{tr}(\Phi^{\frac{N}{2}}) \text{tr}(\Phi^{\frac{N}{2}}) \rangle} \sim \frac{1}{6\sqrt{2}} \left(\frac{32}{27} \right)^N \quad (5)$$

which is bigger than 1 and therefore does not yield a well-defined probability.

Similarly the multi-particle-normalized transition (3) for $J \ll N$ is given by

$$\frac{\left| \langle \chi_{[N]}(\Phi^\dagger) (\text{tr}(\Phi^J))^{N/J} \rangle \right|^2}{\langle \chi_{[N]}(\Phi^\dagger) \chi_{[N]}(\Phi) \rangle \langle \text{tr}(\Phi^J) \text{tr}(\Phi^J) \rangle^{N/J}} \sim 2^{-\frac{1}{2}} e^{-N+2N \log(2) - (N/J) \log(J)} \quad (6)$$

The factor multiplying N in the exponential is $-1/2 + \log(2) - (1/2J) \log(J)$, which is positive for all J (because $\log(2)$ dominates). Thus this amplitude exponentially increases with N for all J . This is also inconsistent with a probability interpretation.

When we consider the multi-particle normalized transition from an *AdS* giant into two smaller *AdS* giants, we get similar divergent results

$$\frac{\left| \langle \chi_{[N]}(\Phi^\dagger) \chi_{[\frac{N}{2}]}(\Phi) \chi_{[\frac{N}{2}]}(\Phi) \rangle \right|^2}{\langle \chi_{[N]}(\Phi^\dagger) \chi_{[N]}(\Phi) \rangle \langle \chi_{[\frac{N}{2}]}(\Phi^\dagger) \chi_{[\frac{N}{2}]}(\Phi) \rangle \langle \chi_{[\frac{N}{2}]}(\Phi^\dagger) \chi_{[\frac{N}{2}]}(\Phi) \rangle} \sim \frac{3}{\sqrt{8}} \left(\frac{32}{27} \right)^N \quad (7)$$

Note however that the multi-particle normalization does not always give divergent results. For example the transition from a *sphere* giant state into KK gravitons with $J \ll N$ is given by

$$\frac{\left| \langle \chi_{[1N]}(\Phi^\dagger) (\text{tr}(\Phi^J))^{N/J} \rangle \right|^2}{\langle \chi_{[1N]}(\Phi^\dagger) \chi_{[1N]}(\Phi) \rangle \langle \text{tr}(\Phi^J) \text{tr}(\Phi^J) \rangle^{N/J}} \sim (2\pi)^{\frac{1}{2}} e^{-N + \frac{1}{2} \log(N) - (N/J) \log(J)} \quad (8)$$

which is exponentially decreasing for all J .

The second part of the puzzle is that there is no clear way to decide which normalization to use. In this paper we solve both puzzles. We will show that the multi-particle normalization requires us to divide by the two-point function on a higher genus manifold. This will yield well-defined probabilities for transitions from a single giant graviton state into a collection of smaller objects. We will also find that different transition probability interpretations require different normalizations.

A final subtlety is that for transitions from a giant state to states described by single trace operators, we cannot just naively take the square of the absolute value of the overlap amplitude of the giant graviton operator with a bunch of traces. Instead we should take the overlap of the giant graviton operator with traces and multiply with the overlap amplitude involving the duals of the trace operators. The dual is defined in terms of the metric on the space of traces: $\mathcal{G}^{ij} \mathcal{O}_j$.

Details of the calculations presented in this section, as well as several other computations, are given in Appendix A. The correctly normalized results for the processes discussed here are given in Section 6. These are exponentially suppressed in N as expected.

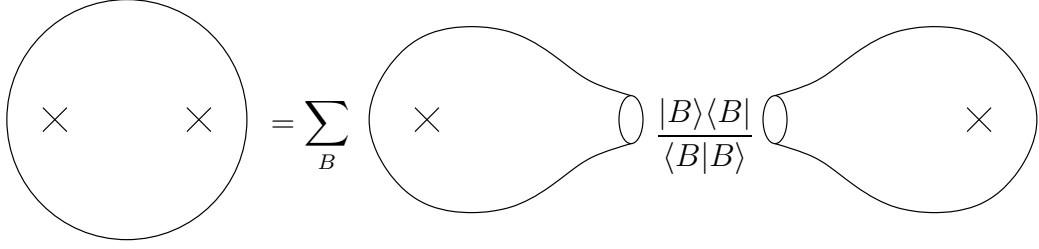


Figure 1: A sphere correlator by gluing two spheres

3 From factorization to probability interpretation of correlators

3.1 Factorization on S^4 and probabilities

Factorization in conformal field theory relates n-point correlators on the sphere to lower point correlators. Consider

$$|\langle A^\dagger(x^*)B(Q) \rangle|^2 = \langle A^\dagger(x^*)B(Q) \rangle \langle B^\dagger(Q^*)A(x) \rangle \quad (9)$$

Factorization implies that we can interpret a normalized version of this as a probability for the state created by the operator A at x to evolve into the state created by the operator B at Q^* . The action of conjugation acts by reversing the sign of the Euclidean time coordinate.

Using a basis B for the set of all possible operators, which we choose to diagonalize the metric on the space of local operators, the factorization equation takes the form

$$\langle A^\dagger(x^*)A(x) \rangle = \sum_B \frac{\langle A^\dagger(x^*)B(Q) \rangle \langle B^\dagger(Q^*)A(x) \rangle}{\langle B^\dagger(Q^*)B(Q) \rangle} \quad (10)$$

See Figure 1. Dividing by the term on LHS we have

$$1 = \sum_B P(A(x) \rightarrow B(Q)) \quad (11)$$

where P is interpreted as the probability for A to evolve into B , given by

$$P(A(x) \rightarrow B(Q)) = \frac{\langle A^\dagger(x^*)B(Q) \rangle \langle B^\dagger(Q^*)A(x) \rangle}{\langle A^\dagger(x^*)A(x) \rangle \langle B^\dagger(Q^*)B(Q) \rangle} \quad (12)$$

In the context of the 2D Matrix CFT model (see section 4) where the fields have matrix oscillators in their mode expansion, the operation of conjugation acts as $\alpha_{-n} \rightarrow \alpha_n^\dagger$ in the holomorphic sector. This is a symmetry of L_0 . Similarly in the antiholomorphic sector, we have that $\bar{\alpha}_{-n} \rightarrow \bar{\alpha}_n^\dagger$, which is a symmetry of \bar{L}_0 . Hence the conjugation is a symmetry of the Hamiltonian $H = L_0 + \bar{L}_0$ which generates translations in time.

In Euclidean theories, the proper definition of the adjoint of an operator involves the usual conjugation as well as the reversal of the Euclidean time. This operation guarantees that self-adjoint operators remain self-adjoint under Euclidean time evolution: $A(\tau) = e^{H\tau} A(0) e^{-H\tau}$.

It also means that for a physical theory $\langle A^\dagger(-\tau, \theta) A(\tau, \theta) \rangle$ must be positive, a condition called reflection positivity [31]. Thus the RHS of eq. (12) is positive as it must be the case for a proper probability interpretation.

The same thing can be said about extremal correlators which involve holomorphic operators at a number of different points:

$$\begin{aligned} & \langle A_1^\dagger(x_1^*) A_2^\dagger(x_2^*) \dots A_k^\dagger(x_k^*) A_1(x_1) A_2(x_2) \dots A_k(x_k) \rangle \\ &= \sum_B \frac{\langle A_1^\dagger(x_1^*) A_2^\dagger(x_2^*) \dots A_k^\dagger(x_k^*) B(Q) \rangle \langle B^\dagger(Q^*) A_1(x_1) A_2(x_2) \dots A_k(x_k) \rangle}{\langle B^\dagger(Q^*) B(Q) \rangle} \end{aligned} \quad (13)$$

Then we can still derive a sum of probabilities equal to 1 with

$$\begin{aligned} & P(A_1(x_1), A_2(x_2) \dots A_k(x_k) \rightarrow B(Q)) \\ &= \frac{|\langle A_1^\dagger(x_1^*) A_2^\dagger(x_2^*) \dots A_k^\dagger(x_k^*) B(Q) \rangle|^2}{\langle A_1^\dagger(x_1^*) A_2^\dagger(x_2^*) \dots A_k^\dagger(x_k^*) A_1(x_1) A_2(x_2) \dots A_k(x_k) \rangle \langle B^\dagger(Q^*) B(Q) \rangle} \end{aligned} \quad (14)$$

Note that these arguments involve the overlap-of-states normalization, not the multi-particle normalization. If we replace $|B(Q)\rangle$ by a state created by more than one operator e.g. $|B_1(y_1) B_2(y_2)\rangle$ the formula (14) can be used but it will not give an answer corresponding to a probability for separate detectors measuring $B_1(y_1)$ and $B_2(y_2)$. We will describe the case of multiple detectors and multi-particle normalization in the next subsection.

We will describe the detailed factorization equations later on, which follow from conformal invariance and the sewing properties of path integrals. These equations involve sums over all operators. There is a limit of large separations where the factorization can be restricted to BPS states, and gives the combinatoric (position independent) factorization equations in terms of the Littlewood-Richardson coefficients obtained in [17].

If we use the trace basis for the B 's in (12), we still have a factorization equation. In this basis, the probability is defined by

$$P(A \rightarrow B) = \frac{\langle A^\dagger B \rangle \langle \tilde{B}^\dagger A \rangle}{\langle A^\dagger A \rangle} \quad (15)$$

where \tilde{B} is the dual operator to B , with duality being given by the inner product defined by the 2-point function (see the Appendix Section G.2.1 for more details).

3.2 Higher topology and multi-particle normalization

We can extend these arguments to derive the probability interpretation for the case of multiple outgoing particles.

We need to consider correlators of higher topology. Take the \mathbb{R}^4 manifold with two B^4 's cut out and an operator insertion. This gives a manifold with two S^3 boundaries and a puncture. Take a second copy of \mathbb{R}^4 with the B^4 's cut out and an operator inserted. Glue each S^3 boundary with a corresponding S^3 boundary on the other \mathbb{R}^4 . Call this manifold X and consider a two-point function on X :

$$\langle A^\dagger(x^*) A(x) \rangle_{G=1} \quad (16)$$

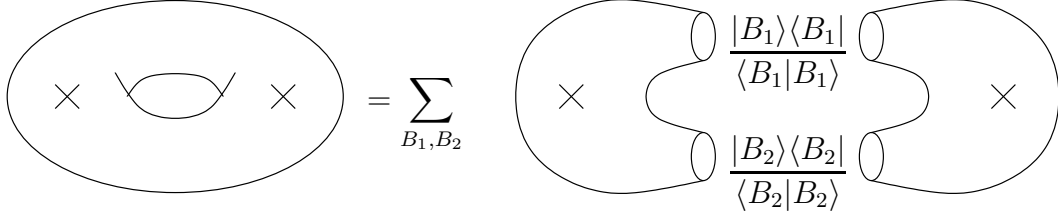


Figure 2: A torus correlator by gluing two spheres

This procedure is analogous to that of gluing two cylinders in 2d CFT to get a genus one surface with two punctures. Here we are doing the gluing in a 4d CFT, but we have used the notation $G = 1$ by analogy. We introduce the notation $\Sigma_4(G)$, to denote the four dimensional analog of a genus G surface in two dimensions. It can be obtained by taking two copies of S^4 with $G + 1$ non-intersecting balls removed, and gluing the two along the S^3 boundaries. To define probabilities for some set of states to go into $G + 1$ states we need to normalize with correlators on $\Sigma_4(G)$.

We can argue for this as follows. By the factorization argument we have

$$\langle A^\dagger(x^*)A(x) \rangle_{G=1} = \sum_{B_1, B_2} \frac{\langle A^\dagger(x^*)B_1(C_1)B_2(C_2) \rangle \langle B_2^\dagger(C_2^*)B_1^\dagger(C_1^*)A(x) \rangle}{\langle B_1^\dagger(C_1^*)B_1(C_1) \rangle \langle B_2^\dagger(C_2^*)B_2(C_2) \rangle} \quad (17)$$

See Figure 2. C_1 and C_2 are circles along which we cut the torus. The operators $B_i(C_i)$ create states localized on these circles. By scaling, these are related to the more familiar states which, in the operator-state correspondence, are obtained by local operators acting on the vacuum. Hence the equation above can be related to correlation functions of usual local operators. Eq. (17) is explained in more detail in section 4 in the two dimensional case, and in section 5 in the four dimensional case.

It follows from (17) that

$$1 = \sum_{B_1, B_2} \frac{\langle A^\dagger(x^*)B_1(C_1)B_2(C_2) \rangle \langle B_2^\dagger(C_2^*)B_1^\dagger(C_1^*)A(x) \rangle}{\langle A^\dagger(x^*)A(x) \rangle_{G=1} \langle B_1^\dagger(C_1^*)B_1(C_1) \rangle \langle B_2^\dagger(C_2^*)B_2(C_2) \rangle} \quad (18)$$

More generally

$$1 = \sum_{B_1, B_2} \frac{\langle A_1^\dagger(x_1^*) \cdots A_k^\dagger(x_k^*)B_1(C_1)B_2(C_2) \rangle \langle B_2^\dagger(C_2^*)B_1^\dagger(C_1^*)A_k(x_k) \cdots A_1(x_1) \rangle}{\langle A_1^\dagger(x_1^*) \cdots A_k^\dagger(x_k^*)A_k(x_k) \cdots A_1(x_1) \rangle_{G=1} \langle B_1^\dagger(C_1^*)B_1(C_1) \rangle \langle B_2^\dagger(C_2^*)B_2(C_2) \rangle} \quad (19)$$

Since every summand is real and positive, it can be interpreted as a probability. We conclude that to normalize correlators in order to get a probability for the case of multiple outgoing objects we need to divide by factors involving higher genus correlators. This corrects the naive multi-particle prescription used in the previous section.

We conclude this section with some comments:

- Notice that the probabilities we describe are defined subject to the constraint that the number of final states is fixed. Multi-particle states in this context are obtained by

the action of products of well separated operators on the vacuum. A brief discussion of conditional probabilities subject to additional conditions, such as fixing one of the outgoing states, is given in Appendix Section B.

- In this paper we focus on Euclidean correlators on \mathbb{R}^4 (or S^4) and higher genus spaces. A Lorentzian interpretation can be developed by choosing an appropriate time direction so that the out-states appear at a later time. When the factorization equations are appropriately continued to Lorentzian signature, they still provide relations between correlators. We have not described the normalization procedure in a purely Lorentzian set-up, but we expect that the probabilities continue to be relevant. Certainly in the large distance limits where the probabilities are independent of separations (see section 6), this is the case. A more thorough investigation of the Lorentzian picture is desirable, where issues of bulk causality of the results can be explored along the lines of [32].
- We work in a basis where the states are characterized by the action of a local operator on the CFT vacuum. These states are natural to consider from the CFT point of view. In general, such states are linear superpositions of states carrying arbitrary four-momentum. Definite momentum states must be constructed so as to recover the S-matrix of type IIB string theory in the flat space limit, as described in [33][34][35]. It would be interesting to express the factorization equation in the momentum basis and study which features survive in the flat space limit.

4 Factorization and gluing amplitudes in two dimensions

4.1 Matrix Model CFT

Consider the 2-dimensional CFT with action

$$S = \frac{1}{4\pi} \int d^2z \text{Tr} (\partial X \bar{\partial} X + \partial Y \bar{\partial} Y) \quad (20)$$

where X and Y are Hermitian $N \times N$ matrices. For these fields the two point functions on the sphere are given by

$$\langle X_j^i(z_1, \bar{z}_1) X_l^k(z_2, \bar{z}_2) \rangle = -\delta_l^i \delta_j^k \log |z_1 - z_2|^2 = \langle Y_j^i(z_1, \bar{z}_1) Y_l^k(z_2, \bar{z}_2) \rangle \quad (21)$$

We also introduce the complex fields

$$Z = \frac{X + iY}{\sqrt{2}}, \quad Z^\dagger = \frac{X - iY}{\sqrt{2}} \quad (22)$$

for which the two-point functions on the sphere are given by

$$\begin{aligned} \langle Z_j^{\dagger i}(z_1, \bar{z}_1) Z_l^k(z_2, \bar{z}_2) \rangle &= -\delta_l^i \delta_j^k \log |z_1 - z_2|^2 \\ \langle Z_j^i(z_1, \bar{z}_1) Z_l^k(z_2, \bar{z}_2) \rangle &= \langle Z_j^{\dagger i}(z_1, \bar{z}_1) Z_l^{\dagger k}(z_2, \bar{z}_2) \rangle = 0 \end{aligned} \quad (23)$$

Our goal is to study factorization properties for correlators of this matrix model CFT. The sums that enter in the factorization identities run over the space of local operators of the conformal field theory. It is natural to consider polynomials in the derivatives $\partial Z, \partial^2 Z, \dots$, and $\partial Z^\dagger, \partial^2 Z^\dagger, \dots$, along with exponentials of the matrices Z, Z^\dagger which generate non-zero momentum sectors. The non-zero momentum states decouple in most sectors of interest. As discussed in Section 4.6.1, in some cases of interest it is also consistent to truncate to the space of local operators invariant under global $U(N)$ transformations³

$$Z \rightarrow U^\dagger Z U \quad (24)$$

This subspace of local operators is given by traces of all matrix words built using $Z, \partial^n Z, Z^\dagger$ and $\partial^n Z^\dagger$ ($n > 0$) as letters. If we consider factorization equations for $U(N)$ invariant operators in the limit of large separations, it is possible to further restrict to just those words built using letters ∂Z or ∂Z^\dagger only. This is discussed further in Section 4.3. A basis for this subspace is provided by the loops

$$\mathcal{A}_n(z) = \text{Tr} ((\partial Z)^n), \quad \mathcal{A}_n^\dagger(z) = \text{Tr} ((\partial Z^\dagger)^n) \quad (25)$$

along with their products, i.e. multi-traces. Although this basis is complete and so perfectly acceptable, it is awkward. In particular, the two point function on the space of local operators is not diagonal with respect to this basis. This is a significant complication because the matrix inverse of this two point function enters the factorization equations. Since the two point functions

$$\langle \partial Z_j^i(z_1) \partial Z_l^k(z_2) \rangle = \frac{-\delta_l^i \delta_j^k}{(z_1 - z_2)^2} \quad (26)$$

have the same index structure as those corresponding to the elementary free field Φ_j^i in the four dimensional super Yang Mills case, we can use results of [8][17] for the color combinatorics. Thus as in the four dimensional case, a far more convenient basis is provided by the Schur polynomials. This basis is complete and further, the two point function on the space of Schur polynomials is diagonal.

4.2 An inner product on the states

In unitary two-dimensional conformal field theories, we can express the Hermitian inner product on the set of states as a product on the space of local operators $\{\mathcal{A}_i(z, \bar{z})\}$:

$$\mathcal{G}_{ij} = \langle i|j \rangle = \left\langle \mathcal{A}_i^\dagger(z', \bar{z}' = 0) \mathcal{A}_j(z, \bar{z} = 0) \right\rangle_{S^2} \quad (27)$$

where z and z' are related by $zz' = 1$, and we denote by $|i\rangle$ the state corresponding to the operator $\mathcal{A}_i(z, \bar{z})$. Note that the prime on the first operator indicates the z' -frame, and the operation of conjugation on it conjugates all *explicit* factors of i and transposes

³In the case of the four dimensional Super Yang Mills theory it is always consistent to truncate to the subspace of local gauge invariant operators (see Section 4.6.1).

matrix indices, but leaves the z and \bar{z} indices unchanged. This is essentially the operation of Euclidean conjugation, which we review in the Appendix C.

When the inner product of states is defined as an operator product, the hermiticity property $\langle i|j\rangle = \langle j|i\rangle^*$ follows from the properties of conformal invariance and operator conjugation [36][37]. In a unitary theory, the inner product of states is nonnegative, $\langle i|i\rangle \geq 0$ for all i , implying a positivity property for the metric \mathcal{G}_{ij} .

As an example, consider correlators involving holomorphic derivatives of Z , of arbitrary order, in the complex matrix model CFT. By direct computation, these are given by (see Appendix D)

$$\left\langle \partial^m Z_j^\dagger(z'=0) \partial^n Z_l^k(z=0) \right\rangle_{S^2} = m((m-1)!)^2 \delta_{nm} \delta_l^i \delta_j^k \quad (28)$$

The same result also follows if we use the operator-state map $\partial^k Z_j^i \leftrightarrow -i(k-1)! \alpha_{-k;j}^i$ and the inner product on states

$$\langle 0 | (i(p-1)! \alpha_{p;j}^\dagger)^i (-i(k-1)! \alpha_{-k;q}^l | 0 \rangle = k[(k-1)!]^2 \delta_{pk} \delta_q^i \delta_j^l \quad (29)$$

Correlators involving products of derivatives of Z and Z^\dagger split up into sums and products of correlators given by eq. (28).

Since the metric $\mathcal{G}_{ij} = \langle i|j\rangle$ is Hermitian and positive definite it is diagonalizable with positive real eigenvalues. In an appropriate basis we then have

$$\mathcal{G}_{ij} = \langle i|i\rangle \delta_{ij} \quad (30)$$

with inverse

$$\mathcal{G}^{ij} = \frac{1}{\langle i|i\rangle} \delta^{ij} \quad (31)$$

From the form of eq. (28), we know that part of this diagonal basis is given by derivatives of Z . Gauge invariant Schur polynomials of the primary field ∂Z are also part of this diagonal basis. This follows since the structure of the two-point function of $\langle \partial Z^\dagger \partial Z \rangle$ is the same as that for free four dimensional fields studied in [8].

4.3 Sphere factorization

For multi-point functions with a simple choice of operator positions, the spacial dependence factors out very simply and all the interesting structure is in the dependence on N and the choice of operators. For example

$$\left\langle \prod_{i=1}^l \chi_{R_i}(\partial Z^\dagger)(z) \prod_{j=1}^k \chi_{S_j}(\partial Z)(0) \right\rangle = z^{-2\Delta} \sum_S g(R_1, \dots, R_l; S) \frac{n_S! \text{Dim}_N(S)}{d_S} g(S_1, \dots, S_k; S), \quad (32)$$

Here Δ is the sum of the number of boxes in the Young diagrams $R_1, R_2 \dots R_n$. Further, $n_S = \Delta$ is the number of boxes in Young diagram S , $\text{Dim}_N(S)$ is the dimension of S taken as a representation of $U(N)$, d_S is the dimension of S taken as a representation of the symmetric group S_n and $g(R_1, R_2, \dots, R_l; S)$ is a Littlewood-Richardson (LR) coefficient. It is possible

to derive fusion and factorization identities for appropriate ratios of such correlators [17]. These identities are a direct consequence of the sum rule

$$g(R_1, R_2, \dots, R_n; S) = \sum_{S_1, S_2, \dots, S_{n-2}} g(R_1, R_2; S_1) g(S_1, R_3; S_2) \cdots g(S_{n-2}, R_n; S) \quad (33)$$

satisfied by the LR coefficients. It is natural to expect that the CFT factorization will reduce to these combinatoric (position independent) factorization identities in some limit. In this section we describe this in the simplest possible setting, where two S^2 correlators are glued to give another S^2 correlator. The local coordinates on the first S^2 are denoted by z ; the local coordinates on the second S^2 are denoted by w . The two spheres are glued around $z, \bar{z} = 0$ and $w, \bar{w} = 0$ with $zw = 1$.

The CFT factorization equation states

$$\langle \mathcal{O}_1(p_1) \mathcal{O}_2(p_2) \rangle_{S^2} = \sum_{ij} \mathcal{G}^{ij} \langle \mathcal{O}_1(p_1) \mathcal{A}_i(z, \bar{z} = 0) \rangle_{S^2} \langle \mathcal{A}_j^\dagger(w, \bar{w} = 0) \mathcal{O}_2(p_2) \rangle_{S^2} \quad (34)$$

This equation involves a sum over all operators. We will now argue that there is a limit of large separations where the factorization can be restricted to “BPS states”, and gives the combinatoric (position independent) factorization equations in terms of the LR coefficients. To see this, focus on the leading contribution to the factorization equations in the large separation limit. By a large separation limit, we mean that we take the distance between the operators, and the distance between the puncture and operators in the correlators to be large. From now on we will assume that we are in this limit and check the N dependence that follows from factorization. Since we are considering a large separation limit, it is clear that operators that dominate the sum will be those with the smallest conformal dimension. In addition, the only non-zero correlators have an equal number of Z s and Z^\dagger s. Taken together, these facts imply that we can restrict to Schur polynomials in ∂Z (or in ∂Z^\dagger). The operators that are dropped from the factorization sum, are polynomials that include at least one letter of the form $\partial^n Z$, with $n > 1$. These higher derivative terms lead to a faster fall off of the correlator as one increases the separation between operator locations, so that they don’t contribute in the leading order. With this restriction, the color combinatorics for the CFT are identical to the zero dimensional model so that the only difference between the two is extra spacial dependence in the CFT correlators. For concreteness, consider the correlator

$$\langle \prod_i \chi_{R_i}(\partial Z^\dagger(z_i)) \prod_j \chi_{S_j}(\partial Z(w_j)) \rangle \quad (35)$$

Using the two point functions, in the large separation limit,

$$\begin{aligned} \langle \partial Z_j^{\dagger i}(z_1) \partial Z_l^k(w_1) \rangle &= -(w'_1)^2 \langle \partial Z_j^{\dagger i}(z_1) \partial Z_l^k(w'_1) \rangle = \frac{(w'_1)^2}{(w'_1 - z_1)^2} \delta_l^i \delta_j^k \\ &= \frac{1}{(1 - z_1 w_1)^2} \delta_l^i \delta_j^k \approx \frac{1}{(z_1)^2} \frac{1}{(w_1)^2} \delta_l^i \delta_j^k \\ \langle \partial Z_j^{\dagger i}(z_1) \partial Z_l^k(0) \rangle &= -\frac{1}{(z_1)^2} \delta_l^i \delta_j^k \\ \langle \partial Z_j^{\dagger i}(0) \partial Z_l^k(w_1) \rangle &= -\frac{1}{(w_1)^2} \delta_l^i \delta_j^k \end{aligned} \quad (36)$$

the spacial dependence factors out on both sides leaving the combinatoric (position independent) factorization equations of [17]. The role of the higher derivatives that have been dropped is to modify the spacial dependences so that the two sides match for any separation. This is illustrated explicitly, in a simple setting, in Appendix D.

4.4 Geometrical gluing and factorization of higher genus correlators

4.4.1 The torus gluing

We will now describe a procedure for getting correlators on a torus by gluing together 3-punctured spheres. The procedure can be generalized to the case of higher topology Riemann surfaces following the description in [37, 38, 39, 40, 41].

Suppose the first sphere is covered with coordinate patches z and z' glued together by $zz' = 1$, while the second sphere is covered with coordinate patches w and w' glued together by $ww' = 1$. Let the first sphere have punctures at $z, \bar{z} = 0$, $z', \bar{z}' = 0$ and $z, \bar{z} = e^{2\pi s}$ ($s > 0$) and the second at $w, \bar{w} = 0$, $w', \bar{w}' = 0$ and $w, \bar{w} = e^{2\pi s}$.

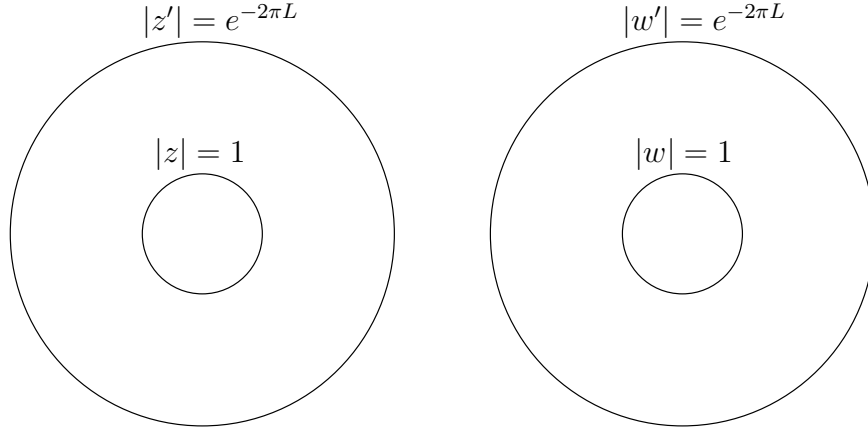


Figure 3: The z -annulus and the w -annulus

We cut out from the first sphere a region around $z, \bar{z} = 0$ and another region around $z', \bar{z}' = 0$ to give the first annulus. We cut out from the second sphere a region around $w, \bar{w} = 0$ and a region around $w', \bar{w}' = 0$ to give a second annulus. The cuts around $z, \bar{z} = 0$ and $w, \bar{w} = 0$ can be described as cutting out $|z| < e^{-2\pi\delta}$ and $|w| < 1$ for $\delta > 0$. We glue the two annuli by identifying points in the regions $e^{-2\pi\delta} \leq |z| \leq 1$ and $1 \leq |w| \leq e^{2\pi\delta}$ with $zw = 1$. Thus if we are approaching $|z| = 1$ from $|z| > 1$, once we enter the overlap region, we are now moving away from $|w| = 1$ in the direction of increasing $|w|$. The cut regions around $z', \bar{z}' = 0$ and $w', \bar{w}' = 0$ can be described by $|z'| < e^{-2\pi(L+\delta)}$ and $|w'| < e^{-2\pi L}$. Points on the two annuli regions $e^{-2\pi(L+\delta)} \leq |z'| \leq e^{-2\pi L}$ and $e^{-2\pi L} \leq |w'| \leq e^{-2\pi(L-\delta)}$ respectively are identified by the equation $z'w' = e^{-4\pi L}$. The gluing procedure produces a torus. If we continuously increase $|z|$ from the region near $|z| = 1$ we move into the z' patch with decreasing $|z'|$, via $zz' = 1$. This maps to increasing $|w'|$ in the w' patch via $z'w' = e^{-4\pi L}$.

This maps in turn into decreasing $|w|$ in the region near $|w| = 1$ on the second annulus, via $ww' = 1$, which maps back to the region near $|z| = 1$ on the first annulus, thus completing the periodic Euclidean time cycle of the torus. The δ factors can be taken to zero.

4.4.2 Factorization of torus correlators

We know from general arguments [37, 38, 39, 40, 41] that for operators \mathcal{O}_1 and \mathcal{O}_2 on a torus with modular parameter τ , $q = e^{2\pi i\tau}$,

$$\begin{aligned} \langle \mathcal{O}_1(p_1) \mathcal{O}_2(p_2) \rangle_{T^2} = & (q\bar{q})^{-c/24} \sum_{ij} \sum_{kl} q^{h_{ij}} \bar{q}^{\tilde{h}_{ij}} \mathcal{G}^{ij} \mathcal{G}^{kl} \left\langle \mathcal{O}_1(p_1) \mathcal{A}_j^\dagger(z', \bar{z}' = 0) \mathcal{A}_k(z, \bar{z} = 0) \right\rangle_{S^2} \\ & \times \left\langle \mathcal{A}_l^\dagger(w, \bar{w} = 0) \mathcal{A}'_i(w', \bar{w}' = 0) \mathcal{O}_2(p_2) \right\rangle_{S^2} \end{aligned} \quad (37)$$

where z and z' , related by $zz' = 1$, are coordinates on one sphere and w and w' , related by $ww' = 1$, are coordinates on another sphere. The two spheres are sewn together around $z, \bar{z} = 0$ and $w, \bar{w} = 0$ with $zw = 1$ and around $z', \bar{z}' = 0$ ($z, \bar{z} = \infty$) and $w', \bar{w}' = 0$ ($w, \bar{w} = \infty$) with $z'w' = q = e^{-4\pi L}$ to get a torus with $\tau = 2iL$.

We shall work with a basis of operators for which the metric is diagonal so that $\mathcal{G}^{ij} = (1/\langle i|i \rangle) \delta^{ij}$. Then the expression above can be written as

$$\begin{aligned} \langle \mathcal{O}_1(p_1) \mathcal{O}_2(p_2) \rangle_{T^2} = & (q\bar{q})^{-c/24} \sum_i \sum_k q^{h_i} \bar{q}^{\tilde{h}_i} \frac{1}{\langle i|i \rangle \langle k|k \rangle} \left\langle \mathcal{O}_1(p_1) \mathcal{A}_i^\dagger(z', \bar{z}' = 0) \mathcal{A}_k(z, \bar{z} = 0) \right\rangle_{S^2} \\ & \times \left\langle \mathcal{A}_k^\dagger(w, \bar{w} = 0) \mathcal{A}'_i(w', \bar{w}' = 0) \mathcal{O}_2(p_2) \right\rangle_{S^2} \end{aligned} \quad (38)$$

Since the metric only mixes operators of the same dimension, the operators $\mathcal{A}_i, \mathcal{A}_k$ can be chosen to be eigenstates of the scaling operator. Notice that when both the operators $\mathcal{O}_1, \mathcal{O}_2$ are set equal to the unit operator, we recover the modular invariant torus partition function.

The geometrical gluing picture described in the previous section provides a set up to demonstrate how a factorization equation such as (38) arises. The basic features of the following manipulations are in Figure 4. The result can be understood naturally in terms of the operator-state correspondence of conformal field theories. We let the operator \mathcal{O}_1 to be located at $z, \bar{z} = e^{2\pi s}$ and the operator \mathcal{O}_2 to be located at $w, \bar{w} = e^{2\pi s}$ with $0 < s < L$.

Consider first the z -correlator appearing in eq. (38)

$$\left\langle \mathcal{A}_i^\dagger(z', \bar{z}' = 0) \mathcal{O}_1(z, \bar{z} = e^{2\pi s}) \mathcal{A}_k(z, \bar{z} = 0) \right\rangle_{S^2} \quad (39)$$

where we choose to order the operator insertions radially with respect to $|z|$. To construct the z -annulus we remove the interior of the unit disk, $|z| < 1$, and replace the operator at $z, \bar{z} = 0$, $\mathcal{A}_k(z, \bar{z} = 0)$, by a state on the boundary at $|z| = 1$. We also remove the patch $|z'| < e^{-2\pi L}$ and replace the operator at $z', \bar{z}' = 0$ ($z, \bar{z} = \infty$), $\mathcal{A}_i^\dagger(z', \bar{z}' = 0)$, by a state on the boundary at $|z'| = e^{-2\pi L}$.

These states arise as follows. Using the operator/state correspondence we associate to the operator $\mathcal{A}_k(z, \bar{z} = 0)$ an “in-state” $|\mathcal{A}_k\rangle$ defined by $\lim_{z, \bar{z} \rightarrow 0} \mathcal{A}_k(z, \bar{z})|0\rangle$. We can think of this state as living on a small circle of radius $|z| = \epsilon$ surrounding the origin $z, \bar{z} = 0$, and consider the limit $\epsilon \rightarrow 0$. Notice that there are no other operator insertions in the unit disk.

$$\begin{aligned}
& \sum \frac{C_2^L \text{ (disk with } \times \text{)} C_2^R}{C_2^L \text{ (disk with } \times \text{)} C_2^R} = \sum_i \frac{|i; C_2^L\rangle \langle i; C_2^R|}{\langle i; C_2^L | i; C_2^R \rangle} \\
& \begin{array}{c} |z'| = e^{-2\pi L} \quad |w'| = e^{-2\pi L} \\ \text{Diagram: A central region with two horizontal ovals labeled } C_2^L \text{ and } C_2^R \text{ at the top, and } C_1^L \text{ and } C_1^R \text{ at the bottom. The top ovals have } \times \text{ marks. The bottom ovals have } \times \text{ marks. The region is bounded by a large oval with } \times \text{ marks on the left and right. Inside, there are labels } |z| = 1 \text{ and } |w| = 1 \text{ near the bottom ovals.} \\ |z| = 1 \quad |w| = 1 \end{array} \\
& \sum \frac{C_1^L \text{ (disk with } \times \text{)} C_1^R}{C_1^L \text{ (disk with } \times \text{)} C_1^R} = \sum_k \frac{|k; C_1^L\rangle \langle k; C_1^R|}{\langle k; C_1^L | k; C_1^R \rangle}
\end{aligned}$$

Figure 4: The torus correlator obtained after gluing - see equation (47)

Then the path integral over the unit disk amounts to radially propagating (or scaling) this state to a state at $|z| = 1$. This operation is equivalent to acting with the radial evolution operator $(1/\epsilon)^{-L_0 - \tilde{L}_0}$ on $|\mathcal{A}_k\rangle$. The end result is that the states differ by a scale factor: $|k; |z| = 1\rangle = \epsilon^{h_k + \tilde{h}_k} |\mathcal{A}_k\rangle$. The new state is an eigenstate of the dilatation operator.

In a similar way, we associate to the operator $\mathcal{A}_i^\dagger(z', \bar{z}' = 0)$ an “out-state”⁴ $\langle \mathcal{A}_i |$ defined by $\lim_{z', \bar{z}' \rightarrow 0} \langle 0 | \mathcal{A}_i^\dagger(z', \bar{z}') \rangle$. This state can be thought of as living on a circle of radius $|z'| = \epsilon$ surrounding $z', \bar{z}' = 0$, in the limit $\epsilon \rightarrow 0$. Now consider the path integral over the region $0 \leq |z'| < e^{-2\pi L}$. This amounts to radially propagating a state at $|z'| = e^{-2\pi L}$ to the state at $z', \bar{z}' = 0$. Notice that we have chosen radial evolution in the direction of increasing $|z|$ or equivalently in the direction of decreasing $|z'|$. To find the finite radius state, we consider the left action of the inverse radial evolution operator $(e^{-2\pi L}/\epsilon)^{L_0 + \tilde{L}_0}$ on $\langle \mathcal{A}_i |$. This operation gives $\langle i; |z'| = e^{-2\pi L} | = \langle \mathcal{A}_i | (e^{2\pi L} \epsilon)^{-h_i - \tilde{h}_i}$.

Now consider the w -correlator in eq. (38)

$$\left\langle \mathcal{A}_k^\dagger(w, \bar{w} = 0) \mathcal{O}_2(w, \bar{w} = e^{2\pi s}) \mathcal{A}_i'(w', \bar{w}' = 0) \right\rangle_{S^2} \quad (40)$$

⁴The “in” and “out- states” thus defined, are conjugates of each other: $\langle \mathcal{A} | = |\mathcal{A}\rangle^\dagger$ [36].

where we choose to radially order the operators with respect to $|w'|$. The w -annulus is constructed in a similar way. The patch $0 \leq |w'| < e^{-2\pi L}$ is removed replacing the operator at $w', \bar{w}' = 0$, $\mathcal{A}'_i(w', \bar{w}' = 0)$, by the state $|i; |w'| = e^{-2\pi L}\rangle = (e^{2\pi L}\epsilon)^{h_i + \tilde{h}_i}|\mathcal{A}_i\rangle$. Similarly the patch $0 \leq |w| < 1$ is removed replacing the operator at $w, \bar{w} = 0$, $\mathcal{A}'_k(w, \bar{w} = 0)$, by the state $\langle k; |w| = 1| = \langle \mathcal{A}_k | \epsilon^{-h_k - \tilde{h}_k}$.

In this way each correlator is replaced with a matrix element of a single operator. The z -correlator (39) is replaced with

$$\frac{(e^{2\pi L}\epsilon)^{h_i + \tilde{h}_i}}{\epsilon^{h_k + \tilde{h}_k}} \left\langle i; |z'| = e^{-2\pi L} \left| \mathcal{O}_1(z, \bar{z} = e^{2\pi s}) \right| k; |z| = 1 \right\rangle \quad (41)$$

while the w -correlator (40) is replaced with

$$\frac{\epsilon^{h_k + \tilde{h}_k}}{(e^{2\pi L}\epsilon)^{h_i + \tilde{h}_i}} \left\langle k; |w| = 1 \left| \mathcal{O}_2(w, \bar{w} = e^{2\pi s}) \right| i; |w'| = e^{-2\pi L} \right\rangle \quad (42)$$

Notice that the multiplicative scale factors cancel when we multiply the two expressions together.

The norms in the denominator of eq. (38) can be also written in terms of the finite radius states. We can think of the norms as normalized sphere amplitudes obtained by gluing each cut-off disk from the original z -sphere with the corresponding cut-off disk from the w -sphere, as shown in Figure 4. From the definition of the metric, eq. (27), and the local gluing relation $zw = 1$, we may write

$$\langle k|k \rangle = \left\langle \mathcal{A}_k^\dagger(w, \bar{w} = 0) \mathcal{A}_k(z, \bar{z} = 0) \right\rangle = \left\langle k; |w| = 1 \left| k; |z| = 1 \right. \right\rangle \quad (43)$$

Since the gluing relation of the prime coordinates is $w'z' = q$, we have that

$$\begin{aligned} \langle i|i \rangle &= q^{h_i} \bar{q}^{\tilde{h}_i} \left\langle \mathcal{A}_i^\dagger(z', \bar{z}' = 0) \mathcal{A}_i(w', \bar{w}' = 0) \right\rangle = \\ &= q^{h_i} \bar{q}^{\tilde{h}_i} \left\langle i; |z'| = e^{-2\pi L} \left| i; |w'| = e^{-2\pi L} \right. \right\rangle \end{aligned} \quad (44)$$

To obtain the last equation, we rescale from the coordinate z' to $\tilde{z} = z'/q$ so that $w'\tilde{z} = 1$. The factors of $q^{h_i} \bar{q}^{\tilde{h}_i}$ transform the operator at $z', \bar{z}' = 0$ to the \tilde{z} -frame. We see that when the norm $\langle i|i \rangle$ is expressed as an inner product between finite radius states at $|z'| = e^{-2\pi L}$ and $|w'| = e^{-2\pi L}$, the relative factor appearing cancels the factors of $q^{h_i} \bar{q}^{\tilde{h}_i}$ in the numerator of eq. (38).

Therefore we can replace the RHS of eq. (38) with

$$\begin{aligned} & (q\bar{q})^{-c/24} \sum_i \sum_k \frac{\left\langle i; |z'| = e^{-2\pi L} \left| \mathcal{O}_1(z, \bar{z} = e^{2\pi s}) \right| k; |z| = 1 \right\rangle_{annulus}}{\left\langle i; |z'| = e^{-2\pi L} \left| i; |w'| = e^{-2\pi L} \right. \right\rangle \left\langle k; |w| = 1 \left| k; |z| = 1 \right. \right\rangle} \\ & \times \left\langle k; |w| = 1 \left| \mathcal{O}_2(w, \bar{w} = e^{2\pi s}) \right| i; |w'| = e^{-2\pi L} \right\rangle_{annulus} \\ & = \sum_i \sum_k \frac{\langle i; x = iL | \mathcal{O}_1^{[x]}(x = is) | k; x = 0 \rangle_{cyl} \langle k; x = 0 | \mathcal{O}_2^{[x]}(x = -is) | i; x = -iL \rangle_{cyl}}{\langle i; x = -iL | i; x = -iL \rangle \langle k; x = 0 | k; x = 0 \rangle} \end{aligned} \quad (45)$$

In the second line, we express the equation in terms of cylinder amplitudes described by coordinates x, \bar{x} ($z = e^{-2\pi i x}, w = e^{2\pi i x}$). The coordinate x will be periodically identified, $x \sim x + 2iL$, to be made compatible with the gluing relations. Notice that the operators \mathcal{O}_1 and \mathcal{O}_2 must be transformed properly under the coordinate change. The power of $(q\bar{q})^{-c/24}$ in the first line is absorbed in the change in the overall normalization of the partition function under the change of coordinates from annulus to cylinder, which follows from the constant shift in the Hamiltonian: $H_{cyl} = L_0 + \tilde{L}_0 - (c + \tilde{c})/24$.

The first gluing of the two annuli along circle $|z| = |w| = 1$, using $zw = 1$, gives a single annulus or equivalently a cylinder of length $2L$, and is accompanied with a sum over a complete set of states $|k\rangle$ on the unit circle. Thus (45) can now be written as

$$\begin{aligned} & (q\bar{q})^{-c/24} \sum_i \frac{\left\langle i; |z'| = e^{-2\pi L} \left| \mathcal{O}_1(z, \bar{z} = e^{2\pi s}) \mathcal{O}_2(w, \bar{w} = e^{2\pi s}) \right| i; |w'| = e^{-2\pi L} \right\rangle_{annulus}}{\left\langle i; |z'| = e^{-2\pi L} \left| i; |w'| = e^{-2\pi L} \right\rangle_{sph}} \\ &= \sum_i \frac{\left\langle i; x = iL \left| \mathcal{O}_1^{[x]}(x = is) \mathcal{O}_2^{[x]}(x = -is) \right| i; x = -iL \right\rangle_{cylinder}}{\left\langle i; x = -iL \left| i; x = -iL \right\rangle} \end{aligned} \quad (46)$$

We emphasize that the numerator in the first line is an annulus transition amplitude and the denominator is a sphere amplitude. The final gluing identifies the inner and outer radii of the annulus, at $|w'| = e^{-2\pi L}$ and $|z'| = e^{-2\pi L}$, through $z'w' = e^{-4\pi L}$, or equivalently the ends of the cylinder by $x \sim x + 2iL$, to produce the torus with $\tau = 2iL$. Then the final sum over states in (46) allows us to express it as a trace, or equivalently as the torus two-point function $\langle \mathcal{O}_1(z, \bar{z} = e^{2\pi s}) \mathcal{O}_2(w, \bar{w} = e^{2\pi s}) \rangle_{T^2}$.

It is useful to rewrite eq. (45) more geometrically (see figure 4) in order to exhibit its coordinate independence

$$\begin{aligned} & \langle \mathcal{O}_1(p_1) \mathcal{O}_2(p_2) \rangle_{T^2} \\ &= \sum_{i,k} \frac{\langle i; C_2^L | \mathcal{O}_1(p_1) | k; C_1^L \rangle \langle k; C_1^R | \mathcal{O}_2(p_2) | i; C_2^R \rangle}{\langle i; C_2^L | i; C_2^R \rangle \langle k; C_1^R | k; C_1^L \rangle} \\ &= \sum_{i,k} \frac{\langle \mathcal{O}_1(p_1) \mathcal{A}_i^\dagger(C_2^L) \mathcal{A}_k(C_1^L) \rangle \langle \mathcal{O}_2(p_2) \mathcal{A}_i(C_2^R) \mathcal{A}_k^\dagger(C_1^R) \rangle}{\langle \mathcal{A}_i^\dagger(C_2^L) \mathcal{A}_i(C_2^R) \rangle \langle \mathcal{A}_k^\dagger(C_1^L) \mathcal{A}_k(C_1^R) \rangle} \end{aligned} \quad (47)$$

In the final line we have expressed the factorization in terms of operators which create states on finite size circles. The action of these operators on the vacuum is defined in terms of the radial evolution of states created by local operators. For example $\mathcal{A}_k(|z| = 1)|0\rangle \equiv |k; |z| = 1\rangle$, where the operator $\mathcal{A}_k(|z| = 1)$ can be viewed as creating a state at finite radius. Macroscopic loop operators are discussed in CFT and 2D gravity in [42]. The final line of (47) is identical to the RHS of (17).

We have presented the factorization equation in terms of the gluing of two annuli. It is instructive to view it conversely in terms of the cutting of the torus. Start with a path integral on a torus, expressed in terms of a generic set of fields ϕ

$$\langle \mathcal{O}_1(p_1) \mathcal{O}_2(p_2) \rangle_{G=1} = \int [d\phi] e^{-S(\phi)} \mathcal{O}_1(p_1) \mathcal{O}_2(p_2) \quad (48)$$

Now we cut along two circles denoted by C_1 and C_2 to get two cylinders. These cylinders can be conformally mapped to the annuli in Figure 3. The fields on the left and right are denoted by ϕ_L and ϕ_R . The boundary values on the circles are written as ϕ_{b_1}, ϕ_{b_2} . Hence the correlator can be written as

$$\begin{aligned} & \langle \mathcal{O}_1(p_1) \mathcal{O}_2(p_2) \rangle_{G=1} \\ &= \int [d\phi_{b_1}] [d\phi_{b_2}] \int [d\phi_L] |_{\phi_{b_1}}^{\phi_{b_2}} e^{-S(\phi_L)} \mathcal{O}_1(p_1) \int [d\phi_R] |_{\phi_{b_1}}^{\phi_{b_2}} e^{-S(\phi_R)} \mathcal{O}_2(p_2) \end{aligned} \quad (49)$$

The fields ϕ_L and ϕ_R are integrated subject to boundary conditions ϕ_{b_1}, ϕ_{b_2} at the circles C_1, C_2 . Each of the left/right path integrals give rise to wavefunctionals of fields on these circles that are correlated by the insertions of the local operators. Using the correspondence between wavefunctionals and Hilbert space states, the integrals $\int d\phi_{b_1} \int d\phi_{b_2}$ can be replaced by sums over states. These are the states summed over in eqs. (47) (45). These cutting and gluing relations appear in their simplest form in topological field theories, see for example [43][44].

4.4.3 Reflection Positivity

Consider again putting \mathcal{O}_2 at $w, \bar{w} = e^{2\pi s}$ in eq. (38), which corresponds to $z, \bar{z} = e^{-2\pi s}$ since z and w are glued with $zw = 1$, and choose now \mathcal{O}_1 to be its conjugate at $z, \bar{z} = e^{2\pi s}$. Then eq. (38) becomes

$$\begin{aligned} & \left\langle \mathcal{O}_2^\dagger(z, \bar{z} = e^{2\pi s}) \mathcal{O}_2(w, \bar{w} = e^{2\pi s}) \right\rangle_{T^2} \\ &= (q\bar{q})^{-c/24} \sum_i \sum_k q^{h_i} \bar{q}^{\tilde{h}_i} \frac{1}{\langle i|i \rangle \langle k|k \rangle} \left\langle \mathcal{O}_2^\dagger(z, \bar{z} = e^{2\pi s}) \mathcal{A}_i^\dagger(z', \bar{z}' = 0) \mathcal{A}_k(z, \bar{z} = 0) \right\rangle_{S^2} \\ & \quad \times \left\langle \mathcal{A}_k^\dagger(w, \bar{w} = 0) \mathcal{A}_i(w', \bar{w}' = 0) \mathcal{O}_2(w, \bar{w} = e^{2\pi s}) \right\rangle_{S^2} \\ &= (q\bar{q})^{-c/24} \sum_i \sum_k q^{h_i} \bar{q}^{\tilde{h}_i} \frac{\left| \left\langle \mathcal{O}_2^\dagger(z, \bar{z} = e^{2\pi s}) \mathcal{A}_i^\dagger(z', \bar{z}' = 0) \mathcal{A}_k(z, \bar{z} = 0) \right\rangle_{S^2} \right|^2}{\langle i|i \rangle \langle k|k \rangle} \end{aligned} \quad (50)$$

Finally note that the set $\{\mathcal{A}_i\}$ contains all local operators of the theory. If $\mathcal{A}(z, \bar{z})$ is an operator in this set, then so is $\mathcal{A}^\dagger(z, \bar{z})$. The two have the same weights and norm with respect to the metric \mathcal{G}_{ij} defined in (27). Thus we can also write the formula above as

$$\begin{aligned} & \left\langle \mathcal{O}^\dagger(z, \bar{z} = e^{2\pi s}) \mathcal{O}(w, \bar{w} = e^{2\pi s}) \right\rangle_{T^2} \\ &= (q\bar{q})^{-c/24} \sum_i \sum_k q^{h_i} \bar{q}^{\tilde{h}_i} \frac{\left| \left\langle \mathcal{O}^\dagger(z, \bar{z} = e^{2\pi s}) \mathcal{A}_i^\dagger(z', \bar{z}' = 0) \mathcal{A}_k(z, \bar{z} = 0) \right\rangle_{S^2} \right|^2}{\langle i|i \rangle \langle k|k \rangle} \end{aligned} \quad (51)$$

If the modular parameter τ is purely imaginary, so that q is real and positive, then each and every summand is real and positive. This demonstrates reflection positivity for the torus. Because every summand is real and positive we can discard some of the intermediate states in the sum to get an inequality with the left-hand side larger than the right-hand side. In the case of the matrix CFT, we choose to keep only states that are totally holomorphic

or totally antiholomorphic. Furthermore we throw away all states except those with first derivatives ∂Z and ∂Z^\dagger . We only keep gauge-invariant polynomials in these fields, which can be written as Schur polynomials. These are diagonal

$$\langle \chi_R(\partial Z^\dagger) \chi_S(\partial Z) \rangle \propto \delta_{RS} \quad (52)$$

4.5 Probabilities and Inequalities in 2D

We will now do some specific checks of the factorization equation (51). We keep gauge-invariant products of the primary field ∂Z in the sum only. We choose to work in the Schur polynomial basis $\chi_R(\partial Z(z))$ for which the metric is diagonal. We will obtain an inequality with the position dependences and torus moduli appearing explicitly.

In the following we will write $R(z)$ for $\chi_R(\partial Z(z))$ and $R^\dagger(z)$ for $\chi_R(\partial Z^\dagger(z))$. By the analysis above, we get an inequality for the torus correlator of the form

$$\begin{aligned} & (q\bar{q})^{c/24} \langle R^\dagger(z = e^{2\pi s}) R(w = e^{2\pi s}) \rangle_{T^2, \tau} \\ & > \sum_{R_1, R_2} e^{-4\pi L \Delta_1} \frac{\langle R^\dagger(z = e^{2\pi s}) R'_1(z' = 0) R_2(z = 0) \rangle \langle R_2^\dagger(w = 0) R'_1(w' = 0) R(w = e^{2\pi s}) \rangle}{\langle R_1 | R_1 \rangle \langle R_2 | R_2 \rangle} \end{aligned} \quad (53)$$

where Δ_1 is the conformal dimension of the operator R_1 , and $q = e^{2\pi i \tau} = e^{-4\pi L}$ since $\tau = 2iL$. We denote the conformal dimension of R_2 by Δ_2 . In order for the pair of operators R_1 and R_2 to contribute, $\Delta_1 + \Delta_2 = \Delta_R$ where Δ_R is the conformal dimension of R . To check this inequality explicitly, we must work out all the individual terms appearing in the inequality. Note that the left hand side is an unnormalized correlator, given by the insertion of operators in the path integral, without dividing by the torus partition function. The right hand side is insensitive to the normalization of the sphere correlators, so we will set the sphere normalization factor to 1 in the following.

4.5.1 The metric on the Schur Polynomials

We follow conventions so that for a single real scalar field, the 2-point function of its holomorphic derivatives on the sphere is given by

$$\langle \partial X(z_1) \partial X(z_2) \rangle_{S^2} = -\frac{1}{(z_1 - z_2)^2} \quad (54)$$

and similarly for a single complex scalar field Z :

$$\langle \partial Z(z_1) \partial Z(z_2) \rangle_{S^2} = -\frac{1}{(z_1 - z_2)^2} \quad (55)$$

Then the Schur polynomials satisfy

$$\langle \chi_R(\partial Z^\dagger(z_1)) \chi_S(\partial Z(z_2)) \rangle_{S^2} = \delta_{RS} f_R \frac{(-1)^{\Delta_R}}{(z_1 - z_2)^{2\Delta_R}} \quad (56)$$

where f_R is defined by

$$f_R = \frac{\text{Dim}_R \Delta_R!}{d_R} \quad (57)$$

In this expression, Dim_R is the dimension of the $U(N)$ representation R and d_R is the dimension of the symmetric group S_{Δ_R} representation R . To derive this 2-point function, we repeat all the steps of the corresponding four dimensional computation of [8], but noting that now each field contraction will give a factor of the propagator (55). The relevant color combinatorics are the same as in the case of [8].

Using eq. (56), we can compute the diagonal elements of the metric given by

$$\langle R_i | R_i \rangle = \left\langle R_i^\dagger(z' = 0) R_i(z = 0) \right\rangle_{S^2} \quad (58)$$

Changing the coordinate of R_i^\dagger to z using $z'z = 1$, and remembering that it is a primary field, we get

$$\begin{aligned} \langle R_i | R_i \rangle &= \lim_{z_0 \rightarrow \infty} \left\langle (-z_0^2)^{\Delta_i} R_i^\dagger(z = z_0) R_i(z = 0) \right\rangle \\ &= \lim_{z_0 \rightarrow \infty} \left[\frac{(-z_0^2)^{\Delta_i} (-1)^{\Delta_i} f_{R_i}}{(0 - z_0)^{2\Delta_i}} \right] \\ &= f_{R_i} \end{aligned} \quad (59)$$

4.5.2 Three point function calculations

We want to work out

$$\langle R^\dagger(z = e^{2\pi s}) R'_1(z' = 0) R_2(z = 0) \rangle_{S^2} \quad (60)$$

which we will do by changing the coordinate of R_1^\dagger to z via $zz' = 1$, and using the general formula of [8]

$$\langle R^\dagger(z) R_1(z_1) R_2(z_2) \rangle = g(R_1, R_2; R) f_R \frac{(-1)^{\Delta_1 + \Delta_2}}{(z_1 - z)^{2\Delta_1} (z_2 - z)^{2\Delta_2}} \quad (61)$$

We get

$$\begin{aligned} &\langle R^\dagger(z = e^{2\pi s}) R'_1(z' = 0) R_2(z = 0) \rangle \\ &= \lim_{z_0 \rightarrow \infty} \langle R^\dagger(z = e^{2\pi s}) (-z_0^2)^{\Delta_1} R_1(z = z_0) R_2(z = 0) \rangle \\ &= \lim_{z_0 \rightarrow \infty} \left[\frac{(-z_0^2)^{\Delta_1} (-1)^{\Delta_1 + \Delta_2} g(R_1, R_2; R) f_R}{(e^{2\pi s} - z_0)^{2\Delta_1} (e^{2\pi s} - 0)^{2\Delta_2}} \right] \\ &= g(R_1, R_2; R) f_R (-1)^{\Delta_2} e^{-4\pi s \Delta_2} \end{aligned} \quad (62)$$

Here, $g(R_1, R_2; R)$ is the group theoretic LR coefficient associated with the three representations R_1 , R_2 and R of $U(N)$. For the other 3-point correlator we obtain the same result:

$$\left\langle R_2^\dagger(w = 0) R_1^\dagger(w' = 0) R(w = e^{2\pi s}) \right\rangle_{S^2} = g(R_1, R_2; R) f_R (-1)^{\Delta_2} e^{-4\pi s \Delta_2} \quad (63)$$

4.5.3 The torus two point function

The torus Green's function in complex x coordinates, such that $x \sim x + 1 \sim x + \tau$, is given by

$$G'(x, \bar{x}; y, \bar{y}) = -\log |\theta_1(x - y; \tau)|^2 + \frac{2\pi}{\tau_2} [\text{Im}(x - y)]^2 \quad (64)$$

where θ_1 is a theta function⁵. For a single complex field, this implies

$$\begin{aligned} Z_{T^2}^{-1} \langle \partial_x Z^\dagger(x) \partial_y Z(y) \rangle_{T^2} &= -Z_{T^2}^{-1} \partial_x^2 \langle Z^\dagger(x) Z(y) \rangle_{T^2} \\ &= \partial_x^2 (\log \vartheta_{11}(x - y; \tau)) - \frac{2\pi}{\tau_2} \\ &= -\wp(x - y; \tau) \end{aligned} \quad (65)$$

where \wp is the Weierstrass elliptic function. The factor of Z_{T^2} , the torus partition function, appears because the Weierstrass function is the *normalized* correlator. Notice that factorization produces the un-normalized torus path integrals. Transforming to $z = e^{-2\pi i x}$ and $w = e^{2\pi i y}$ coordinates, we also have that

$$\langle \partial_z Z^\dagger(z) \partial_w Z(w) \rangle_{T^2} = \frac{1}{(-2\pi i z)} \frac{1}{(2\pi i w)} \langle \partial_x Z^\dagger(x) \partial_y Z(y) \rangle_{T^2} \quad (66)$$

We are interested in the two point function for which the operators are inserted at $x = is$ ($z = e^{2\pi s}$) and $y = -is$ ($w = e^{2\pi s}$), with $\tau = 2iL$ —see Figure 5. So we obtain that

$$\begin{aligned} Z_{T^2}^{-1} \langle \partial_z Z^\dagger(z = e^{2\pi s}) \partial_w Z(w = e^{2\pi s}) \rangle_{T^2} &= \frac{e^{-4\pi s}}{(2\pi)^2} Z_{T^2}^{-1} \langle \partial_x Z^\dagger(x = is) \partial_y Z(y = -is) \rangle_{T^2} \\ &= -\frac{1}{(2\pi)^2} e^{-4\pi s} \wp(2is; 2iL) \equiv \Gamma(is, -is) \end{aligned} \quad (67)$$

where we introduced the notation $\Gamma(is, -is)$ for brevity. The function $-\wp(2is; 2iL)$ is positive for all real values of s , as expected from the property of reflection positivity.

We can check that (67) leads to the correct pole structure in the limit of small s . Using the expansion of the Weierstrass elliptic function (65) for small $x - y = 2is$ and $\tau = 2iL$, we obtain

$$\begin{aligned} \Gamma(is, -is) &= -\frac{1}{(2\pi)^2} e^{-4\pi s} \wp(2is; 2iL) \\ &= -\frac{1}{(2\pi)^2} e^{-4\pi s} \left[\frac{1}{-4s^2} + \sum_{m, n \in \mathbb{Z}: m, n \neq 0} \left\{ \frac{1}{(2is + n + 2miL)^2} - \frac{1}{(n + 2miL)^2} \right\} \right] \\ &\simeq \frac{1}{16\pi^2 s^2} \end{aligned} \quad (68)$$

The same result can be obtained from the sphere 2-point function, eq. (55), for $z_1 = e^{-2\pi is}$, $z_2 = e^{2\pi is}$ in the limit $s \rightarrow 0$. The pole structure is dictated by the operator product expansion.

⁵ α' has been set equal to 2 in the corresponding formula of [37].

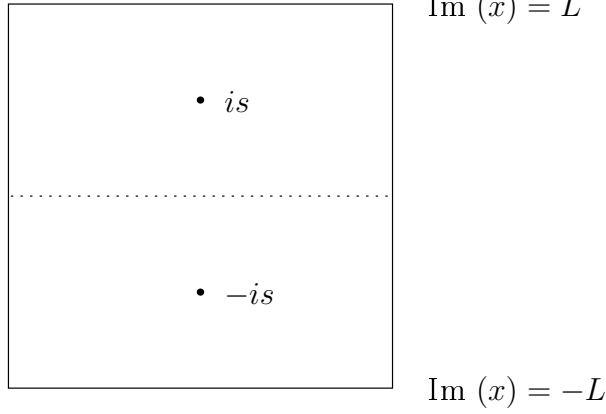


Figure 5: The torus correlator obtained after gluing

Now we can compute the torus 2-point function of the Schur polynomial R . The color combinatorics are the same as in the sphere-case. Each field contraction gives a factor of $\Gamma(is, -is)$. The number of such contractions is set by the (integer) conformal dimension of R . So we obtain

$$\langle R^\dagger(z = e^{2\pi s}) R(w = e^{2\pi s}) \rangle_{T^2} = Z_{T^2} \Gamma(is, -is)^{\Delta_R} f_R \quad (69)$$

4.5.4 The inequality

If we insert into (53) all the elements, the inequality becomes

$$Z_{T^2} \Gamma(is, -is)^{\Delta_R} f_R > (q\bar{q})^{-c/24} \sum_{R_1, R_2} e^{-4\pi L \Delta_1} \frac{e^{-8\pi s \Delta_2} g(R_1, R_2; R)^2 f_R^2}{f_{R_1} f_{R_2}} \quad (70)$$

In terms of the Weierstrass elliptic function, we obtain

$$\left(-\frac{1}{(2\pi)^2} \wp(2is; 2iL) \right)^{\Delta_R} > \frac{(q\bar{q})^{-c/24}}{Z_{T^2}} \sum_{R_1, R_2} e^{-4\pi L \Delta_1 + 4\pi s(\Delta_1 - \Delta_2)} \frac{g(R_1, R_2; R)^2 f_R}{f_{R_1} f_{R_2}} \quad (71)$$

In the strict large L limit, the factor $\frac{(q\bar{q})^{-c/24}}{Z_{T^2}}$ is equal to one because only the state corresponding to the unit operator contributes to the partition sum⁶. At finite L it is smaller than one and makes the inequality easier to satisfy. If we embed the Matrix CFT in a supersymmetric theory and use periodic boundary conditions for the fermions in the gluing process, this extra factor is exactly one (assuming that the ground state is unique). Hence in general we expect the stronger inequality

$$\left(-\frac{1}{(2\pi)^2} \wp(2is; 2iL) \right)^{\Delta_R} > \sum_{R_1, R_2} e^{-4\pi L \Delta_1 + 4\pi s(\Delta_1 - \Delta_2)} \frac{g(R_1, R_2; R)^2 f_R}{f_{R_1} f_{R_2}} \quad (72)$$

⁶We can gap non-zero momentum and winding states by considering a compact version of the CFT.

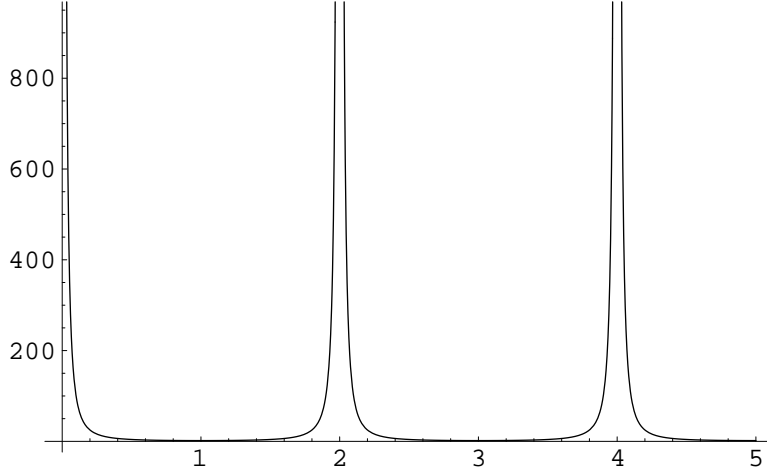


Figure 6: A plot of $-\wp(2is; 2iL)$ against s with $L = 1$

to be valid, although our main interest is at large L .

We can now do various checks of the inequality (72). If we further restrict to intermediate operators for which $\Delta_1 = \Delta_2 = \Delta$ ($\Delta = \Delta_R/2$), we get

$$\left(-\frac{1}{(2\pi)^2} \wp(2is; 2iL) \right)^{2\Delta} > e^{-4\pi\Delta L} \sum_{R_1, R_2} \frac{g(R_1, R_2; R)^2 f_R}{f_{R_1} f_{R_2}} \quad (73)$$

where the RHS is now a constant as a function of s . The function $-\wp(2is; 2iL)$ is a real, positive function of s which is periodic. The period is L with respect to s (or $2L$ with respect to the separation of the two operator insertions, $2s$). In each period this function reaches a minimum at the middle of its period. Thus the LHS of the inequality reaches a minimum at $s = L/2$ (see Figure 6). At this point we have

$$-\wp(iL; 2iL) = \pi^2 \left(4 \sum_{n>0} \{ \coth(2n\pi L) \operatorname{cosech}(2n\pi L) \} + \frac{1}{3} \right) \quad (74)$$

For this and other limits of the Weierstrass elliptic function see Appendix E.

This means that the inequality will be true for all s provided that

$$\left(\sum_{n>0} \{ \coth(2n\pi L) \operatorname{cosech}(2n\pi L) \} + \frac{1}{12} \right)^{2\Delta} > e^{-4\pi\Delta L} \sum_{R_1, R_2} \frac{g(R_1, R_2; R)^2 f_R}{f_{R_1} f_{R_2}} \quad (75)$$

We can see how this is satisfied for all values of L . For large L , the LHS tends to $(1/12)^{2\Delta}$ which will be much bigger than $e^{-4\pi\Delta L}$. For small L the hyperbolic functions $\coth(2n\pi L)$ and $\operatorname{cosech}(2n\pi L)$ both blow up.

We will now check our result for the transition from a size N AdS giant, a single-row representation written $R = [N]$, to two smaller AdS giants, $R_1, R_2 = [N/2]$, so that $\Delta = N/2$.

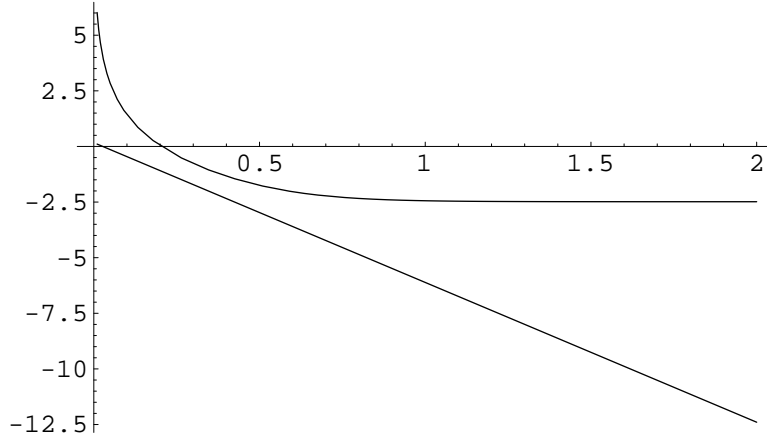


Figure 7: A plot of the logarithms of the LHS of (75) (top) against (76) (bottom) against L for our chosen representations. We have in fact taken the N th root of each side. We can ignore the $3/\sqrt{8}$ factor in (76) because it adds a small constant to the lower graph which does not affect the inequality for any value of N .

Then the RHS of (75) is given by

$$\begin{aligned} \frac{f_{[N]}}{f_{[N/2]}^2} e^{-2\pi N L} &= \frac{(2N-1)!(N-1)!}{((3N/2-1)!)^2} e^{-2\pi N L} \\ &\sim \frac{3}{\sqrt{8}} \left(\frac{32}{27}\right)^N e^{-2\pi N L} (1 + \mathcal{O}(1/N)) \end{aligned} \quad (76)$$

In Figure 7, the LHS of (75) is plotted against (76), for the specific Schur polynomials chosen, as a function of L to verify that the inequality holds for all L and N .

For $\Delta_1 \neq \Delta_2$ the s -dependence of the RHS of (72) is no longer trivial. Some numerical checks of the inequality have been made for this situation.

4.5.5 Probability interpretation in the large L , N limits

We can now obtain a well defined probability for a transition to occur, from a state of charge N , created by the operator $\chi_{[N]}(\partial Z)$, to two states of charge $N/2$ each created by the operator $\chi_{[N/2]}(\partial Z)$ in the large L and N limits.

The large L limit is the appropriate limit. The discussion in Section 4.4.1, of gluing at two punctures, should be related to the limit in moduli space where $\tau = 2iL$ and $L \rightarrow \infty$. This can be seen as follows. Consider a sphere with disks of radii $e^{-2\pi r_1}, e^{-2\pi r_2}$ removed near the N and S poles. The region from the equator to the first disk is mapped to a cylinder of radius one and length r_1 using the exponential map $z = e^{-2i\pi x}$. The region from the equator to the second disk is mapped to a cylinder of radius 1 and length r_2 by the map $z' = e^{-i2\pi y}$. Hence we have a cylinder with radius 1 and length $r_1 + r_2$. When this is glued to another similar cylinder of unit radius and size $r_1 + r_2$, we get a torus with τ parameter $2i(r_1 + r_2)$. As the disks reach zero size in the limit $r_1, r_2 \rightarrow \infty$, we get a torus with $\tau \rightarrow i\infty$.

Because the LHS of (72) approaches a constant for large L , the probability is given by

$$P([N] \rightarrow [N/2], [N/2]) \sim \frac{3}{\sqrt{8}} \exp \{(-2\pi L + \log(32/27) + \log 12)N\} \quad (77)$$

which is less than 1 because L is taken large. We have used (76), which computes the contribution to the RHS for this particular process. Notice that the factor L governs the spatial separation of the states on the cylinder.

4.6 Miscellaneous comments

4.6.1 Zero coupling gauge theory v/s unconstrained free fields

The two dimensional Matrix CFT we are considering is invariant under global $U(N)$ transformations. The symmetry imposes restrictions on the type of internal states that contribute in factorization relations.

Suppose that the external states in a factorization equation are invariant under global $U(N)$ transformations:

$$Q_a|A\rangle = 0, \quad Q_a|B\rangle = 0 \quad (78)$$

where the operators Q_a denote the generators of $U(N)$ transformations. These satisfy $[Q_a, Q_b] = if_{abc}Q_c$, with f_{abc} the $U(N)$ Lie algebra structure constants. Consider the overlap

$$\langle B|U(t_1, t_2)|A\rangle \quad (79)$$

where $U(t_1, t_2)$ is the time (radial) evolution operator. The Hamiltonian (dilatation operator) is invariant under global $U(N)$ transformations so that $[Q_a, U] = 0$. Now we insert a complete set of orthonormal states at time t' (or radius r'), which can be taken to be eigenstates of the mutually commuting Cartan generators, to obtain a factorization relation

$$\langle B|U(t_1, t_2)|A\rangle = \sum_C \langle B|U(t_1, t')|C\rangle \langle C|U(t', t_2)|A\rangle \quad (80)$$

Then the intermediate states $|C\rangle$ must also be invariant under global $U(N)$ transformations. We can argue for this as follows:

$$\begin{aligned} \langle B|U(t_1, t')|C\rangle &= \langle B| (e^{i\alpha_a Q_a} U(t_1, t') e^{-i\alpha_a Q_a}) |C\rangle \\ &= (\langle B| e^{i\alpha_a Q_a}) U(t_1, t') (e^{-i\alpha_a Q_a} |C\rangle) = \langle B|U(t_1, t')|C\rangle e^{-i\alpha_a q_a} \end{aligned} \quad (81)$$

where the vector q_a denotes the charges of the state $|C\rangle$. Since the above must hold for arbitrary α_a , it is clear that only intermediate states with $q_a = 0$ contribute. Therefore, the operator corresponding to $|C\rangle$ must also be invariant. So only $U(N)$ invariant operators contribute in the genus zero factorization. If we consider a factorization equation of a genus-1 correlator such as eq. (17), then the symmetry implies that the net charge of the internal operators B_1 and B_2 contributing must add to zero, assuming that the external operators are invariant.

If a theory has a local gauge symmetry, such as the four dimensional $\mathcal{N} = 4$ Super Yang Mills theory we are interested in, then there are further constraints on the types of internal

operators contributing in factorization equations. Consider for example correlators of local gauge invariant operators of the $\mathcal{N} = 4$ theory on the $S^3 \times S^1$ manifold. Suppose we factorize such higher genus correlators in terms of correlators of local operators on S^4 . Invariance of the theory under local gauge transformations implies that in order for the internal local operators to contribute, each must be a local gauge invariant operator.

The considerations above address the following puzzle. Consider the $\mathcal{N} = 4$ Super Yang Mills theory on $S^3 \times S^1$ in the limit of vanishing coupling constant. Even in this limit, the zero mode of A_0 on the sphere does not decouple from matter fields, and because of the non-trivial topology of the manifold, it cannot be gauged away. The relevant gauge invariant quantity is the Wilson line of A_0 around the S^1 circle. As a consequence, thermal two point functions of local gauge invariant operators composed of adjoint scalars are different from the two point functions of the same operators in a theory with unconstrained, free scalar fields only—see [45]. This difference is also reflected in factorization equations in terms of local operators: in the zero coupling gauge theory, each of the internal local operators must be a local gauge invariant operator to contribute, while in the unconstrained free scalar theory only the net charge of the operators has to vanish. We expect that correlators of local gauge invariant operators in the two theories should agree in the limit of large radius for the S^1 circle. When the circle becomes uncompact, A_0 can be gauged away. This was discussed, in the case of large N in [45]. In addition, it was argued in [45] that to leading order in $1/N$, non-renormalization theorems protecting the two point and three point functions of $1/2$ BPS operators against 't Hooft coupling corrections survive in the low temperature phase of the theory. The large N and large radius limits are the relevant limits for our computations in section 5.6.

4.6.2 Windings from torus factorization sums

If our intermediate states \mathcal{A}'_i and \mathcal{A}_j appearing in the factorization equation differ in their holomorphicity, then we can interpret some of the summands in the torus factorization as paths winding around a non-trivial cycle in the torus. For example, when $\mathcal{A}'_i(z', \bar{z}' = 0) = \partial Z^{\dagger}(z', \bar{z}' = 0)$ and $\mathcal{A}_k(z, \bar{z} = 0) =: \partial Z(z, \bar{z} = 0) \partial Z(z, \bar{z} = 0) :$, we obtain a path with winding number 1. See the Appendix section F for a detailed discussion.

5 Factorization in the 4D CFT

5.1 Introduction

The factorization arguments described in the previous section extend naturally to conformal field theories in four dimensions. To obtain sphere factorization identities, we glue together two S^4 s around one puncture to produce a single S^4 . To obtain genus-1 factorization identities, we glue together two S^4 s at two punctures to get a genus-1 surface which is conformally equivalent to the $S^1 \times S^3$ manifold. The argument for the factorization of the correlation functions in the $3 + 1$ -dimensional CFT follows from the path integral discussion in Section 4.4.2. In the sum over intermediate states we keep only the Schur polynomials in a single complex scalar Φ .

5.2 Metric

In order to define a positive metric on the space of operators, we choose the scalar 2-point function on \mathbb{R}^4 to satisfy the convention

$$\Delta_x G(x-y) = -\delta^4(x-y) \quad (82)$$

This gives

$$G(x-y) = \frac{1}{4\pi^2|x-y|^2} \quad (83)$$

The metric on the space of Schur polynomials is given by

$$\langle R^\dagger(r'=0)R(r=0) \rangle \quad (84)$$

where $r' = 1/r$. To compute the correlator, we map R^\dagger back to the r -coordinate frame. Under the coordinate transformation $r' \rightarrow r = 1/r'$, the metric changes as follows

$$dr'^2 + r'^2 d\Omega^2 \rightarrow \frac{1}{r^4}(dr^2 + r^2 d\Omega^2) \quad (85)$$

and so the primary fields transform as

$$\Phi'(x') \rightarrow \Omega(x)^{-\Delta/2} \Phi(x) = r^{2\Delta} \Phi(x) \quad (86)$$

where $\Omega(x) = 1/r^4$ is the conformal factor [36]. Thus for the metric element we obtain

$$\begin{aligned} \langle R^\dagger(r'=0)R(r=0) \rangle &= \lim_{r_0 \rightarrow \infty} \langle r_0^{2\Delta} R^\dagger(r=r_0)R(r=0) \rangle \\ &= \left(\frac{1}{4\pi^2} \right)^\Delta f_R \end{aligned} \quad (87)$$

5.3 The genus zero factorization in four dimensions

Following the two dimensional example, we start with two 4-spheres, one with coordinates (r, Ω_i) and the other with coordinates (s, Ω'_i) . Next we cut out a 4-ball of unit radius around the origin in each, and glue them together using $rs = 1$. The factorization identity implies an inequality given by

$$\begin{aligned} &\langle R_1^\dagger(s=e^{x_1}) \cdots R_k^\dagger(s=e^{x_k}) R_k(r=e^{x_k}) \cdots R_1(r=e^{x_1}) \rangle \\ &> \sum_R \frac{\langle R_1^\dagger(s=e^{x_1}) \cdots R_k^\dagger(s=e^{x_k}) R(r=0) \rangle \langle R^\dagger(s=0) R_k(r=e^{x_k}) \cdots R_1(r=e^{x_1}) \rangle}{\langle R^\dagger R \rangle} \end{aligned} \quad (88)$$

where we set $x_j > 0$ for $j = 1, \dots, k$ so that the operator insertions are outside the cut-off region. We have suppressed the angular coordinates of the operators R_j in (88), but these can be arbitrary in general.

In general the correlator on the LHS of the inequality is not extremal, so it may have a non-trivial dependence on the 't Hooft coupling constant. To avoid this complication, we do our calculations in the limit that the correlator becomes extremal, i.e. when $x_1 = x_2 = \dots = x_k$.

In the large separations limit, $x_j \rightarrow \infty$, we recover the combinatorial factorization identities discussed in [17].

5.4 The genus one factorization in four dimensions

We parameterize four dimensional flat space \mathbb{R}^4 with spherical coordinates so that the metric is given by

$$ds^2 = dr^2 + r^2 d\Omega_3^2 \quad (89)$$

This metric is conformal to the standard metric on $S^3 \times \mathbb{R}$ under the coordinate transformation $r = e^\tau$:

$$ds^2 = e^{2\tau} (d\tau^2 + d\Omega_3^2) \quad (90)$$

In the two dimensional example, we started with two copies of $S^1 \times I$ described by coordinates $1 \leq |z| \leq e^{2\pi L}$ and $1 \leq |w| \leq e^{2\pi L}$. In the four dimensional case, we start with two cylinders $S^3 \times I$ described by coordinates (r, Ω_i) and (s, Ω'_i) with the radial variables in the range

$$\begin{aligned} 1 &\leq r \leq e^T \\ 1 &\leq s \leq e^T \end{aligned} \quad (91)$$

In most of the following expressions, we suppress the angular dependence since the angles, in all of the gluings, are identified trivially.

Introduce also the coordinates $r' = 1/r$ and $s' = 1/s$. We now glue the two cylinders $S^3 \times I$ at the inner ends $r = 1, s = 1$ with $rs = 1$. We then glue the outer ends at $r = e^T, s = e^T$ with $r's' = e^{-2T}$ (i.e. $rs = e^{2T}$). The gluing produces an $S^3 \times S^1$ manifold with $\tau \sim \tau + 2T$ ⁷.

5.5 The genus one factorization and inequality

The derivation of factorization of correlators on genus-1 surfaces in two dimensions uses basic features of CFT, such as the operator-state correspondence and properties of the path integral representation of correlators. The same steps can be run through in four dimensions. Now we are looking at correlators on $\Sigma_4(G=1)$, which is obtained by gluing two copies of $S^3 \times I$, each obtained by cutting out the neighborhoods of two points in an S^4 manifold. We obtain

$$\begin{aligned} &\langle R^\dagger(P_1)R(P_2) \rangle_{G=1} \\ &= \sum_{i,j} \frac{\langle R^\dagger(P_1)\mathcal{A}_i^\dagger(C_2^L)\mathcal{A}_k(C_1^L) \rangle \langle \mathcal{A}_k^\dagger(C_1^R)\mathcal{A}_i(C_2^R)R(P_2) \rangle}{\langle \mathcal{A}_i^\dagger(C_2^L)\mathcal{A}_i(C_2^R) \rangle \langle \mathcal{A}_k^\dagger(C_1^L)\mathcal{A}_k(C_1^R) \rangle} \end{aligned} \quad (92)$$

The surfaces C_i^L and C_i^R are now 3-spheres. Eq. (92) is the 4d analog of eq. (47). By scaling, we can express the RHS in terms of correlators of local operators on \mathbb{R}^4

$$\langle R^\dagger(r = e^x, \Omega_i)R(s = e^x, \Omega_i) \rangle$$

⁷ In our notation, $2T$ stands for the inverse temperature with regards to the thermal theory on $S^3 \times S^1$. We hope that the notation does not cause confusion to the reader.

$$= Z_0 \sum_{i,j} e^{-2T\Delta_i} \frac{\langle R^\dagger(r=e^x, \Omega_i) \mathcal{A}_i^\dagger(r'=0) \mathcal{A}_k(r=0) \rangle \langle \mathcal{A}_k^\dagger(s=0) \mathcal{A}_i(s'=0) R(s=e^x, \Omega_i) \rangle}{\langle i|i \rangle \langle k|k \rangle} \quad (93)$$

This is the 4d analog of eq. (37). Z_0 is the large T limit of the Euclidean partition function on $S^3 \times S^1$, analogous to the $(q\bar{q})^{-c/24}$ term in two dimensions. It depends only on the Casimir energy of the ground state. We will not need it explicitly. In going from a path integral expression to an operator expression, we must specify a time-ordering. We specialize to the case where P_2 and P_1 are related by Euclidean time reversal so that we can expect positivity of the RHS of the equations above. We will further restrict the sum to the case where \mathcal{A}_i^\dagger and \mathcal{A}_k are given respectively by the Schur Polynomials $\chi_{R_1}(\Phi)$ and $\chi_{R_2}(\Phi)$. By checking the resulting inequality, we will obtain well-behaved probabilities.

We want to demonstrate the inequality

$$\begin{aligned} & \langle R^\dagger(s=e^x, \Omega_i) R(r=e^x, \Omega_i) \rangle_{G=1} \\ & > Z_0 \sum_{R_1, R_2} e^{-2T\Delta_1} \frac{\langle R^\dagger(r=e^x, \Omega_i) R_1'(r'=0) R_2(r=0) \rangle \langle R_2^\dagger(s=0) R_1^\dagger(s'=0) R(s=e^x, \Omega_i) \rangle}{\langle R_1^\dagger R_1 \rangle \langle R_2^\dagger R_2 \rangle} \end{aligned} \quad (94)$$

We work out the first three-point function to get

$$\begin{aligned} & \langle R^\dagger(r=e^x, \Omega_i) R_1'(r'=0) R_2(r=0) \rangle \\ & = \lim_{r_0 \rightarrow \infty} \langle R^\dagger(r=e^x, \Omega_i) r_0^{2\Delta_1} R_1(r=r_0) R_2(r=0) \rangle \\ & = (4\pi^2)^{-\Delta_1-\Delta_2} e^{-2x\Delta_2} g(R_1, R_2; R) f_R \end{aligned} \quad (95)$$

Similarly for the second correlator we get

$$\langle R_2^\dagger(s=0) R_1^\dagger(s'=0) R(s=e^x, \Omega_i) \rangle = (4\pi^2)^{-\Delta_1-\Delta_2} e^{-2x\Delta_2} g(R_1, R_2; R) f_R \quad (96)$$

Hence the right-hand side of the inequality (94) becomes

$$\sum_{R_1, R_2} (4\pi^2)^{-\Delta_1-\Delta_2} \frac{g(R_1, R_2; R)^2 f_R^2}{f_{R_1} f_{R_2}} e^{-2T\Delta_1} e^{-4x\Delta_2} \quad (97)$$

Because of charge conservation, the only terms contributing to the RHS are those for which $\Delta_1 + \Delta_2 = \Delta_R$, where Δ_R is the conformal dimension of the Schur operator R .

5.6 The correlator on $S^3 \times S^1$

Let the metric on $S^3 \times S^1$ be given by

$$ds^2 = d\tau^2 + d\chi^2 + \sin^2 \chi (d\theta^2 + \sin^2 \theta d\phi^2) \quad (98)$$

where $\tau \in [0, 2T]$, $\chi, \theta \in [0, \pi]$ and $\phi \in [0, 2\pi]$.

If the differential operator K admits a complete set of eigenvectors $\Psi_n(x)$ with $K\Psi_n = \lambda_n\Psi_n$, then the corresponding Green's function is given by

$$G(x, y) = \sum_{n|\lambda_n \neq 0} \frac{\Psi_n^*(x)\Psi_n(y)}{\lambda_n} \quad (99)$$

and it satisfies

$$\begin{aligned} KG(x, y) &= \sum_{n|\lambda_n \neq 0} \Psi_n^*(x)\Psi_n(y) \\ &= \delta(x - y) - \sum_{n|\lambda_n = 0} \Psi_n^*(x)\Psi_n(y) \end{aligned} \quad (100)$$

For a conformally coupled scalar field in four dimensions, the differential operator K is given by

$$K = \Delta - \frac{1}{6}R \quad (101)$$

where Δ is the Euclidean Laplacian and the second term is the coupling to the 4-dimensional curvature [46]. It is like a mass term and has the same sign as a positive mass term in a Euclidean theory. For $S^1 \times S^3$ with unit radii, only the curvature of S^3 contributes, giving for the Ricci scalar curvature $R = 6$. Thus $K = \Delta - 1$.

On S^3 the spherical harmonics are given by [46]

$$\mathcal{Y}_{\mathbf{k}}(\Omega_i) = \Pi_{kJ}(\chi)Y_J^M(\theta, \phi) \quad (102)$$

where $\mathbf{k} = (k, J, M)$, Y_J^M are spherical harmonics on S^2 and Π_{kJ} is given by

$$\Pi_{kJ} = \left[\frac{1}{2}\pi k^2(k^2 - 1) \cdots (k^2 - J^2) \right]^{-1/2} \sin^J \chi \left(\frac{d}{d \cos \chi} \right)^{1+J} \cos k\chi \quad (103)$$

The quantum numbers k , J and M lie in the following ranges

$$\begin{aligned} k &= 1, 2, \dots, \\ J &= 0, 1, \dots, k - 1 \\ M &= -J, -J + 1, \dots, J \end{aligned} \quad (104)$$

The harmonics $\mathcal{Y}_{\mathbf{k}}(\Omega_i)$ satisfy

$$\Delta_{S^3} \mathcal{Y}_{\mathbf{k}}(\Omega_i) = -(k^2 - 1)\mathcal{Y}_{\mathbf{k}}(\Omega_i) \quad (105)$$

and they are orthonormal. Spherical harmonics on S^1 are given by

$$h_m(\tau) = \mathcal{N} e^{im\pi\tau/T} \quad (106)$$

where $\mathcal{N} = (2T)^{-\frac{1}{2}}$ is the normalization factor. They satisfy

$$\Delta_{S^1} h_m = -\left(\frac{m\pi}{T} \right)^2 h_m \quad (107)$$

Thus if

$$\Psi_n = h_m(\tau) \mathcal{Y}_{\mathbf{k}}(\Omega_i) \quad (108)$$

where $n = (m, \mathbf{k})$, then

$$\Delta_{S^3 \times S^1} \Psi_n = (\Delta_{S^3} + \Delta_{S^1}) \Psi_n = \left[-(k^2 - 1) - \left(\frac{m\pi}{T} \right)^2 \right] \Psi_n \quad (109)$$

If we add the conformal coupling term as in (101), we get

$$K \Psi_n = (\Delta_{S^3 \times S^1} - 1) \Psi_n = \left[-k^2 - \left(\frac{m\pi}{T} \right)^2 \right] \Psi_n \quad (110)$$

This eigenvalue problem has no zero-mode solution. In accordance with the \mathbb{R}^4 correlator (82), we actually choose the Green's function to satisfy

$$KG(x, y) = -\delta^4(x - y) \quad (111)$$

so that we get a positive metric on the space of operators. So the desired Green's function is given by

$$\begin{aligned} G(x, y) &= - \sum_n \frac{\Psi_n(x)^* \Psi_n(y)}{\lambda_n} \\ &= \sum_{m, k, J, M} \frac{h_m(\tau)^* \mathcal{Y}_{\mathbf{k}}^*(\Omega_i) h_m(\tau') \mathcal{Y}_{\mathbf{k}}(\Omega'_i)}{k^2 + \left(\frac{m\pi}{T} \right)^2} \end{aligned} \quad (112)$$

where k, J and M are in the ranges set out in (104) and m is an integer.

We want to work out

$$\langle R^\dagger(s = e^x) R(r = e^x) \rangle_{G=1} \quad (113)$$

where the angular coordinates are fixed to coincide.

If we change coordinates to $s = e^{-\tau}$, $r = e^\tau$, we get

$$\begin{aligned} \langle \Phi^\dagger(s = e^x) \Phi(r = e^x) \rangle_{G=1} &= \frac{1}{rs} \langle \Phi^\dagger(\tau = -x) \Phi(\tau = x) \rangle_{G=1} \\ &= e^{-2x} \langle \Phi^\dagger(\tau = -x) \Phi(\tau = x) \rangle_{G=1} \end{aligned} \quad (114)$$

Now insert the Green's function (112) to get

$$Z_{G=1}^{-1} \langle \Phi^\dagger(\tau = -x) \Phi(\tau = x) \rangle_{G=1} = \sum_{m, k, J, M} \frac{h_m(0)^* \mathcal{Y}_{\mathbf{k}}^*(\Omega_i) h_m(2x) \mathcal{Y}_{\mathbf{k}}(\Omega_i)}{k^2 + \left(\frac{m\pi}{T} \right)^2} \quad (115)$$

where we put each S^3 spherical harmonic at the same point on the S^3 and $Z_{G=1}$ is the thermal partition function. A clever choice of the angular point simplifies the sum. Let that point be where $\chi = 0$ so that Π_{kJ} is zero for $J > 0$, since the term $\sin^J \chi$ at the front of the

expression is zero ($\cos k\chi$ is a polynomial in $\cos \chi$ so for $\chi = 0$ the derivatives of $\cos k\chi$ give a constant). Then the only terms that contribute are those with $J = M = 0$. We get

$$\begin{aligned}\Pi_{k0} &= \left[\frac{1}{2} \pi k^2 \right]^{-1/2} \frac{d}{d \cos \chi} \cos k\chi \Big|_{\chi=0} \\ &= 2^{1/2} \pi^{-1/2} k\end{aligned}\tag{116}$$

Then noting that $Y_0^0(\theta, \phi) = 2^{-1}(\pi)^{-1/2}$, we get

$$\begin{aligned}\Gamma(-x, x) &\equiv \frac{\langle \Phi^\dagger(\tau = -x) \Phi(\tau = x) \rangle_{G=1}}{Z_{G=1}} \\ &= \sum_{m \in \mathbb{Z}, k \geq 1} \frac{\mathcal{N}^2 e^{im2\pi x/T} 2^{-1} \pi^{-2} k^2}{k^2 + \left(\frac{m\pi}{T}\right)^2} \\ &= \frac{1}{4\pi^2 T} \sum_{m \in \mathbb{Z}, k \geq 1} \frac{k^2 e^{im2\pi x/T}}{k^2 + \left(\frac{m\pi}{T}\right)^2} \\ &= \frac{1}{4\pi^2 T} \left[2 \sum_{m>0, k \geq 1} \frac{k^2 \cos(m2\pi x/T)}{k^2 + \left(\frac{m\pi}{T}\right)^2} + \sum_{k \geq 1} \frac{k^2}{k^2} \right]\end{aligned}\tag{117}$$

where the second term in the last expression is the $m = 0$ term. When plotted the truncated sums converge everywhere, except when x is an integer multiple of T .

5.6.1 The Inequality

The computations above lead to the spacetime inequality

$$\begin{aligned}&e^{-2x(\Delta_1 + \Delta_2)} (\Gamma(-x, x))^{\Delta_1 + \Delta_2} f_R Z_{G=1} \\ &> Z_0 \left(\frac{1}{4\pi^2} \right)^{\Delta_1 + \Delta_2} \sum_{R_1, R_2} \frac{g(R_1, R_2; R)^2 f_R^2}{f_{R_1} f_{R_2}} e^{-2T\Delta_1} e^{-4x\Delta_2}\end{aligned}\tag{118}$$

or

$$\begin{aligned}&\left(\frac{1}{4\pi^2 T} \left[2 \sum_{m>0, k \geq 1} \frac{k^2 \cos(m2\pi x/T)}{k^2 + \left(\frac{m\pi}{T}\right)^2} + \sum_{k \geq 1} 1 \right] \right)^{\Delta_1 + \Delta_2} \\ &> \frac{Z_0}{Z_{G=1}} \left(\frac{1}{4\pi^2} \right)^{\Delta_1 + \Delta_2} \sum_{R_1, R_2} \frac{g(R_1, R_2; R)^2 f_R}{f_{R_1} f_{R_2}} e^{-2T\Delta_1 + 2x(\Delta_1 - \Delta_2)}\end{aligned}\tag{119}$$

After canceling the $4\pi^2$ constants, we obtain

$$\left(\frac{1}{T} \left[2 \sum_{m>0, k \geq 1} \frac{k^2 \cos(m2\pi x/T)}{k^2 + \left(\frac{m\pi}{T}\right)^2} + \sum_{k \geq 1} 1 \right] \right)^{\Delta_1 + \Delta_2} > \frac{Z_0}{Z_{G=1}} \sum_{R_1, R_2} \frac{g(R_1, R_2; R)^2 f_R}{f_{R_1} f_{R_2}} e^{-2T\Delta_1 + 2x(\Delta_1 - \Delta_2)}\tag{120}$$

This expression is very similar to the $S^1 \times S^1$ inequality. Note however that the LHS does not have the analog of the $(1/12)$ term of eq. (75), since the zero mode has been lifted by the conformal mass term.

As in the 2d case, in the large T limit, the factor $\frac{Z_0}{Z_{G=1}}$ tends to 1. For the case of the thermal partition function, we have $\frac{Z_0}{Z_{G=1}} < 1$ in general⁸. If we perform the gluing with periodic boundary conditions for the fermions this factor will be 1, also just like the 2d case. Hence we expect the stronger inequality

$$\left(\frac{1}{T} \left[2 \sum_{m>0, k \geq 1} \frac{k^2 \cos(m2\pi x/T)}{k^2 + \left(\frac{m\pi}{T}\right)^2} + \sum_{k \geq 1} 1 \right] \right)^{\Delta_1 + \Delta_2} > \sum_{R_1, R_2} \frac{g(R_1, R_2; R)^2 f_R}{f_{R_1} f_{R_2}} e^{-2T\Delta_1 + 2x(\Delta_1 - \Delta_2)} \quad (121)$$

to hold, although again our main interest in this paper is at large T .

For $\Delta_1 = \Delta_2 = \Delta$ the x dependence of the RHS vanishes, so it is sufficient to check the inequality at the minimum of the LHS. This minimum occurs at $x = \frac{1}{2}T$, i.e. where the points are at maximum separation on the S_1 . At this point, we have

$$\begin{aligned} \frac{1}{T} \left[2 \sum_{m>0, k \geq 1} \frac{k^2 \cos(m\pi)}{k^2 + \left(\frac{m\pi}{T}\right)^2} + \sum_{k \geq 1} 1 \right] &= \frac{1}{T} \left[2 \sum_{m>0, k \geq 1} \frac{k^2 (-1)^m}{k^2 + \left(\frac{m\pi}{T}\right)^2} + \sum_{k \geq 1} 1 \right] \\ &= \frac{1}{T} \sum_{k \geq 1} [(-1 + kT \operatorname{cosech}(kT)) + 1] \\ &= \sum_{k \geq 1} k \operatorname{cosech}(kT) \end{aligned} \quad (122)$$

The sum above is convergent. Thus the inequality becomes

$$\left(\sum_{k \geq 1} k \operatorname{cosech}(kT) \right)^{2\Delta} > \sum_{R_1, R_2} \frac{g(R_1, R_2; R)^2 f_R}{f_{R_1} f_{R_2}} e^{-2T\Delta} \quad (123)$$

For small T the inequality holds because the RHS is constant and the sum in the LHS blows up. For large T we can approximate the sum (122) by only taking the first term in the sum and noticing that in this limit

$$\operatorname{cosech}(T) \rightarrow 2e^{-T} \quad (124)$$

For $R = [N]$, $\Delta_1 = \Delta_2 = N/2$, $R_1, R_2 = [N/2]$, the RHS of (123) is given by

$$\begin{aligned} \frac{f_{[N]}}{f_{[N/2]}^2} e^{-TN} &= \frac{(2N-1)!(N-1)!}{((3N/2-1)!)^2} e^{-TN} \\ &\sim \frac{3}{\sqrt{8}} \left(\frac{32}{27} \right)^N e^{-TN} \end{aligned} \quad (125)$$

⁸For a comprehensive discussion of the thermal partition function of the $\mathcal{N} = 4$ Super Yang Mills theory on S^3 see [47]. For supersymmetric partition sums involving BPS states see [48].

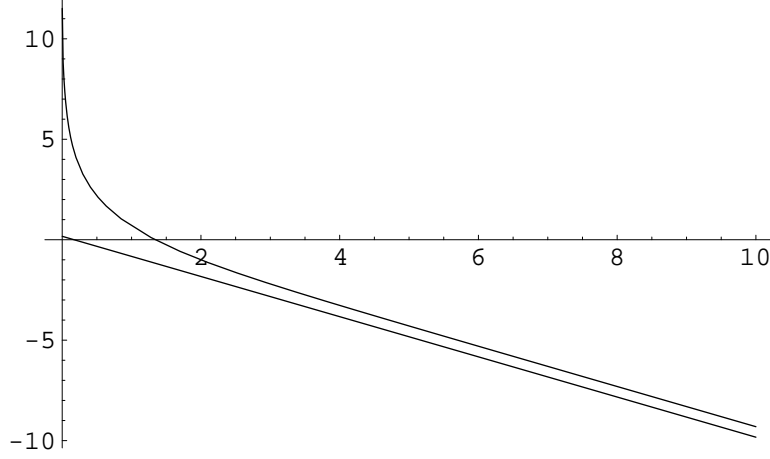


Figure 8: A plot of of the logarithms of the LHS of (123) (top) against the RHS of (123) (bottom) against T for our chosen representations. We have in fact taken the N th root of each side. We can ignore the $3/\sqrt{8}$ factor on the RHS because it adds a small constant to the lower graph which does not affect the inequality for any value of N .

For large T and our choice of R the inequality becomes

$$2^N e^{-NT} > \frac{3}{\sqrt{8}} \left(\frac{32}{27} \right)^N e^{-TN} \quad (126)$$

which is satisfied.

In Figure 8, the LHS of (123) is plotted against the RHS of (123), for our choice of Schur polynomials, as a function of T , to verify that the inequality holds for all T . For large T , as expected the graphs are separated by a constant value $\log(27/16)$.

5.7 Probability interpretation in the large T limit

We can now obtain a well-defined probability for a transition. We take the limit $T \rightarrow \infty$ and fix $x = \frac{1}{2}T$ so that the operators are as far apart from each other as they can be.

In this limit we find for general R , R_1 and R_2

$$\begin{aligned} P(R \rightarrow R_1, R_2) &= \frac{1}{(2e^{-T})^{\Delta_1 + \Delta_2}} \frac{g(R_1, R_2; R)^2 f_R}{f_{R_1} f_{R_2}} e^{-T(\Delta_1 + \Delta_2)} \\ &= \frac{1}{2^{\Delta_1 + \Delta_2}} \frac{g(R_1, R_2; R)^2 f_R}{f_{R_1} f_{R_2}} \end{aligned} \quad (127)$$

where we have used the approximation (124) for the large T limit of the genus-1 correlator. This probability is independent both of the spacetime positions of the operators and of T .

6 Results for probabilities

The calculations done here are given in the Appendix G.

6.1 $G = 0$ factorization

For the amplitude of several operators combining into a bigger operator we use genus zero factorization. The correlators are computed on \mathbb{R}^4 and the results for probabilities are invariant under the conformal transformation to S^4 . In a large distance limit, the resulting normalization prescription is equivalent to the overlap of states normalization we naïvely used before. These sphere factorization relations are equivalent to the factorization equations derived in [17]. The gluing procedure is as in section 5.3. For example, the probability for two “in” states to evolve to a single “out” state is given by

$$P(R_1(r = e^x, \Omega_i), R_2(r = e^y, \Omega_i) \rightarrow R(r = 0)) = \frac{\left| \langle R_1^\dagger(r = e^x, \Omega_i) R_2^\dagger(r = e^y, \Omega_i) R(r = 0) \rangle \right|^2}{\langle R_2^\dagger(s = e^y, \Omega_i) R_1^\dagger(s = e^x, \Omega_i) R_1(r = e^x, \Omega_i) R_2(r = e^y, \Omega_i) \rangle \langle R^\dagger R \rangle} \quad (128)$$

In our calculations we put R_1 and R_2 at the same position $x = y$ so that the normalization factor in the denominator is an extremal correlator. The results will then be valid beyond the zero coupling limit $g_{YM}^2 = 0$, where the actual computations are done. If we separate them in spacetime, then we have a non-extremal correlator in the denominator which can be computed at zero coupling, but which will receive non-trivial corrections at finite coupling. We further take the $x, y \rightarrow \infty$ limit. This maximizes the distance of the operators R_1 and R_2 from R and gives a probability independent of the spacetime positions of the operators.

For two giants combining into another giant we get

$$P(2 \text{ size } N/2 \text{ S giants} \rightarrow 1 \text{ size } N \text{ S giant}) = \frac{f_{[1^N]}}{\sum_S g([1^{N/2}], [1^{N/2}]; S)^2 f_S} < 1$$

$$P(2 \text{ size } N/2 \text{ AdS giants} \rightarrow 1 \text{ size } N \text{ AdS giant}) = \frac{f_{[N]}}{\sum_S g([N/2], [N/2]; S)^2 f_S} < 1 \quad (129)$$

For the transition of Kaluza Klein gravitons to a giant we get

$$P(N \text{ size } 1 \text{ KK gravitons} \rightarrow \text{one size } N \text{ S giant}) \sim \frac{1}{N^N}$$

$$P(N \text{ size } 1 \text{ KK gravitons} \rightarrow \text{one size } N \text{ AdS giant}) \sim \left(2^{2N-1} \frac{1}{\sqrt{\pi N}} \right) \frac{1}{N^N} \quad (130)$$

$$P(N/2 \text{ size } 2 \text{ KK gravitons} \rightarrow \text{one size } N \text{ S giant}) \sim \sqrt{\frac{2}{e}} \frac{1}{(eN)^{N/2}}$$

$$P(N/2 \text{ size } 2 \text{ KK gravitons} \rightarrow \text{one size } N \text{ AdS giant}) \sim \left(2^{2N-1} \frac{1}{\sqrt{\pi N}} \right) \sqrt{\frac{2}{e}} \frac{1}{(eN)^{N/2}} \quad (131)$$

We see that larger KK gravitons are more likely to evolve into a giant graviton than several smaller ones. It would be interesting to give a proof that this trend continues to hold when KK states of more general small angular momenta are considered. For the case of N/k

angular momenta equal to k , the obvious guess extrapolating the leading behavior of the above results is $N^{-N/k}$. The results of Appendix A.6 will be useful for the case where only angular momentum 1 and 2 are involved. More generally we will need to establish some general properties of the relevant symmetric group quantities. The information theoretic ideas on overlaps from [29] may be explored as a tool.

Strictly traces can only be interpreted as Kaluza-Klein states when the individual traces involved are small as above. It is of interest, nevertheless, to compute probabilities for extrapolated KK-states where large powers are involved. We find

$$P(1 \text{ size } N \text{ KK graviton} \rightarrow \text{one size } N \text{ S giant}) \sim \sqrt{\pi N} \frac{1}{2^{2N}}$$

$$P(1 \text{ size } N \text{ KK graviton} \rightarrow \text{one size } N \text{ AdS giant}) \sim \left(2^{2N-1} \frac{1}{\sqrt{\pi N}}\right) \sqrt{\pi N} \frac{1}{2^{2N}} = \frac{1}{2} \quad (132)$$

For transitions to outgoing KK gravitons we must use the basis dual to the trace basis. For the case of a single trace, and an initial giant, we find the same probability whether we have a sphere giant or an AdS giant

$$P(\text{one size } N \text{ giant} \rightarrow \text{one size } N \text{ KK graviton}) = \frac{1}{N} \quad (133)$$

These transitions do not decay exponentially as N becomes large. Note also the asymmetry between (133) and (132), which is another illustration of the probabilities on the choice of measurement.

6.2 $G = 1$ factorization

For the amplitude of 1 giant graviton into 2 smaller giants we must use genus-1 factorization. We take two 4-spheres, one with coordinates (r, Ω_i) , the other with (s, Ω'_i) , cut out two 4-balls at radii 1 and e^T from the origin in each, and glue the spheres together so that $rs = 1$ near the first gluing and $rs = e^{2T}$ near the second. Also introduce a primed coordinate r' on the first sphere with $rr' = 1$ and s' on the second with $ss' = 1$.

The probability is then given by

$$P(R(r = e^x, \Omega_i) \rightarrow R'_1(r' = 0)R_2(r = 0))$$

$$= Z_0 e^{-2T\Delta_1} \frac{|\langle R^\dagger(r = e^x, \Omega_i) R'_1(r' = 0) R_2(r = 0) \rangle|^2}{\langle R^\dagger(s = e^x, \Omega_i) R(r = e^x, \Omega_i) \rangle_{G=1} \langle R_1^\dagger R_1 \rangle \langle R_2^\dagger R_2 \rangle} \quad (134)$$

where $x \in [0, T]$ so that the operator is outside the cut-off area. We take the limit $T \rightarrow \infty$, where the factor $Z_0 e^{-2T\Delta_1}$ goes to 1 (see discussion in Section 5.6.1). In addition we fix $x = \frac{1}{2}T$ so that the operators are far apart from each other, maximizing the distance of the insertion of R from the two boundaries of the cut S^4 . This procedure will give a probability independent of the spacetime dependencies of the operators, as discussed in Section 5.7. In this limit we find

$$P(R \rightarrow R_1, R_2) = \frac{1}{2^{\Delta_1 + \Delta_2}} \frac{g(R_1, R_2; R)^2 f_R}{f_{R_1} f_{R_2}} \quad (135)$$

For the transition of a giant into two smaller giants

$$\begin{aligned}
P(1 \text{ size } N \text{ S giant} \rightarrow \text{two size } N/2 \text{ S giants}) &\sim \sqrt{\frac{\pi N}{2}} \left(\frac{1}{2}\right)^{2N} \\
P(1 \text{ size } N \text{ AdS giant} \rightarrow \text{two size } N/2 \text{ AdS giants}) &\sim \frac{3}{\sqrt{8}} \left(\frac{16}{27}\right)^N
\end{aligned} \tag{136}$$

These are well-normalized probabilities and demonstrate that (134) with a higher genus correlator in the denominator gives the proper implementation of the multi-particle normalization. In the old multi-particle normalization prescription, we got a divergent result for this transition of *AdS* giants

$$\frac{\left| \langle \chi_{[N]}(\Phi^\dagger) \chi_{[\frac{N}{2}]}(\Phi) \chi_{[\frac{N}{2}]}(\Phi) \rangle \right|^2}{\langle \chi_{[N]}(\Phi^\dagger) \chi_{[N]}(\Phi) \rangle \langle \chi_{[\frac{N}{2}]}(\Phi^\dagger) \chi_{[\frac{N}{2}]}(\Phi) \rangle \langle \chi_{[\frac{N}{2}]}(\Phi^\dagger) \chi_{[\frac{N}{2}]}(\Phi) \rangle} \sim \frac{3}{\sqrt{8}} \left(\frac{32}{27}\right)^N \tag{137}$$

The factor of 2^{-N} from equation (135) provides the correction to (137) to give the correctly normalized result (136).

We can also compute the transition of a giant to two Kaluza-Klein gravitons giving

$$\begin{aligned}
P(1 \text{ size } N \text{ S giant} \rightarrow \text{two size } N/2 \text{ KK gravitons}) &\sim \left(\frac{2}{N}\right)^2 \sqrt{\frac{\pi N}{2}} \left(\frac{1}{2}\right)^{2N} \\
P(1 \text{ size } N \text{ AdS giant} \rightarrow \text{two size } N/2 \text{ KK gravitons}) &\sim \left(\frac{2}{N}\right)^2 \frac{3}{\sqrt{8}} \left(\frac{16}{27}\right)^N
\end{aligned} \tag{138}$$

These are well-normalized probabilities. In the old multi-particle normalization scheme, we had a diverging result for this transition

$$\frac{\left| \langle \chi_{[N]}(\Phi^\dagger) \text{tr}(\Phi^{\frac{N}{2}}) \text{tr}(\Phi^{\frac{N}{2}}) \rangle \right|^2}{\langle \chi_{[N]}(\Phi^\dagger) \chi_{[N]}(\Phi) \rangle \langle \text{tr}(\Phi^{\frac{N}{2}}) \text{tr}(\Phi^{\frac{N}{2}}) \rangle \langle \text{tr}(\Phi^{\frac{N}{2}}) \text{tr}(\Phi^{\frac{N}{2}}) \rangle} \sim \frac{1}{6\sqrt{2}} \left(\frac{32}{27}\right)^N \tag{139}$$

An interesting question is whether a Schur polynomial operator can only evolve into other Schur polynomials. We might ask whether in the large T limit

$$\sum_{R_1, R_2} P(R \rightarrow R_1, R_2) \tag{140}$$

adds up to 1. We can calculate this sum when R is a sphere (or *AdS*) giant because, by the Littlewood Richardson rules, it can only split into other sphere (or *AdS*) giants. We find that this guess does not work

$$\sum_k P([1^N] \rightarrow [1^k], [1^{N-k}]) < 1 \tag{141}$$

which means that the infinite sums over additional outgoing states do contribute a finite amount.

6.3 Higher genus factorization

For higher genus $G = n - 1$ factorization, a natural guess for the analogous equation to (135) is

$$P(R \rightarrow R_1, R_2, \dots, R_n) = \frac{1}{k_n^{\Delta_1 + \Delta_2 + \dots + \Delta_n}} \frac{g(R_1, R_2, \dots, R_n; R)^2 f_R}{f_{R_1} f_{R_2} \dots f_{R_n}} \quad (142)$$

where k_n is a constant. We know $k_1 = 1$ and $k_2 = 2$. We assume that this equation holds in a long-distance limit, when the operators are in a symmetric configuration far apart from each other.

We can work out limits on k_n by considering the transition of an *AdS* giant into n smaller *AdS* giants

$$\begin{aligned} P([N] \rightarrow n \times [N/n]) &= \frac{1}{k_n^N} \frac{f_{[N]}}{f_{[N/n]}^n} \\ &\sim \frac{1}{\sqrt{2}} \left[\frac{(n+1)}{n} \right]^{\frac{n}{2}} \left[\frac{4n^{n+1}}{k_n(n+1)^{n+1}} \right]^N \end{aligned} \quad (143)$$

in the large N limit. Given that $4n^{n+1}(n+1)^{-n-1}$ tends up to $4/e$, $k_n > 4/e$ would certainly ensure that the probability is not larger than 1, although this condition is clearly too strong for $n = 1$. $k_n = n$ would satisfy this condition and works for $n = 1, 2$ but this is no more than a guess.

For the transition of an *AdS* giant of R -charge Δ_R to KK gravitons we find

$$P([\Delta_R] \rightarrow \text{tr}(\Phi^{\Delta_1}), \dots, \text{tr}(\Phi^{\Delta_n})) = \frac{1}{k_n^{\Delta_R}} \frac{1}{\Delta_1 \dots \Delta_n} \frac{f_{[\Delta_R]}}{f_{[\Delta_1]} \dots f_{[\Delta_n]}} \quad (144)$$

and for a sphere giant

$$P([1^{\Delta_R}] \rightarrow \text{tr}(\Phi^{\Delta_1}), \dots, \text{tr}(\Phi^{\Delta_n})) = \frac{1}{k_n^{\Delta_R}} \frac{1}{\Delta_1 \dots \Delta_n} \frac{f_{[1^{\Delta_R}]}}{f_{[1^{\Delta_1}]} \dots f_{[1^{\Delta_n}]}} \quad (145)$$

For genus $G = 2$ we have for the transition of an *AdS* giant into KK gravitons

$$\begin{aligned} P(1 \text{ size } N \text{ AdS giant} \rightarrow \text{three size } N/3 \text{ KK gravitons}) &= \sqrt{\frac{2}{3}} \frac{36}{N^3} \left(\frac{81}{64k_3} \right)^N \\ P(1 \text{ size } N \text{ AdS giant} \rightarrow \text{one size } N-2 \text{ and 2 size 1 KKs}) &= \frac{(2N-1)(2N-2)}{(N-2)N^2} \frac{1}{k_3^N} \end{aligned} \quad (146)$$

which makes it more likely for a giant to evolve into 3 medium-sized KK gravitons than into one large one and two tiny ones.

7 Bulk interpretation of the gluing properties of correlators

The factorization properties of the CFT correlators allow the construction of correlators on a 4-manifold of more complicated topology in terms of correlators on manifolds of simpler

topology. For example the theory on $S^3 \times S^1$ can be reconstructed by starting from correlators on S^4 . As we have emphasized above, these relations imply that to get properly normalized probabilities from correlators on S^4 (or the conformally equivalent \mathbb{R}^4) we need, in general, correlators on more complicated topologies.

In the CFT the correlators of local operators can be interpreted in terms of transition amplitudes between states. These states can be identified as wavefunctionals of the fields on S^3 boundaries of four dimensional balls, B^4 , cut out around the local operators. Hence the amplitudes are given by path integrals with boundary conditions on the CFT fields, specified at the S^3 boundaries. Using this CFT interpretation of correlators as transition amplitudes, and the bulk-boundary correspondence of AdS/CFT, it is natural to interpret the correlators as gravitational transition amplitudes, obtained by Euclidean bulk path integrals, subject to boundary conditions for bulk fields that are specified in the neighborhood of the local operator insertions in the boundary CFT. This is indeed compatible with perturbative computations [2, 3, 11, 12] for operators of small R -charge. The work of LLM [10] relating local operators to bulk geometries suggests that we can interpret correlators of operators with large R charge in terms of bulk transition amplitudes between geometries (LLM-like in the case of half-BPS operator insertions) defined in the neighborhood of the boundary insertions. Note that although the bulk path integral is over Euclidean metrics, the asymptotic geometries are AdS-like, and so they admit a Lorentzian continuation. For a recent discussion of Euclidean quantum gravity in an M-Theory context see [49]. The above bulk spacetime picture of correlators implies, for example, that a three point function of gauge theory operators can be viewed as a transition from a disjoint union of LLM geometries to a single LLM geometry. This is a topology changing process. We will note, in Section 7.3, that this holographic setup for topology change implies constraints on the interpolating topologies.

In this section we will investigate some of the implications of this picture. Some of our discussion will be in terms of the five-dimensional bulk, where the sphere part of $AdS_5 \times S^5$ is captured through dimensional reduction to gravitational fields on AdS_5 and higher KK modes coming from the five sphere.

One strength of the interpretation of correlators as transition amplitudes computed via bulk Euclidean path integrals is immediately apparent. Since the factorization properties of correlators on the CFT side follow from the path integral implementation of geometrical gluing relations, it is reasonable to expect that a simple bulk-gravitational explanation of these relations among correlators might follow from the postulate that the correlators can also be interpreted as gravitational transition amplitudes defined in terms of path integrals with asymptotic geometries (LLM-like geometries in the case of half-BPS operators of large R charge). Gluing on the CFT side is then lifted to gluing on the gravity side. In CFT, an important ingredient in relating path integral gluing to relations among correlators of operators is the correspondence between operators and states, viewed as wavefunctionals. Such a connection in gravity is not directly understood, but we will be lead to some discussion of it based on AdS/CFT considerations in Section 7.5.

In addition to SYM correlators on S^4 we will be interested in correlators on manifolds which can be obtained by simple cutting and pasting procedures of copies of S^4 . We can cut out the open four-ball neighborhoods B_\circ^4 of n points of S^4 and to get a manifold denoted by $S^4 \setminus \sqcup_{\alpha=1}^n (B_\circ^4)_\alpha$. This can also be written as $\overline{S^4 \setminus \sqcup_{\alpha=1}^n (B^4)_\alpha}$, indicating that we can remove

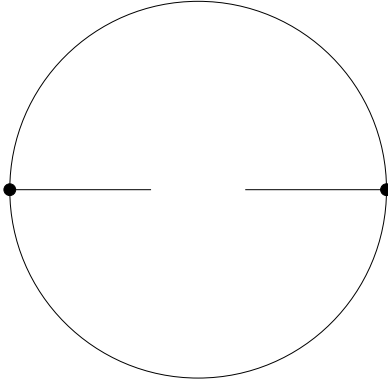


Figure 9: Disconnected graph G_1 in B^5 associated with two insertions on the boundary S^4

closed balls, and then take the closure⁹. Take two copies of $S^4 \setminus \sqcup_{\alpha=1}^n (B^4_{\circ})_{\alpha}$ and glue along the S^3 boundaries. The analogous construction in two dimensions gives the genus $n - 1$ surface. We will denote the corresponding manifold in 4D as $\Sigma_4(n - 1)$ and refer to it as having genus $n - 1$ by analogy to the 2D case. The subscript denotes the dimension, and the argument denotes the genus. These manifolds can also be obtained as the boundary in \mathbb{R}^5 of the neighborhood of a graph with $n - 1$ loops. In the following we will also find it useful to consider neighborhoods of graphs in B^5 , with endpoints of the graph lying on the S^4 boundary of the B^5 . These graphs, denoted as Witten graphs, appear in the perturbative computation of correlators in AdS. They will play a role in understanding how to lift gluings of $S^4 \setminus \sqcup_{\alpha=1}^n (B^4_{\circ})_{\alpha}$ to the bulk.

7.1 Bulk geometries for $S^3 \times S^1$ boundary from Witten graphs

Consider the case of $S^3 \times S^1$. Start from 2-point functions on S^4 . Cut out two disjoint copies of B^4_{\circ} around the insertion points, obtaining a manifold with topology $S^3 \times I$. Using the scaling symmetry on S^4 , we can obtain states at the boundaries of $S^3 \times I$. Two copies of $S^3 \times I$ can be glued to get $S^3 \times S^1$. The S^4 is the boundary of Euclidean AdS_5 , which has topology B^5 . We would like to understand how the gluing lifts to the bulk. It is well known that the supergravity partition function for the $S^3 \times S^1$ manifold receives contributions from two different bulk topologies, namely $B^4 \times S^1$ and $S^3 \times B^2$ [3][50]. Hence the procedure for lifting the gluings from boundary to bulk should account for both these possibilities. We will demonstrate that this is accomplished simply by using Witten graphs.

Given two points on S^4 bounding a B^5 , a very simple graph to consider is the disconnected one consisting of two lines, joining points in the bulk to the points on the boundary (see Figure 9). We will denote this disconnected graph G_1 . The neighborhood of each line is a B^4 fibered over an interval and collapsing to zero size at one end. This is homeomorphic to B^5 . Hence the neighborhood of the graph is a disjoint union of two small B^5 's. Now consider the original B^5 with this neighborhood removed, i.e the complement in B^5 of the neighborhood of the graph. Take the closure. Let us call this $\overline{B^5 \setminus N(G_1, B^5)}$ where $N(G_1, B^5)$ indicates a

⁹ B^k will denote closed balls and B^k_{\circ} open ones.

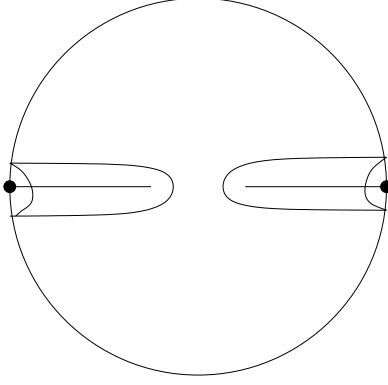


Figure 10: Neighborhood of the graph G_2

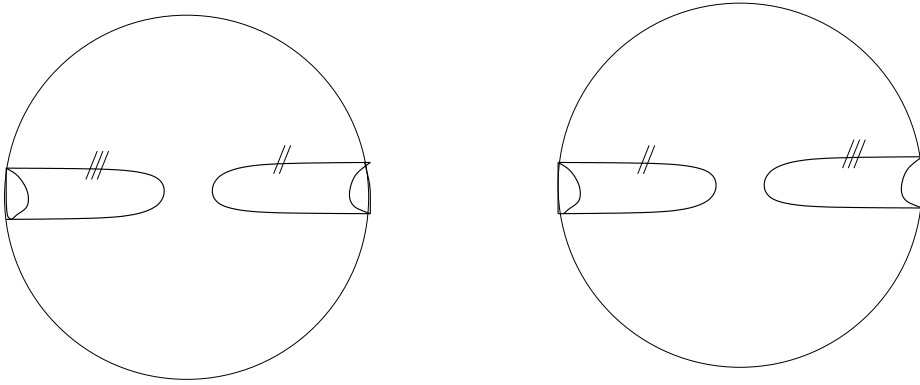


Figure 11: Gluing two copies of the B^5 with graph neighborhood removed

neighborhood¹⁰ in the B^5 of the graph fixed by a small number ϵ . The original S^4 boundary now has two B^4_\circ removed. It has two S^3 boundaries (see Figure 10), exactly the geometry we would consider purely from the point of view of CFT on S^4 . After excising these graph neighborhoods from B^5 (and taking the closure), the original S^4 boundary has become $S^3 \times I$. The remaining 5D manifold still has topology B^5 , and its S^4 boundary can be described as

$$B^4 \cup (S^3 \times I) \cup B^4$$

The two B^4 's are joined to $S^3 \times I$ at the two ends of I on S^3 's.

Take two copies of this $\overline{B^5 \setminus N(G_1, B^5)}$ which is topologically the same as $B^4 \times B^1 \cong B^5$, and do two gluings (see Figure 11). The outcome is $B^4 \times S^1$ with boundary $S^3 \times S^1$. Thus we have obtained one of the bulk geometries holographically dual to $S^3 \times S^1$ by lifting to the bulk the CFT gluing of two copies of $S^3 \times I$.

Now we want to understand, through the bulk lifting of boundary gluings, the bulk geometry $S^3 \times B^2$ which also has boundary $S^3 \times S^1$. Again we start with two points in the S^4 boundary of B^5 . Now draw the graph which joins the two points and extends through the

¹⁰More exactly we write $N(G, B^5) = \{x \in B^5 : \|G - x\| \leq \epsilon\}$ where we are using the metric inherited from the trivial embedding of B^5 in \mathbb{R}^5 . We do not use the metric of Euclidean AdS in this definition.

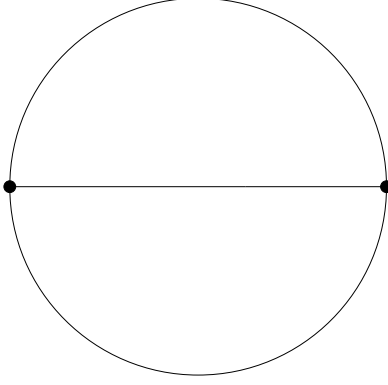


Figure 12: Connected graph G_2 in B^5 associated with two insertions on S^4

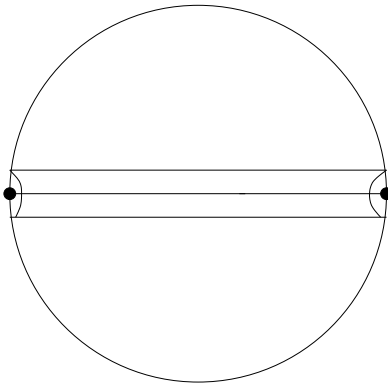


Figure 13: Neighborhood of the connected graph G_2 of topology $B^4 \times I$

bulk (see Figure 12). We will call this graph G_2 . The neighborhood of the graph is $B^4 \times I$. Excise this neighborhood from the B^5 . The manifold $\overline{B^5 \setminus N(G_2, B^5)}$ (see Figure 13), has topology $S^3 \times B^2$, which has boundary $S^3 \times S^1$. The S^1 consists of the interval I which bounds the excised region, joined to a semicircular interval on the original S^4 boundary. Now take two of these $\overline{B^5 \setminus N(G_2, B^5)}$. Glue along the interior $S^3 \times I$ as indicated in Figure 14. Since B^2 joined to another B^2 along an interval is B^2 , the outcome of this gluing of $S^3 \times B^2$ to $S^3 \times B^2$ along $S^3 \times I$ is $S^3 \times B^2$. This is the second topology with boundary $S^3 \times S^1$ which appears in [3].

7.1.1 Further topologies with $S^3 \times S^1$ boundary

If we use more complicated Witten graphs, with loops inside the bulk B^5 , we get more complicated bulk manifolds with boundary topology $S^3 \times S^1$. We do not know if they support metrics which are extrema of the supergravity action. But they will certainly contribute in the bulk path integral corresponding to the partition function on $S^3 \times S^1$. A natural question is whether, using the most general Witten graphs and the most general gluing maps, we can produce the most general bulk topology with the specified boundary topology.

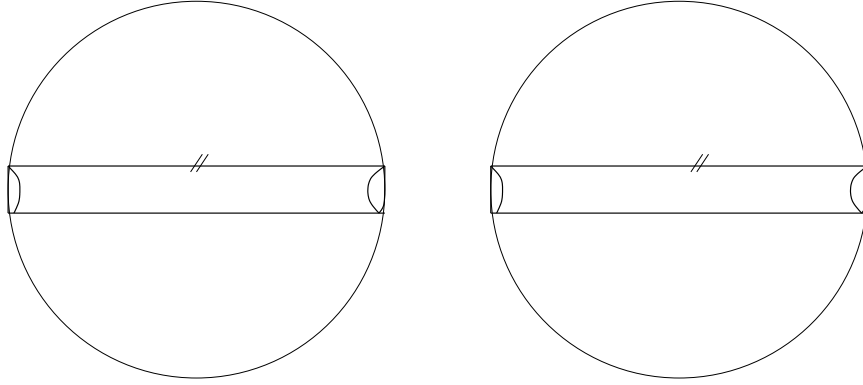


Figure 14: Gluing two copies of the B^5 with graph neighborhood removed

7.2 Gluing to higher genus 4-manifolds and corresponding bulk topologies

In this section we will show how to build bulk topologies corresponding to the higher genus four-manifolds $\Sigma_4(n-1)$. As mentioned earlier we can obtain $\Sigma_4(n-1)$ by starting with two copies of S^4 with n punctures, excising n copies of B^4_\circ around the punctures and gluing along the S^3 boundaries. Following the lead from the discussion of $\Sigma_4(1)$, we will consider tree-level Witten graphs with n boundary points. For our topological considerations, graphs related by merging two internal vertices by shrinking a connecting edge will be equivalent. Distinct graphs will correspond to different ways of separating the n points into subsets. This is the same as the number of ways of partitioning n , usually denoted by $p(n)$. All the points in one subset will be joined up by one vertex in the bulk. When all the n points are connected by one vertex, we have a connected graph V_n . When they are separated into different subsets, we have disconnected graphs. In the description of the bulk topologies corresponding to disconnected graphs, it will be useful to use the concept of handle attachment, which appears in the theory of handlebody decompositions [51]. We will start with a brief review of handlebody decompositions. For a physics discussion of these see [52, 53].

7.2.1 Handlebody decompositions

To give a handlebody decomposition of a manifold M , we start with a d -dimensional ball B^d (a 0-handle) and then add handles to it until we obtain a manifold homeomorphic to M . A k -handle is a manifold $B^k \times B^{d-k}$ which we glue onto M along the boundary $\partial B^k \times B^{d-k} = S^{k-1} \times B^{d-k}$.

For the different handles in three dimensions, $d = 3$, see Figure 15. A 0-handle B^3 is a filled ball. A 1-handle $B^1 \times B^2$ is a filled cylinder which we can bend to attach it to the manifold at the two ends of the cylinder ($S^0 \times B^2$, two disconnected filled circles). A 2-handle $B^2 \times B^1$ can be thought of as a thickened hemisphere (like a squash ball cut down the middle) which we glue along the base $S^1 \times B^1$. The B^1 interval provides the thickening. A 3-handle B^3 is a filled ball which we glue along its surface S^2 . In general handlebody decompositions are not unique.

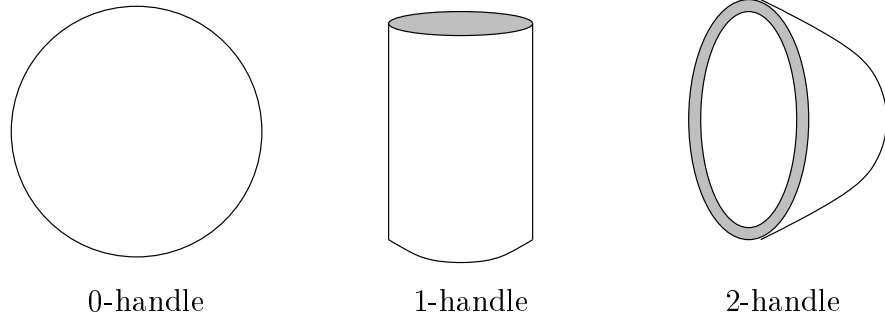


Figure 15: The different handles in 3 dimensions

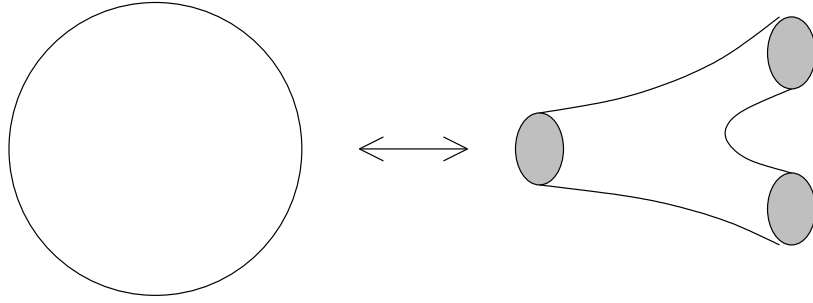


Figure 16: B^3 is homeomorphic to $N(V_3, B^3)$

7.2.2 Gluing for the complements of connected Witten graphs

Now we want to understand how to glue the five-manifolds related to connected Witten graphs. We have two copies of $\overline{B^5 \setminus N(V_n, B^5)}$. Each is obtained by removing from B^5 the neighborhood $N(V_n, B^5)$ of the Witten graph V_n , and taking the closure of the resulting manifold. This procedure restricts, on the boundary of the B^5 , to the excision of n copies of B^4_\circ around n points on the S^4 . It thus provides a bulk lifting of the usual CFT construction of removing open neighborhoods of operator insertions. The neighborhood $N(V_n, B^5)$ has topology B^5 and boundary S^4 . The interior boundary of this neighborhood will be defined as the intersection of the boundary of $N(V_n, B^5)$ with $\overline{B^5 \setminus N(V_n, B^5)}$. This interior boundary¹¹ will be denoted by $\partial^{(i)}N(V_n, B^5)$. For concreteness see the left picture in Figure 17 for $\overline{B^3 \setminus N(V_3, B^3)}$. It is clear that $\partial^{(i)}N(V_3, B^3)$ is the usual two dimensional pants diagram. We will be gluing two copies of $\overline{B^5 \setminus N(V_n, B^5)}$ along $\partial^{(i)}N(V_n, B^5)$.

The crucial observation is that $\overline{B^5 \setminus N(V_n, B^5)}$ is homeomorphic to the thickening, $\partial^{(i)}N(V_n, B^5) \times B^1$, of the internal surface $\partial^{(i)}N(V_n, B^5)$. We see this by first noting that B^5 is homeomorphic to $N(V_n, B^5)$ (see Figure 16 for the case $d = 3$, $n = 3$). Then if we remove $N(V_n, B^5)$ from the B^5 , and take the closure, we just get a thickening $\partial^{(i)}N(V_n, B^5) \times B^1$ of the internal surface (see Figure 17 for the case of $d = 3$, $n = 3$). Since $\overline{B^5 \setminus N(V_n, B^5)}$ is homeomorphic to $\partial^{(i)}N(V_n, B^5) \times B^1$, $\overline{B^5 \setminus N(V_n, B^5)}$ is homotopic to $\partial^{(i)}N(V_n, B^5)$ by the

¹¹More formally $\partial^{(i)}N(G, B^5) = \{x \in B^5 : \|G - x\| = \epsilon\}$. $\partial^{(i)}N(G, B^5)$ differs from $\partial N(G, B^5)$ because $\partial N(G, B^5)$ includes the four-balls around the insertion points of the Witten graphs.

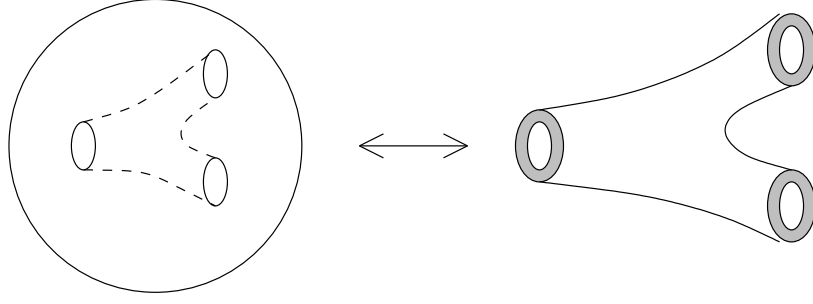


Figure 17: $\overline{B^3 \setminus N(V_3, B^3)}$ is homeomorphic to $\partial^{(i)}N(V_3, B^3) \times B^1$: thickened pants

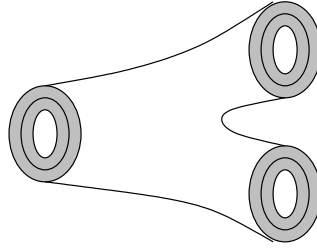


Figure 18: $\partial^{(i)}N(V_3, B^3) \times B^1$ glued to $\partial^{(i)}N(V_3, B^3) \times B^1$ along the internal surface

trivial homotopy retract that shrinks the B^1 to a point.

This means that we can ‘invert’ the second copy of $\overline{B^5 \setminus N(V_n, B^5)}$ and glue it inside the internal surface $\partial^{(i)}N(V_n, B^5)$ of the first copy of $\overline{B^5 \setminus N(V_n, B^5)}$ (see Figure 18 for $d = 3, n = 3$). To invert the second copy we take the manifold $\partial^{(i)}N(V_n, B^5) \times B^1$ and invert the direction of the B^1 coordinate.

The resulting manifold is the same as $\partial^{(i)}N(V_n, B^5) \times B^1$, but now double the thickness. Thus it has the same topology as the original manifold $\overline{B^5 \setminus N(V_n, B^5)}$. It is interesting to note that $\partial \overline{B^5 \setminus N(V_n, B^5)}$ is made of two copies of $S^4 \setminus \sqcup_{\alpha=1}^n B_{\circ}^4$ joined at the S^3 ’s, hence it is $\Sigma_4(n-1)$. This is consistent with the result that the gluing has not changed the topology of the bulk manifold or its boundary.

7.2.3 Gluing for the complements of disconnected graphs

Suppose a Witten graph G is composed of m disconnected components $G = V_{n_1} \sqcup V_{n_2} \sqcup \dots \sqcup V_{n_m}$ where \sqcup means disjoint union.

If we now glue $\overline{B^5 \setminus N(G, B^5)}$ to a copy of itself along the internal surface $\partial^{(i)}N(G, B^5)$ the resulting manifold is the same one $\overline{B^5 \setminus N(G, B^5)}$ with $(m-1)$ 1-handles attached.

We can see this if we deform $\overline{B^5 \setminus N(G, B^5)}$ into $\overline{B^5 \setminus N(V_{n_1}, B^5)}$, $\overline{B^5 \setminus N(V_{n_2}, B^5)}$, \dots and $\overline{B^5 \setminus N(V_{n_m}, B^5)}$ linked in a line by 1-handles (see Figure 19). Locally each $\overline{B^5 \setminus N(V_{n_i}, B^5)}$ glues to its copy as above for the connected Witten graphs. Now there are two 1-handles in each link between the connected parts, generating $(m-1)$ non-trivial 1-cycles. We can also obtain this manifold by starting with $\overline{B^5 \setminus N(G, B^5)}$ and attaching $(m-1)$ 1-handle loops.

The figure also makes it clear that the boundary of $\overline{B^5 \setminus N(G, B^5)}$ is a connected sum of

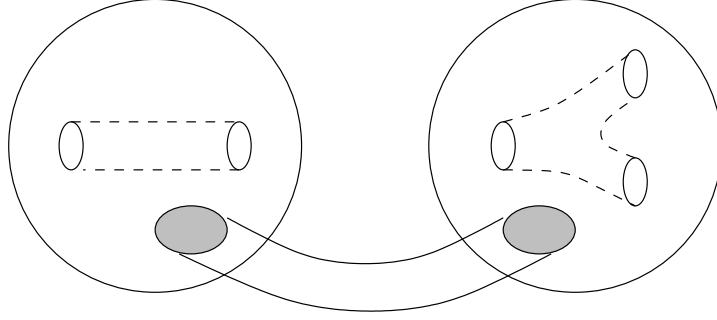


Figure 19: $\overline{B^3 \setminus N(V_3 \sqcup V_2, B^3)}$; a 1-handle links the connected parts

$\Sigma(n_1-1), \Sigma(n_2-1) \cdots \Sigma(n_m-1)$. This boundary is topologically $\Sigma(n-m)$ where $n = \sum_{i=1}^m n_i$. After the gluing we have $\overline{B^5 \setminus N(G, B^5)}$ with $(m-1)$ 1-handles attached. Each 1-handle increases the genus by one, so the glued manifold has boundary $\Sigma(n-1)$, as expected.

7.2.4 Homology groups

For the complement of the connected Witten graph, $\overline{B^5 \setminus N(V_n, B^5)}$, the homology groups, derived in Appendix Section H.3, are

- $H_0(\overline{B^5 \setminus N(V_n, B^5)}) = \mathbb{Z}$
- $H_1(\overline{B^5 \setminus N(V_n, B^5)}) = \{0\}$
- $H_2(\overline{B^5 \setminus N(V_n, B^5)}) = \{0\}$
- $H_3(\overline{B^5 \setminus N(V_n, B^5)}) = \mathbb{Z}^{n-1}$
- $H_4(\overline{B^5 \setminus N(V_n, B^5)}) = \{0\}$
- $H_5(\overline{B^5 \setminus N(V_n, B^5)}) = \{0\}$

The Euler character follows

$$\chi(\overline{B^5 \setminus N(V_n, B^5)}) = \sum_j (-1)^j b_j = 1 + (-1)^3(n-1) = 2 - n \quad (147)$$

For the homology of $\overline{B^5 \setminus N(V_{n_1} \sqcup V_{n_2} \sqcup \cdots \sqcup V_{n_m}, B^5)}$, the complement of a disconnected Witten graph, see Appendix Section H.4.

For the genus $n-1$ 4-manifold $\Sigma_4(n-1)$ the homology groups, derived in Appendix Section H.5, are

- $H_0(\Sigma_4(n-1)) = \mathbb{Z}$
- $H_1(\Sigma_4(n-1)) = \mathbb{Z}^{n-1}$
- $H_2(\Sigma_4(n-1)) = \{0\}$

- $H_3(\Sigma_4(n-1)) = \mathbb{Z}^{n-1}$
- $H_4(\Sigma_4(n-1)) = \mathbb{Z}$

For the case of a 2-dimensional boundary the same methods give the standard homology of a Riemann surface with genus $g = n - 1$

- $H_0(\Sigma_2(n-1)) = \mathbb{Z}$
- $H_1(\Sigma_2(n-1)) = \mathbb{Z}^{2(n-1)}$
- $H_2(\Sigma_2(n-1)) = \mathbb{Z}$

A simple check on these results is provided by the Mayer-Vietoris sequence, which relates homology groups associated with $X \cup Y$, $X \times Y$ and $X \cap Y$. In our case $X = \overline{B^5 \setminus N(V_n, B^5)}$. Y is $N(V_n, B^5)$, the closed neighborhood of the graph, which has the topology of a ball. $X \cup Y$ is B^5 . $X \cap Y$ is the interior part of the boundary of $N(V_n, B^5)$, called $\partial^{(i)}N(V_n, B^5)$. The Mayer-Vietoris sequence implies that

$$\chi(X) + \chi(Y) = \chi(X \cap Y) + \chi(X \cup Y) \quad (148)$$

In this case

$$\begin{aligned} \chi(Y) &= \chi(B^5) = 1 \\ \chi(X \cap Y) &= 2 - n \\ \chi(X \cup Y) &= \chi(B^5) = 1 \end{aligned} \quad (149)$$

Hence we deduce $\chi(X) = 2 - n$. In the above we have used the fact that the Euler character of $X \cap Y = \partial^{(i)}N(V_n, B^5)$ is $2 - n$. In the case of 3D bulk and 2D boundary this is the familiar Euler character of S^2 with n disks removed. In the case of 5D bulk and 3D boundary this is derived in the Appendices. One way is to use an explicit cell decomposition (see Appendix Section H.3). The other way is to use the fact that $S^4 \setminus \sqcup_\alpha (B^4_\circ)_\alpha$ is a quotient of $B^4 \setminus \sqcup_\alpha (B^4_\circ)_\alpha$, which retracts to an n -wedge of spheres (see Appendix Section H.1).

Note that we expected $\chi(\overline{B^5 \setminus N(V_n, B^5)}) = \chi(\partial^{(i)}N(V_n, B^5))$ since $\overline{B^5 \setminus N(V_n, B^5)}$ is homotopic to $\partial^{(i)}N(V_n, B^5)$ and the Euler characteristic is homotopy invariant.

Now we take the gluing of X with another copy of X along $\partial^{(i)}N(V_n, B^5)$. Let us call the resulting space Z . Then

$$\begin{aligned} X \cup X &= Z \\ X \cap X &= \partial^{(i)}N(V_n, B^5) \end{aligned} \quad (150)$$

Use 148 again to find

$$\chi(X) + \chi(X) = \chi(Z) + (2 - n) \quad (151)$$

which gives $\chi(Z) = 2 - n$. We have explained that $X \cong Z$ so we have here checked that $\chi(Z) = \chi(X)$, i.e. the Euler characters before and after gluing are the same.

7.3 Holographic topology change

A clear prescription for the computation of correlators in Euclidean AdS space is given in [3, 2] in the context of perturbation theory, using the correspondence between single trace CFT operators and Kaluza-Klein states in the bulk. As emphasized in [7] the perturbative set-up does not work for operators of large R charge. A clear extension of the perturbative prescription for the computation of Euclidean correlators is not available. The work of LLM suggests that for the Schur polynomial operators, in the regime of sufficiently large R charge, the right way to find the bulk computation of the correlators is to use the LLM geometries. For a Euclidean setting it is natural to do a Wick rotation of the LLM geometry and cutoff the region where the S^3 of AdS is larger than a fixed size.

For concreteness consider a three-point function. For each operator insertion we have a cut-off LLM-like geometry, which determines boundary conditions for the bulk path integral over metrics (and other fields). The three-point correlator can be viewed as a transition amplitude between a disconnected pair of LLM-like geometries and a single LLM-like geometry. This is reminiscent of cobordisms, where a manifold interpolates between several disconnected boundary components. These appear in formal discussions of 2D CFT and topological field theory [44]. In low dimensional Matrix models, this is discussed as macroscopic loop amplitudes [42]. A 2-dimensional example is the pants diagram which describes a transition from a disjoint union of two circles to a single circle (see Figure 20).

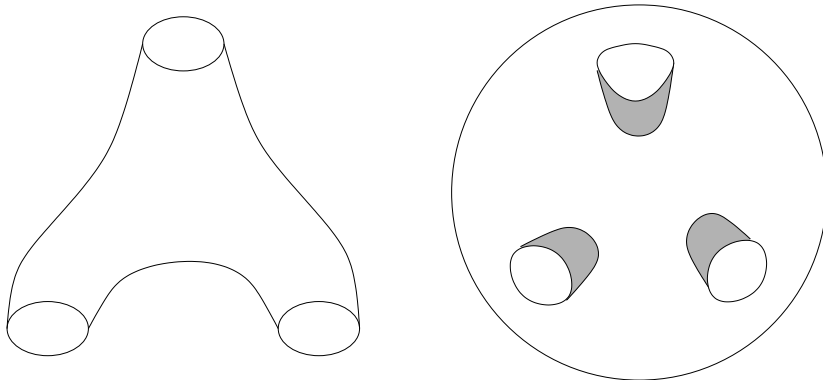


Figure 20: On the left is a cobordism between two S^1 's (or S^3 's) and one S^1 (or S^3); on the right is the analogous interpolation for the bulk

In the CFT we can think of our transition amplitudes in terms of cobordisms. For a three-point function for example, we take S^4 and cut out 3 balls around the operator insertions. We then map our operators to states in Hilbert spaces associated to the three S^3 boundaries. The S^4 with three balls removed is an interpolation (cobordism) between the disjoint union of two S^3 's and a single S^3 . The correlator is computed as a CFT path integral on this cobordism. To lift this picture to the bulk let us assume for simplicity that we can discuss this in the purely five dimensional perspective. We take our Euclidean AdS, which we think of as a 5-dimensional ball, and remove B^5 's at the boundary around the operator insertions (see Figure 20). We can then insert cut-off LLM-like geometries associated with the operators in the balls. We integrate over all metrics (and other fields)

in the remaining bulk. At the interface of the bulk with the LLM geometries (shaded gray in Figure 20) the boundary conditions are specified by the cut-off LLM. The bulk must also be asymptotically Euclidean AdS in the remaining boundary regions. We have a transition from a pair of disjoint geometries to a single one. This is not a cobordism because the initial and final conditions do not correspond to distinct boundaries of the bulk, but rather to different marked regions of the single boundary, with boundary conditions determined by LLM geometries.

It is worth emphasizing an important difference between this picture of topology change with the one natural from a traditional gravitational path integral perspective, which uses cobordisms and does not implement holography. From the traditional perspective, a five dimensional gravity theory would sum over all possible topologies consistent with the initial and final topologies living at 4D boundaries, using some appropriate weights [54, 52]. But from the holographic picture, we have 5D geometries which provide 4D boundary conditions on separate regions of the 4D boundary. The topology of the complete 4D boundary is fixed, since this is where the dual non-gravitational field theory lives. Fixing the boundary topology constrains the bulk topology. This is easiest to see in the even simpler case of 2D boundary theory and 3D bulk. There are many ways to interpolate between two copies of $B^2 \times I$ and a single copy, involving boundary topology of arbitrary genus (with three boundary circles). Figure 21 gives the genus zero and genus one cases. But the boundary CFT gives a well-defined amplitude for each fixed genus. The CFT does not give a prescription for summing over these different topologies. The story is the same in the case of 4D CFT/5D bulk. We are given, from super-Yang Mills theory, a three point function for a fixed boundary topology. We can construct bulk topologies interpolating between two balls $B^4 \times I$ and a single one by using neighborhoods of graphs with three vertices, with any number of loops (note that in previous discussions we considered graphs with no loops). SYM does not give a way of summing over these different 4D topologies. Hence holography acts as a constraint on interpolating topologies.

Given that the bulk-boundary correspondence in ADS/CFT [55] can be interpreted in terms of a Hartle-Hawking wavefunction [56], it is interesting to note that we here have a situation where different regions of the Hartle-Hawking boundary are associated with different geometries (LLM-like for the case of half-BPS operators). The search for a framework that can handle probabilities for multiple geometries (universes) appearing in a multiverse in the context of eternal inflation scenarios has been an active topic of discussion [57, 58, 59, 60]. It will be interesting to apply the lessons on the correct normalization of probabilities in quantum gravity, given by AdS/CFT, to the spacetimes of interest in eternal inflation. One qualitative lesson we may extract from sections 3-6 in this paper, is that properly normalized answers to questions regarding physics on one spacetime, require knowledge of correlators on more complicated topologies. A systematic framework for exploring the relevance of these ideas to eternal inflation could perhaps be found along the lines [61].

Finally we note that a different perspective on topology change in the context of LLM has been discussed in [62]. In the latter discussion, the topology changing process is described entirely in terms of the Fermi sea. In the present picture the fermions are only relevant as a description of the half BPS states in the asymptotic regions, while the bulk involves fluctuating geometries and in general goes beyond the half BPS sector.

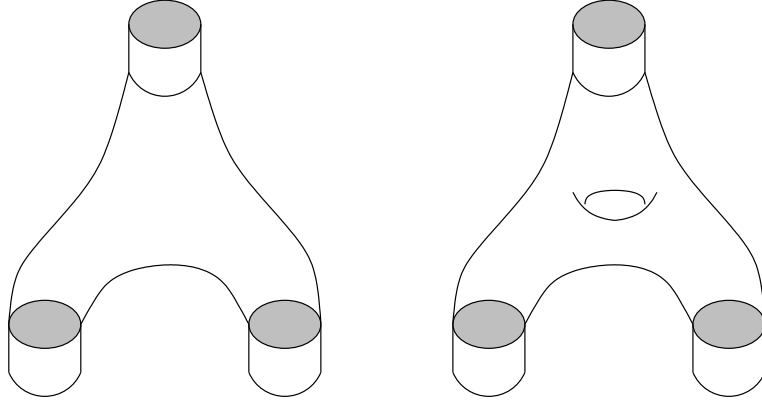


Figure 21: Two different interpolating bulk geometries

7.4 Towards holographic topological gravity theory

The observations in this section can be viewed as hints towards the definition of axioms for a holographic topological gravity theory. Such a theory in D dimensions is related to a conformal or topological field theory in $D - 1$ dimensions. The partition function of the holographic topological theory, obtained by a sum over topologies with fixed boundary, is equal to that of the boundary field theory. Operator insertions at a point in the $(D - 1)$ dimensional theory are associated to states in a Hilbert space, living on the $D - 2$ dimensional boundary of a neighborhood of the point. The usual gluing relations of the boundary theory are lifted to the bulk via the Witten graph construction we have described. The above remarks on holographic topology change should also have a natural role in an axiomatic holographic topological gravity theory.

7.5 Operator-Wavefunctional correspondence in quantum gravity

In Section 7.1 we posed a geometrical question on how to lift boundary gluings, associated to a choice of punctures for insertions of local CFT operators, to bulk gluings. The solution we described made use of Witten graphs which have the punctures as end-points and join them up through vertices in the bulk. The same gluing on the base space of the CFT was lifted to different gluings of the bulk manifolds, along the interior boundary of the neighborhoods of the Witten graphs. From the CFT perspective, geometrical gluing relations translate into relations between amplitudes, after we use the correspondence between local operators and wavefunctionals of fields on a sphere surrounding the local operator. Interpreting the bulk gluings in an analogous manner in terms of wavefunctionals of gravity (and other fields) in AdS , we are lead to conclude that the insertion of a physical observable (corresponding to a CFT operator) on the boundary of AdS leads to wavefunctionals on the interior boundaries of the neighborhoods of all the possible Witten graphs. This is to be contrasted with the much simpler operator-wavefunctional correspondence in CFT. Admittedly we have only given indirect evidence for this more complicated operator-wavefunctional correspondence in gravity, and it would be interesting to derive it more directly. It appears superficially to be a consequence of the greater non-locality we expect in a quantum theory of gravity

[63, 64]. A more direct derivation of this multiplicity of wavefunctionals related to a set of operator insertions on the boundary should also clarify the relation between the topological use of Witten graphs here and their perturbative use. The work of [65] has some of the elements needed to make this connection. In that work, Feynman integrals I_Γ are related to expectation values of observables (in a spin foam model), i.e $I_\Gamma = \langle 0|\mathcal{O}|0\rangle$. Since our gluing story suggests the consideration of wavefunctionals associated to Feynman graphs, it is natural to explore if they are related to states $\mathcal{O}|0\rangle$ appearing in [65]. It is an interesting future direction to explore the extension of this kind of connection between observables and wavefunctionals in quantum gravity to more general spacetimes.

8 Summary and Outlook

We started with a puzzle regarding the unexpected growth of normalized correlators of gauge theory operators on S^4 (or \mathbb{R}^4) corresponding to AdS giants. We have found a resolution of the paradox by observing that the proper normalization which leads to a probabilistic interpretation involves the division by correlators on 4-manifolds of more complicated topology, which we called higher genus manifolds by analogy to the two dimensional case. The appropriate behavior of the probabilities, that they are less than one and add up to one when all outcomes are taken into account, follows from factorization equations of 4D CFT which relate correlators on higher genus to those on lower genus. These points were illustrated in two dimensions before moving on to the 4D case.

These factorization properties follow by implementing geometrical gluing relations at the level of the path integral of the CFT. In AdS/CFT the CFT can be viewed as living on a 4D boundary of a 5D bulk, where the extra five dimensions are reduced away à la Kaluza Klein. As a first step towards a bulk understanding of these properties, we considered how to lift the gluings of the 4D boundaries to the 5D bulk. Witten graphs played a central role in this story.

There are several avenues for future research suggested by this work.

- We have observed a trend that products of traces are more likely to overlap with Schur operators $\chi_R(\Phi)$, if they involve traces of higher powers. It will be instructive to see how general this is. If these results are extended to the case of decay of brane-antibrane systems in AdS, they could be related to the fact that brane decay is more likely to produce longer strings.
- We have explored the idea that LLM geometries determine boundary conditions for the bulk path integrals. The results of section 7 can be viewed as indirect supporting evidence for such a point of view. A more direct approach is desirable. A satisfactory formulation should allow an extension of the Euclidean gravitational path integral prescription for computation of perturbative correlators of single trace operators to the case of operators of very large charge corresponding to Young diagrams (or fermion excitations).
- We have outlined some aspects of a holographic topological gravity theory in Section 7. It is an open problem to give complete definitions and exhibit non-trivial examples.

- While our discussion has focused on local operators, there is also a substantial literature on Wilson loops in $\mathcal{N} = 4$ SYM, including connections to free fermions, see for example [66, 67, 68]. We may expect that while summing over local operators leads to gluing along S^3 , summing over Wilson loops will be related to gluing along $S^1 \times S^2$. One does have to deal with the additional subtlety that, in the case of a general Wilson loop, conformal transformations (which were used in the operator-state map) will also transform the loop itself. We expect that many aspects of our discussion of the lifts from boundary gluings to bulk gluings will carry over. The topological role of neighborhoods of Witten graphs would now be extended to neighborhoods of worldsheets of strings, bounded by the Wilson loops, and extending into the bulk. It will be interesting to calculate normalized probabilities in the larger context involving both Wilson loops and local operators.
- The lessons we have learned on the correct normalization of probabilities should be applied more generally in quantum gravity, in particular to the problem of probabilities in the multiverse. We have made some preliminary remarks in this direction in Section 7.3.

Acknowledgements We thank Andreas Brandhuber, Nick Dorey, Patrick Dorey, Paul Heslop, Simon McNamara, Costis Papageorgakis, Andrew Sellers, Rodolfo Russo, Gabriele Travaglini and Jan Troost for discussions. SR is supported by a PPARC Advanced Fellowship and in part by the EC Marie Curie Research Training Network MRTN-CT-2004-512194.

A Appendix

A.1 Multiparticle-normalized transitions of S and AdS -giants

We want to work out the normalized correlators for transitions from AdS and S giant graviton states into multiple KK gravitons. We will use two normalizations: the multi-particle normalization and the overlap-of-states normalization.

For example the multi-particle-normalized S transition amplitude is given by

$$\frac{\langle \chi_{[1^L]}(\Phi^\dagger)(\text{tr}(\Phi^J))^{L/J} \rangle}{||\chi_{[1^L]}(\Phi)|| ||\text{tr}(\Phi^J)||^{L/J}} \quad (152)$$

and the overlap-of-states-normalized AdS transition is given by

$$\frac{\langle \chi_{[L]}(\Phi^\dagger)(\text{tr}(\Phi^J))^{L/J} \rangle}{||\chi_{[L]}(\Phi)|| ||\text{tr}(\Phi^J)||^{L/J}} \quad (153)$$

where we do not insist that $L \sim N$ so that we can be as general as possible.

The norms of the S and AdS giants are given respectively by

$$||\chi_{[1^L]}(\Phi)||^2 = f_{[1^L]} = \frac{N!}{(N-L)!} \quad (154)$$

$$||\chi_{[L]}(\Phi)||^2 = f_{[L]} = \frac{(N+L-1)!}{(N-1)!} \quad (155)$$

We can compute the norms involving traces in certain limits. These tractable cases are:

- $L \ll N$ and any $J \leq L$ for the overlap normalization;
- $J \ll N$ and any L for the multi-particle normalization;
- $J = 1, 2$ and any L for the overlap normalization (see Sections A.3 and A.4);
- $J = L, L/2$ for both normalizations (see Section A.5).

For $L \ll N$ for the overlap-of-states normalization and $J \ll N$ for the multi-particle normalization, we can use the result proved below that for large N and $JM \ll N$

$$||(\text{tr}(\Phi^J))^M||^2 = \langle (\text{tr}(\Phi^J))^M (\text{tr}(\Phi^{\dagger J}))^M \rangle \sim M! J^M N^{JM} \quad (156)$$

from which we see that the multi-particle normalization factor for $J \ll N$ is

$$||(\text{tr}(\Phi^J))||^{L/J} \sim J^{L/2J} N^{L/2} \quad (157)$$

If we fix L and vary J , then we find that $J^{L/2J} N^{L/2}$ increases to a peak of $e^{L/2e} N^{L/2}$ at $J = e$ and then decreases sharply approaching zero. The overlap-of-states normalization factor for $L \ll N$ is given by

$$||(\text{tr}(\Phi^J))^{L/J}|| \sim \sqrt{(L/J)!} J^{L/2J} N^{L/2} \quad (158)$$

which decreases even faster as a function of J . It still peaks around $J = 1, 2$. The fact that both of these normalizations are decreasing functions of J in these bounds means that giant gravitons are always more likely to undergo transitions into larger KK modes than smaller ones.

Now we can proceed

$$\begin{aligned}
\langle \chi_{[1^L]}(\Phi^\dagger)(\text{tr}(\Phi^J))^{L/J} \rangle &= \sum_{R_1 \dots R_{L/J}} g(R_1, \dots, R_{L/J}; [1^L]) \chi_{R_1}(J) \cdots \chi_{R_{L/J}}(J) f_{[1^L]} \\
&= (\chi_{[1^J]}(J))^{L/J} f_{[1^L]} \\
&= (-1)^{(J-1)L/J} \|\chi_{[1^L]}(\Phi)\|^2
\end{aligned} \tag{159}$$

We obtain the first line by writing each trace $\text{tr}(\Phi^J)$ as a sum of Schur polynomials¹² over representations of the symmetric group S_J . Each trace sum includes representations R_i corresponding to Young diagrams with J boxes only. $\chi_{R_i}(J)$ is the character of a cycle of length J , e.g. $(12 \dots J)$. In the second line we have noted that we can only build $[1^L]$ in tensor products of representations which are also single columns. Thus the LR coefficient $g(R_1, \dots, R_{L/J}; [1^L])$ is non-zero only when each $R_i = [1^J]$.

Similarly

$$\begin{aligned}
\langle \chi_{[L]}(\Phi^\dagger)(\text{tr}(\Phi^J))^{L/J} \rangle &= \sum_{R_1 \dots R_{L/J}} g(R_1, \dots, R_{L/J}; [L]) \chi_{R_1}(J) \cdots \chi_{R_{L/J}}(J) f_{[1^L]} \\
&= (\chi_{[J]}(J))^{L/J} f_{[1^L]} \\
&= \|\chi_{[L]}(\Phi)\|^2
\end{aligned} \tag{160}$$

The multi-particle-normalized S transition for $J \ll N$ is given by

$$\begin{aligned}
\frac{\langle \chi_{[1^L]}(\Phi^\dagger)(\text{tr}(\Phi^J))^{L/J} \rangle}{\|\chi_{[1^L]}(\Phi)\| \|\text{tr}(\Phi^J)\|^{L/J}} &= \frac{(-1)^{(J-1)L/J} \|\chi_{[1^L]}(\Phi)\|}{\|\text{tr}(\Phi^J)\|^{L/J}} \\
&\sim (-1)^{(J-1)L/J} J^{-L/2J} N^{-L/2} \sqrt{\frac{N!}{(N-L)!}}
\end{aligned} \tag{161}$$

and to get the overlap-normalized version for $L \ll N$ just divide by $\sqrt{(L/J)!}$.

For $L = N$ and $J \ll N$ we get for the multi-particle normalization

$$\begin{aligned}
\frac{\langle \chi_{[1^N]}(\Phi^\dagger)(\text{tr}(\Phi^J))^{N/J} \rangle}{\|\chi_{[1^N]}(\Phi)\| \|\text{tr}(\Phi^J)\|^{N/J}} &\sim (-1)^{(J-1)N/J} J^{-N/2J} N^{-N/2} N^{N/2} e^{-N/2} (2\pi N)^{\frac{1}{4}} \\
&= (-1)^{(J-1)N/J} (2\pi)^{\frac{1}{4}} e^{-N/2 + \frac{1}{4} \log(N) - (N/2J) \log(J)}
\end{aligned} \tag{162}$$

which is exponentially decreasing for all J .

The multi-particle-normalized AdS transition for $J \ll N$ is given by

$$\begin{aligned}
\frac{\langle \chi_{[L]}(\Phi^\dagger)(\text{tr}(\Phi^J))^{L/J} \rangle}{\|\chi_{[L]}(\Phi)\| \|\text{tr}(\Phi^J)\|^{L/J}} &= \frac{\|\chi_{[L]}(\Phi)\|}{\|\text{tr}(\Phi^J)\|^{L/J}} \\
&\sim J^{-L/2J} N^{-L/2} \sqrt{\frac{(N+L-1)!}{(N-1)!}}
\end{aligned} \tag{163}$$

¹²For details for this and other similar identities see Appendix J.

and to get the overlap-normalized version for $L \ll N$ just divide by $\sqrt{(L/J)!}$.

For $L = N$ and $J \ll N$ we get for the multi-particle normalization

$$\begin{aligned} \frac{\langle \chi_{[N]}(\Phi^\dagger)(\text{tr}(\Phi^J))^{N/J} \rangle}{\|\chi_{[N]}(\Phi)\| \|\text{tr}(\Phi^J)\|^{N/J}} &\sim J^{-N/2J} N^{-N/2} 2^N N^{N/2} e^{-N/2} 2^{\frac{1}{4}} \\ &= 2^{-\frac{1}{4}} e^{-N/2 + N \log(2) - (N/2J) \log(J)} \end{aligned} \quad (164)$$

The factor on the N in the exponential is $-1/2 + \log(2) - (1/2J) \log(J)$, which is positive for all J . Thus this exponentially increases for all J . This shows that the multi-particle normalization does not give well-defined probabilities.

A.2 Overlap normalizations : general formulas

Consider the correlator

$$\langle (\text{tr} \Phi^J)^M (\text{tr} \Phi^{\dagger J})^M \rangle \quad (165)$$

which appears in overlap normalizations. By using the diagrammatic method of [17] we can get

$$\langle (\text{tr} \Phi^J)^M (\text{tr} \Phi^{\dagger J})^M \rangle = J^M M! \sum_{\sigma_2 \in [J^M]} N^{C(\sigma_1 \sigma_2)} \quad (166)$$

where σ_1 is a fixed permutation in the symmetric group conjugacy class $[J^M] \subset S_{JM}$, characterized by M cycles of length J , and σ_2 runs over all the elements in this conjugacy class. $C(\sigma_1 \sigma_2)$ is the number of cycles in the permutation $\sigma_1 \sigma_2$. By converting to the Schur basis, we can also get the equivalent form

$$\langle (\text{tr} \Phi^J)^M (\text{tr} \Phi^{\dagger J})^M \rangle = \sum_R \chi_R(\sigma_1) \chi_R(\sigma_1) f_R \quad (167)$$

where σ_1 is again a fixed permutation in the conjugacy class $[J^M]$.

Getting explicit formulas for the sum in (166) requires additional work. For large N and $JM \ll N$ the leading terms will be

$$\langle (\text{tr} \Phi^J)^M (\text{tr} \Phi^{\dagger J})^M \rangle = J^M M! (N^{JM} + O(N^{JM-2})) \quad (168)$$

The first term comes from (166) when $\sigma_1 \sigma_2 = 1^{JM}$. There is no N^{JM-1} term because that would require $\sigma_1 \sigma_2 \in [1^{JM-2} 2]$, a permutation with odd sign. This is impossible because $\sigma_1 \sigma_2$ must have even sign since σ_1 and σ_2 are in the same conjugacy class. This is an important fact because if we now raise (168) to a multiple of N , as we do for the multi-particle normalization, we see that we only need the first term for the large N approximation.

For $J = 1, 2$ we can work out more explicit formulas for the sum in (166) (see Sections A.3 and A.4); also any J for $M = 1$ (see Section A.5).

A.3 Overlap normalization for $(\text{tr} \Phi)^M$

We know that

$$\langle (\text{tr} \Phi)^M (\text{tr} \Phi^\dagger)^M \rangle = M! N^M \quad (169)$$

For $M = N$ we find

$$\langle (\text{tr } \Phi)^N (\text{tr } \Phi^\dagger)^N \rangle \sim N^{2N} e^{-N} \sqrt{2\pi N} \quad (170)$$

which will make both the S and the AdS correlator very small indeed.

For the transition from L KK modes, of angular momentum 1 each, to an S -giant, we get

$$\frac{\langle \chi_{[1^L]}(\Phi) (\text{tr } \Phi^\dagger)^L \rangle}{\|(\text{tr } \Phi)^L\| \|\chi_{1^L}(\Phi)\|} = \sqrt{\frac{1}{N^L} \frac{N!}{L!(N-L)!}} \quad (171)$$

For $L = N$

$$\begin{aligned} \frac{\langle \chi_{[1^N]}(\Phi^\dagger) (\text{tr } \Phi)^N \rangle}{\|\chi_{[1^N]}(\Phi)\| \|(\text{tr } \Phi)^N\|} &= \frac{\|\chi_{[1^N]}(\Phi)\|}{\|(\text{tr } \Phi)^N\|} \\ &= \sqrt{\frac{N!}{N! N^N}} \\ &= N^{-N/2} \end{aligned} \quad (172)$$

For the transition from L KK modes of angular momentum 1 each to an AdS -giant, we get

$$\frac{\langle \chi_{[L]}(\Phi) (\text{tr } \Phi^\dagger)^L \rangle}{\|(\text{tr } \Phi)^L\| \|\chi_{[L]}(\Phi)\|} = \sqrt{\frac{(N+L-1)!}{(N-1)! L! N^L}} \quad (173)$$

When $L = N$

$$\begin{aligned} \frac{\langle \chi_{[N]}(\Phi^\dagger) (\text{tr } \Phi)^N \rangle}{\|\chi_{[N]}(\Phi)\| \|(\text{tr } \Phi)^N\|} &= \frac{\|\chi_{[N]}(\Phi)\|}{\|(\text{tr } \Phi)^N\|} \\ &= \sqrt{\frac{N(2N)!}{2N N!} \frac{1}{N! N^N}} \\ &\sim 2^{N-1/2} (\pi N)^{-1/4} N^{-N/2} \end{aligned} \quad (174)$$

which are both very small.

A.4 Overlap normalization for $(\text{tr } (\Phi^2))^M$

We can show (see below) that

$$\begin{aligned} \langle (\text{tr } \Phi^2)^M (\text{tr } \Phi^{\dagger 2})^M \rangle &= 2^{2M} M! \lambda(\lambda+1)(\lambda+2) \cdots (\lambda+M-1) \\ &= 2^{2M} M! \frac{(\lambda+M-1)!}{(\lambda-1)!} \end{aligned} \quad (175)$$

where $\lambda = N^2/2$. For $M = N/2$ we find that

$$\begin{aligned}
\langle (\text{tr } \Phi^2)^{N/2} (\text{tr } \Phi^{\dagger 2})^{N/2} \rangle &\sim 2^N (N/2)! \frac{(N^2/2 + N/2)!}{(N^2/2)!} \\
&\sim 2^N \sqrt{\pi N} e^{-N} (N/2)^{N/2} (N^2/2 + N/2)^{N^2/2 + N/2} (N^2/2)^{-N^2/2} \\
&= 2^N \sqrt{\pi N} e^{-N} (N/2)^{N/2} (N^2/2)^{N/2} (1 + 1/N)^{N^2/2 + N/2} \\
&= 2^N \sqrt{e\pi N} e^{-N/2} (N/2)^{N/2} (N^2/2)^{N/2} \\
&= \sqrt{e\pi N} e^{-N/2} N^{3N/2}
\end{aligned} \tag{176}$$

where we have used $(1 + 1/N)^N \sim e$ and $(1 + 1/N)^{N^2} \sim e^N$.

For the transition from N KK modes, with angular momentum 2 each, to an S-giant, we get

$$\frac{\langle \chi_{[1^N]}(\Phi^\dagger) (\text{tr } \Phi^2)^{N/2} \rangle}{\|\chi_{[1^N]}(\Phi)\| \|\text{tr } \Phi^2\|} \sim (2/e)^{1/4} N^{-N/4} e^{-N/4} \tag{177}$$

For the transition to the AdS giant we get

$$\frac{\langle \chi_{[N]}(\Phi^\dagger) (\text{tr } \Phi^2)^{N/2} \rangle}{\|\chi_{[N]}(\Phi)\| \|\text{tr } \Phi^2\|} \sim 2^{N-1/4} (e\pi)^{-1/4} N^{-N/4-1/4} e^{-N/4} \tag{178}$$

which are both very small, but larger than the $J = 1$ results.

A.4.1 Overlap normalization for $(\text{tr } \Phi^2)^M$ from Casimir diagrammatics

There is a nice formula, which can be derived using a diagrammatic method for the class-algebra of symmetric groups.

The coefficient of N^{2K} is obtained by summing over all possible ways of writing $K = \sum_{i=1} k_i$ where $k_1, k_2, k_3 \dots$ are non-negative integers which also obey $\sum_i i k_i = M$

$$\begin{aligned}
&\langle (\text{tr } \Phi^2)^M (\text{tr } (\Phi^\dagger)^2)^M \rangle \\
&= \sum_K M!^2 N^{2K} \sum_{\{k_i\}} \prod_i F_i
\end{aligned} \tag{179}$$

The F_i are given by

$$\begin{aligned}
F_i &= \frac{N_i^{k_i}}{k_i! (i!)^{2k_i}} \\
N_i &= (2i)((2i-2)!!)^2 = 2i(2i-2)^2(2i-4)^2 \dots 2^2 = (2i)^{-1} 2^{2i} (i!)^2
\end{aligned} \tag{180}$$

from which we have

$$F_i = \frac{2^{(2i-1)k_i}}{i^{k_i} k_i!} \tag{181}$$

A simple manipulation can be used to rewrite (179) as

$$\begin{aligned} & \langle (\text{tr } \Phi^2)^M (\text{tr } (\Phi^\dagger)^2)^M \rangle \\ &= 2^{2M} (M!)^2 \sum_K 2^{-K} N^{2K} \sum_{\{k_i\}} \prod_i \frac{1}{i^{k_i} k_i!} \end{aligned} \quad (182)$$

We can associate the set k_i with a conjugacy class in S_M , described by k_i cycles of length i , so that K is the total number of cycles. Rewriting (182) in terms of conjugacy classes $[S_M]$, and then as a sum over S_M , we get

$$\begin{aligned} \langle (\text{tr } \Phi^2)^M (\text{tr } (\Phi^\dagger)^2)^M \rangle &= 2^{2M} M! \sum_{[\sigma] \in [S_M]} \frac{M!}{|\text{Sym}([\sigma])|} \left(\frac{N^2}{2} \right)^{C([\sigma])} \\ &= 2^{2M} M! \sum_{[\sigma] \in [S_M]} |\sigma| \left(\frac{N^2}{2} \right)^{C([\sigma])} \\ &= 2^{2M} M! \sum_{\sigma \in S_M} \left(\frac{N^2}{2} \right)^{C(\sigma)} \end{aligned} \quad (183)$$

where $|\sigma|$ is the number of symmetric group elements in the conjugacy class $[\sigma]$. $C([\sigma])$ is the number of cycles in $[\sigma]$. $|\text{Sym}([\sigma])|$ is the size of the symmetry group of the permutation σ . The above happens to be the formula for the dimension of the totally symmetric representation $[M]$ of $U(N^2/2)$. If $\lambda = N^2/2$ then we get

$$\langle \text{tr } (\Phi^2)^M \text{tr } (\Phi^\dagger)^2)^M \rangle = 2^{2M} M! \lambda (\lambda + 1) (\lambda + 2) \cdots (\lambda + M - 1) \quad (184)$$

Proof : The derivation of (182) can be related to the class algebra multiplication of $[2^M].[2^M]$ in S_{2M} . A useful technique for the calculation is based on the realization of these operators in $V^{\otimes 2M}$ in terms of $U(N)$ Casimir operators. For example

$$T_{[2]} = \sum_{\sigma \in [2]} \sigma = \frac{1}{2} \sum_{a_1 \neq a_2} \rho_{a_1}(E_{i_1 i_2}) \rho_{a_2}(E_{i_2 i_1}) \equiv \frac{1}{2} E_{[2]} \quad (185)$$

where $E_{i_1 i_2}$ is the matrix with 1 in the (i_1, i_2) entry and zero elsewhere. The sum of elements in a conjugacy class can in general be related to such Casimirs (called cycle operators) by equations of the form

$$T_{\vec{l}} \equiv \frac{1}{|\text{Sym}([\vec{l}])|} E_{\vec{l}} \quad (186)$$

This is described in detail in [69, 70] and can be used to give a diagrammatic algorithm for computation of products in the class algebra of symmetric groups [71]. The $E_{l_1, l_2, \dots}$ operators are associated with circles having crosses marked on them, with the number of crosses being l_1, l_2, \dots . When we are multiplying two of these operators we sum over ways of joining the crosses from the two sets, with lines. These lines are then simplified with the move in Figure 22. This move is a diagrammatic representation of the effect of multiplying the $U(N)$ generators.

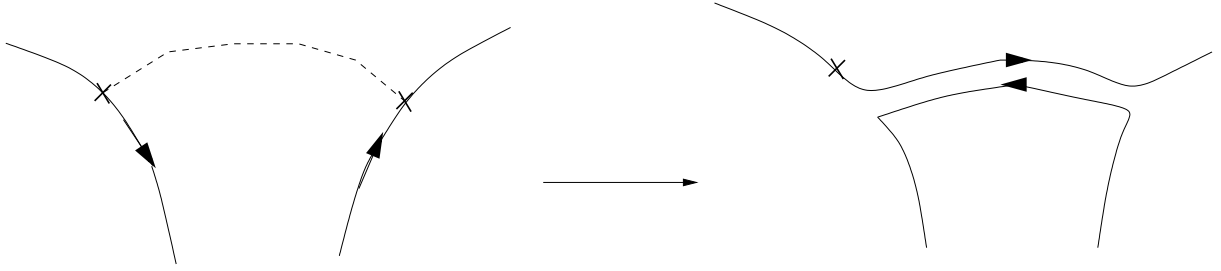


Figure 22: Merging two crosses

The $E_{[2^M]}$ operator can be represented diagrammatically by M oriented circles with two crosses each, which we will describe in words as M copies of C_2 . When multiplying, we can draw the circles from the first $E_{[2^M]}$ on the left and those from the second on the right. The multiplication involves a few basic products of the form

$$\begin{aligned}
 C_2.C_2 &\sim C_1.C_1 \\
 (C_2)^2.(C_2)^2 &\sim C_2.C_2 \\
 (C_2)^3.(C_2)^3 &\sim C_3.C_3 \\
 &\vdots
 \end{aligned} \tag{187}$$

In the first type of multiplication, there are lines joining crosses from one circle on the left and one on the right. In the second type of multiplication, there are lines joining crosses from two circles on the left and two circles on the right. These two types of multiplication are shown in Figure 23. Let k_1 be the number of $(C_1)^2$ coming from the multiplications of the first type. The k_2 is the number of $(C_2)^2$ coming from multiplications of the second type etc. The resulting diagram corresponds to the cycle operator $E_{1^{2k_1}, 2^{2k_2}, \dots}$, related to the conjugacy class $[1^{2k_1}, 2^{2k_2}, \dots]$, which is weighted, according to (166), by N^{2K} .

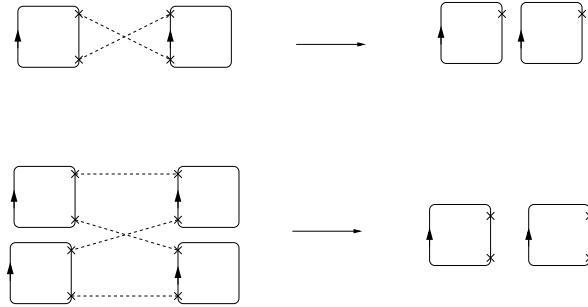


Figure 23: First two types of diagrams for multiplication $[2^M].[2^M]$

The T operators we are multiplying are related to E operators by the factor

$$c_1 = \left(\frac{1}{|\text{Sym}(T_{2^M})|} \right)^2 \tag{188}$$

To get a multiplication labeled by $k_1, k_2..$ we need to choose k_1 operators C_2 from the M in $E_{[2^M]}$, $2k_2$ operators C_2 from the M etc. This gives a factor

$$\frac{M!}{\prod_i (ik_i)!} \quad (189)$$

We square because the same factor occurs in each of the T_{2^M} we are multiplying, to get

$$c_2 = \left(\frac{M!}{\prod_i (ik_i)!} \right)^2 \quad (190)$$

Given the ik_i copies of C_2 we group them in k_i sets of i in the following number of ways

$$\prod_i \frac{(ik_i)!}{(i!)^{k_i} k_i!} \quad (191)$$

We again square since this arises from each factor in the product

$$c_3 = \prod_i \left(\frac{(ik_i)!}{(i!)^{k_i} k_i!} \right)^2 \quad (192)$$

There are $k_i!$ ways of connecting the k_i copies of circles with two crosses, from the two factors giving

$$c_4 = k_i! \quad (193)$$

Having fixed a set of i C_2 to be connected to another i C_2 there is a factor of

$$\begin{aligned} & (2i)(2i-2)^2(2i-4)^2 \dots 2^2 \\ &= (2i)((2i-2)!!)^2 \\ &= N_i \end{aligned} \quad (194)$$

Since this occurs k_i times we have

$$c_5 = N_i^{k_i} \quad (195)$$

The resulting $E_{[i^{2k_i}]}$ -operator must be converted to $T_{[i^{2k_i}]}$ by a factor

$$c_6 = |\text{Sym}([i^{2k_i}])| \quad (196)$$

Finally there is a factor of

$$c_7 = \frac{|\text{Sym}[2^M]|^2}{|\text{Sym}[i^{2k_i}]|} \quad (197)$$

which arises in converting the trace normalization problem to a class algebra problem .

Collecting the factors $c_1..c_7$ we get F_i given in (179).

A.4.2 The recursion method for $||(\text{tr}(\Phi^2))^M||$

A neat derivation of (169) and (175) can be obtained by recursion.

Let \mathcal{A}_M^1 be defined by

$$\mathcal{A}_M^1 \equiv \langle (\text{tr}(\Phi))^M (\text{tr}(\Phi^\dagger))^M \rangle \quad (198)$$

Now choose a single Φ and Wick contract it with a single Φ^\dagger (of which there are M choices). This Wick contraction gives us a factor of N and leaves us with $M-1$ uncontracted Φ s and $M-1$ uncontracted Φ^\dagger s. This gives us a recursion relation

$$\mathcal{A}_M^1 = MN \mathcal{A}_{M-1}^1 \quad (199)$$

Applying this M times and noting that $\mathcal{A}_0^1 = 1$ we get

$$\mathcal{A}_M^1 = M! N^M \quad (200)$$

as expected.

Let \mathcal{A}_M^2 be defined by

$$\mathcal{A}_M^2 \equiv \langle (\text{tr}(\Phi^2))^M (\text{tr}(\Phi^{\dagger 2}))^M \rangle \quad (201)$$

Now choose a $\text{tr}(\Phi^2)$ and Wick contract the two Φ s with two Φ^\dagger s. There are two different ways of doing this. The first way, on the left of Figure 24, is to contract them with a $\text{tr}(\Phi^{\dagger 2})$ giving a factor of N^2 . There are M $\text{tr}(\Phi^{\dagger 2})$ s and two ways of pairing up the Φ s and Φ^\dagger s. This leaves us with $M-1$ uncontracted $\text{tr}(\Phi^2)$ s and $M-1$ uncontracted $\text{tr}(\Phi^{\dagger 2})$ s. The

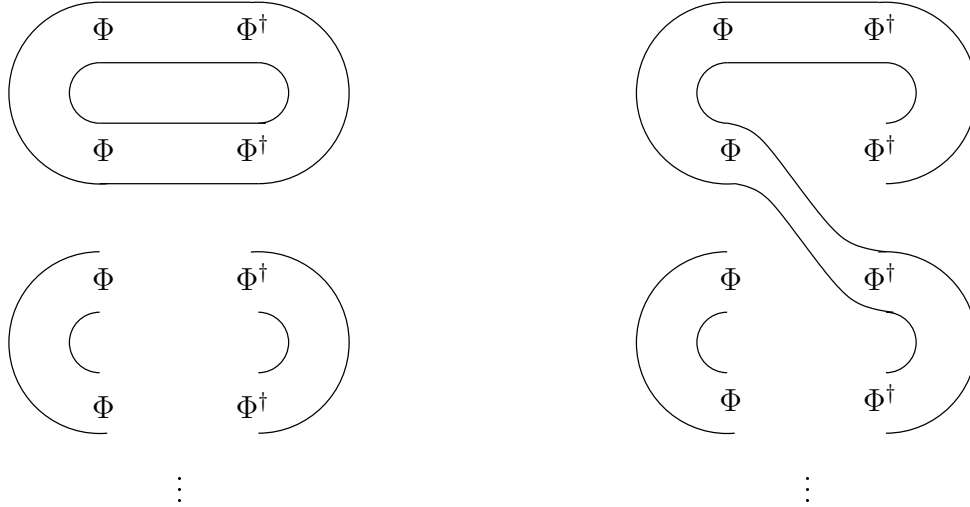


Figure 24: For \mathcal{A}_M^2 there are two different ways of contracting a $\text{tr}(\Phi^{\dagger 2})$ with two Φ^\dagger s.

other way, on the right of Figure 24, is to pair up the Φ s with Φ^\dagger s from different $\text{tr}(\Phi^{\dagger 2})$ s. There are $2M$ choices for the first Φ^\dagger and $2M-2$ for the second. Again this leaves us with $M-1$ uncontracted $\text{tr}(\Phi^2)$ s and $M-1$ uncontracted $\text{tr}(\Phi^{\dagger 2})$ s. Altogether we have

$$\begin{aligned} \mathcal{A}_M^2 &= 2M(N^2 + 2M - 2) \mathcal{A}_{M-1}^2 \\ &= 2^2 M(\lambda + M - 1) \mathcal{A}_{M-1}^2 \end{aligned} \quad (202)$$

where $\lambda = N^2/2$. This becomes

$$\mathcal{A}_M^2 = 2^{2M} M! \frac{(\lambda + M - 1)!}{(\lambda - 1)!} \quad (203)$$

as expected.

A.5 $J = L, L/2$ for both normalizations

We know from [17] that

$$\langle \text{tr}(\Phi^L) \text{tr}(\Phi^{\dagger L}) \rangle = \frac{1}{L+1} \left(\frac{(N+L)!}{(N-1)!} - \frac{N!}{(N-L-1)!} \right) \quad (204)$$

by considering the equation

$$\langle \text{tr}(\Phi^L) \text{tr}(\Phi^{\dagger L}) \rangle = \sum_R \chi_R(L) \chi_R(L) f_R \quad (205)$$

and noting that $\chi_R(L)$ is only non-zero for hooks.

If $L = N$ we find

$$\langle \text{tr}(\Phi^N) \text{tr}(\Phi^{\dagger N}) \rangle \sim \frac{(2N)!}{N!} \quad (206)$$

For the transition of a sphere giant we get

$$\begin{aligned} \frac{\langle \chi_{[1^N]}(\Phi^\dagger) (\text{tr}(\Phi^N)) \rangle^2}{\|\chi_{[1^N]}(\Phi)\|^2 \|\text{tr}(\Phi^N)\|^2} &\sim \frac{(N!)^2}{(2N)!} \\ &\sim (\pi N)^{\frac{1}{2}} 2^{-2N} \end{aligned} \quad (207)$$

which is very small. For the AdS transition we get

$$\begin{aligned} \frac{\langle \chi_{[N]}(\Phi^\dagger) (\text{tr}(\Phi^N)) \rangle^2}{\|\chi_{[N]}(\Phi)\|^2 \|\text{tr}(\Phi^N)\|^2} &\sim \frac{(2N-1)!}{(N-1)!} \frac{N!}{(2N)!} \\ &= \frac{1}{2} \end{aligned} \quad (208)$$

which is a large probability.

We can also write down a formula for $J = L/2$

$$\begin{aligned} \langle (\text{tr}(\Phi^{L/2}))^2 (\text{tr}(\Phi^{\dagger L/2}))^2 \rangle &= \sum_R \sum_{R_1, R_2, S_1, S_2} g(R_1, R_2; R) g(S_1, S_2; R) \\ &\quad \chi_{R_1}(L/2) \chi_{R_2}(L/2) \chi_{S_1}(L/2) \chi_{S_2}(L/2) f_R \end{aligned} \quad (209)$$

given that we know $\chi_{R_1}(L/2)$ will only be non-zero for hooks $\chi_{[(L/2-r), 1^r]}(L/2) = (-1)^r$. This gives us

$$\begin{aligned} \langle (\text{tr}(\Phi^{L/2}))^2 (\text{tr}(\Phi^{\dagger L/2}))^2 \rangle &= \sum_R \sum_{r_1, r_2, s_1, s_2} (-1)^{r_1+r_2+s_1+s_2} g([(L/2-r_1), 1^{r_1}], [(L/2-r_2), 1^{r_2}]; R) \\ &\quad g([(L/2-s_1), 1^{s_1}], [(L/2-s_2), 1^{s_2}]; R) f_R \end{aligned} \quad (210)$$

where r_i and s_i are integers characterizing the hooks.

Another approach to finding (209) is to use the Murnaghan-Nakayama rule on

$$\langle (\text{tr}(\Phi^{L/2}))^2 (\text{tr}(\Phi^{\dagger L/2}))^2 \rangle = \sum_R (\chi_R(L/2 \circ L/2))^2 f_R \quad (211)$$

A.6 General formula for $||(\text{tr} \Phi)^{M_1} (\text{tr} \Phi^2)^{M_2}||^2$

Using the diagrammatic method described in section A.4.1 we obtain a general formula

$$||(\text{tr} \Phi)^{M_1} (\text{tr} \Phi^2)^{M_2}||^2 = (M_2!)^2 (M_1!)^2 2^{2M_2} N^{M_1} \sum_{\{k_i, p_j, q_l^+, q_m^-\}} \frac{N^{2k} 2^{-k-2q}}{(M_1 - 2q - p)!} \prod_{i,j,l,m} \frac{1}{i^{k_i} k_i!} \frac{1}{p_j!} \frac{1}{q_l^+!} \frac{1}{q_m^-!} \quad (212)$$

where the sum is over the sets of non-negative integers $\{k_i, p_j, q_l^+, q_m^-\}$ satisfying

- $k \equiv \sum_i k_i$
- $p \equiv \sum_i p_i$
- $q \equiv \sum_i q_i^+ = \sum_i q_i^-$

All the sums above start at 1. The k_i count diagrams of the type encountered in section A.4.1. The p_i count diagrams with i 2-cross circles on each side. For example, p_2 counts diagrams of the type in Figure 25. q_i^+ counts diagrams with i 2-cross circles on the left and $(i-1)$ 2-cross circles on the right. The diagram in Figure 26 shows the types of diagrams counted by q_2^+ . q_i^- counts diagrams related to those counted by q_i^+ by a left-right reflection.

There are also constraints

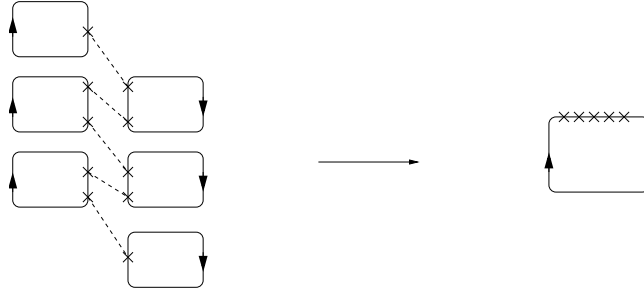


Figure 25: Diagram for p_2

- $2q + p \leq M_1$
- $M_2 = \sum_i i k_i + \sum_j j p_j + \sum_l l (q_l^+ + q_l^-) - q$

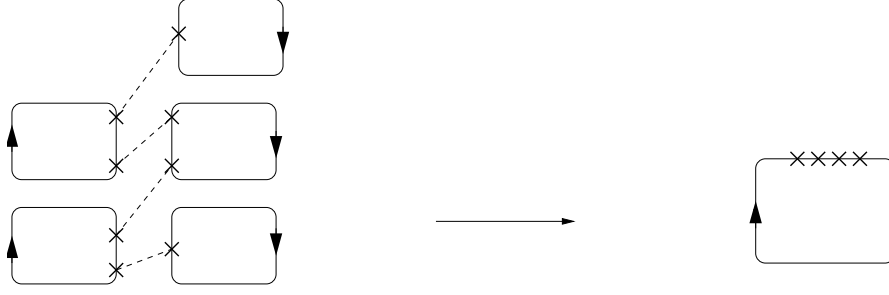


Figure 26: Diagram for q_2^+

We know that if $L_B \equiv \sum_i ik_i$ and $\lambda \equiv N^2/2$

$$\sum_{\{k_i\} | \sum_i ik_i = L_B} \lambda^k L_B! \prod_i \frac{1}{i^{k_i} k_i!} = \frac{(\lambda + L_B - 1)!}{(\lambda - 1)!} \quad (213)$$

so (212) becomes

$$\begin{aligned} & ||(\text{tr}(\Phi))^{M_1} (\text{tr}(\Phi^2))^{M_2} ||^2 = \\ & (M_2!)^2 (M_1!)^2 2^{2M_2} N^{M_1} \sum_{L_B, \{p_j, q_l^+, q_m^-\}} \frac{2^{-2q}}{(M_1 - 2q - p)! L_B!} \frac{(\lambda + L_B - 1)!}{(\lambda - 1)!} \prod_{j,l,m} \frac{1}{p_j!} \frac{1}{q_l^+!} \frac{1}{q_m^-!} \end{aligned} \quad (214)$$

where the sum is over the non-negative integer L_B and the sets of non-negative integers $\{p_j, q_l^+, q_m^-\}$ satisfying

- $p \equiv \sum_j p_j$
- $q \equiv \sum_l q_l^+ = \sum_m q_m^-$
- $2q + p \leq M_1$
- $M_2 = \sum_i ik_i + \sum_j jp_j + \sum_l l(q_l^+ + q_l^-) - q$

We can simplify this further. Let

$$\begin{aligned} Q^\pm &= \sum_i iq_i^\pm \\ P &= \sum_i ip_i \end{aligned}$$

By using the generating function $e^{\frac{y}{1-x}}$ we can show that the sum over p_i constrained by p, P is given by

$$\sum_{p_i} \frac{1}{\prod p_i!} = \frac{(P + p - 1)!}{p! P!} \equiv S(P, p) \quad (215)$$

The same sum appears for Q^\pm . Hence we can rewrite the norm as

$$\begin{aligned} ||(\text{tr}(\Phi))^{M_1}(\text{tr}(\Phi^2))^{M_2}||^2 &= (M_2!)^2 (M_1!)^2 2^{2M_2} N^{M_1} \\ &\sum_{L_B, Q^\pm, P, p, q} S(P, p) S(Q^+, q) S(Q^-, q) \frac{2^{-2q}}{(M_1 - 2q - p)! L_B!} \frac{(\lambda + L_B - 1)!}{(\lambda - 1)!} \end{aligned} \quad (216)$$

where $M_2 = L_B + P + Q^+ + Q^- - q$ and $2q + p \leq M_1$.

We have checked that the above formula specializes correctly to previously derived formulas in the cases $M_1 = 0$ (with M_2 arbitrary) and $M_2 = 0$ (with M_1 arbitrary). In the case $M_1 = 1$ with M_2 general it gives.

$$\begin{aligned} ||\text{tr}(\Phi)(\text{tr}(\Phi^2))^{M_2}||^2 &= (M_2!)^2 2^{2M_2} N \sum_{L_B \leq M_2} \frac{1}{L_B!} \frac{(\lambda + L_B - 1)!}{(\lambda - 1)!} \\ &= M_2! 2^{2M_2} N \frac{(\lambda + M_2)!}{\lambda!} \end{aligned} \quad (217)$$

The case $M_2 = 2$ can also be expanded.

A.7 More general results

Some relevant computations are in Appendix E of [17]. Using these techniques we get, for the overlap between an S-giant and multi-KK

$$\begin{aligned} &\langle \chi_{[1^L]}(\Phi^\dagger) \text{tr}(\Phi^{c_1}) \text{tr}(\Phi^{c_2}) \dots \text{tr}(\Phi^{c_k}) \rangle \\ &= \sum_{R_1, \dots, R_k} g(R_1, R_2, \dots, R_k; [1^L]) f_{[1^L]} \chi_{R_1}(c_1) \chi_{R_2}(c_2) \dots \chi_{R_k}(c_k) \\ &= (-1)^{c_1 + c_2 + \dots + c_k - k} \frac{N!}{(N - L)!} \\ &= (-1)^{L - k} \frac{N!}{(N - L)!} \end{aligned} \quad (218)$$

where $\sum_i c_i = L$ by charge conservation.

For single AdS giant, we have

$$\begin{aligned} &\langle \chi_{[L]}(\Phi^\dagger) \text{tr}(\Phi^{c_1}) \text{tr}(\Phi^{c_2}) \dots \text{tr}(\Phi^{c_k}) \rangle \\ &= \sum_{R_1, \dots, R_k} g(R_1, R_2, \dots, R_k; [L]) f_{[L]} \chi_{R_1}(c_1) \chi_{R_2}(c_2) \dots \chi_{R_k}(c_k) \\ &= f_L = \frac{(N + L - 1)!}{(N - 1)!} \end{aligned}$$

A special case of interest is

$$\langle \text{tr}(\Phi^L) \chi_R(\Phi^\dagger) \rangle \quad (219)$$

This is a character of the symmetric $\chi_R(\{L\})$, where $\{L\}$ is a permutation with a single cycle of length L . This character is non-zero only if R is a hook. Among the giants, this includes a single sphere giant or a single AdS giant, but not two AdS giants or two Sphere giants.

To compute the above in overlap normalization, we need to look at correlators of traces. Using the notation above it is relatively simple to prove a general formula for the products of traces

$$\langle \text{tr}(\Phi^{c_1}) \cdots \text{tr}(\Phi^{c_k}) \text{tr}(\Phi^{\dagger d_1}) \cdots \text{tr}(\Phi^{\dagger d_l}) \rangle \quad (220)$$

where $\sum_i c_i = \sum_j d_j = n$. If c_i is a cycle of length c_i , e.g. $(12 \dots c_i)$, then

$$\langle \text{tr}(\Phi^{c_1}) \cdots \text{tr}(\Phi^{c_k}) \text{tr}(\Phi^{\dagger d_1}) \cdots \text{tr}(\Phi^{\dagger d_l}) \rangle = \sum_R \chi_R(c_1 \cdots c_k) \chi_R(d_1 \cdots d_l) f_R \quad (221)$$

Now use the same trick on the $\text{Dim} R$ to get

$$\begin{aligned} & \langle \text{tr}(\Phi^{c_1}) \cdots \text{tr}(\Phi^{c_k}) \text{tr}(\Phi^{\dagger d_1}) \cdots \text{tr}(\Phi^{\dagger d_l}) \rangle \\ &= \frac{n!}{|[c_1 \cdots c_k]|} \sum_{\sigma \in [c_1 \cdots c_k]} N^{C((d_1 \cdots d_l)^{-1} \sigma)} \end{aligned} \quad (222)$$

It is fairly easy to show that

$$|[c_1 \cdots c_k]| = \frac{n!}{1^{l_1} l_1! 2^{l_2} l_2! \cdots m^{l_m} l_m!} \quad (223)$$

where l_1 of the cycles have length 1, l_2 of length 2, etc. How can we work this out? There are a total of $n!$ ways of slotting n things into n boxes. But some of these configurations will be the same. For example, if we mix up the l_j boxes of length j it won't make any difference, giving us a factor of $l_j!$. Also in each box we can cycle round the entries without changing it. This gives us j per l_j box.

If we plug this into (222) we get

$$\begin{aligned} & \langle \text{tr}(\Phi^{c_1}) \cdots \text{tr}(\Phi^{c_k}) \text{tr}(\Phi^{\dagger d_1}) \cdots \text{tr}(\Phi^{\dagger d_l}) \rangle \\ &= 1^{l_1} l_1! 2^{l_2} l_2! \cdots m^{l_m} l_m! \sum_{\sigma \in [c_1 \cdots c_k]} N^{C((d_1 \cdots d_l)^{-1} \sigma)} \end{aligned} \quad (224)$$

If $\{c_i\} = \{d_i\}$ (the order doesn't matter) then we can find the leading term

$$\begin{aligned} & \langle \text{tr}(\Phi^{c_1}) \cdots \text{tr}(\Phi^{c_k}) \text{tr}(\Phi^{\dagger c_1}) \cdots \text{tr}(\Phi^{\dagger c_k}) \rangle \\ &= 1^{l_1} l_1! 2^{l_2} l_2! \cdots m^{l_m} l_m! (N^n + O(N^{n-1})) \end{aligned} \quad (225)$$

B Conditional probabilities

Consider operators \mathcal{O}_i for $i = 1, 2, 3$ with zero charge. Given the starting state \mathcal{O}_1 the joint probability of getting \mathcal{O}_2 and \mathcal{O}_3 as the outgoing states is

$$P(\mathcal{O}_2, \mathcal{O}_3) = \frac{|\langle \mathcal{O}_1^\dagger \mathcal{O}_2 \mathcal{O}_3 \rangle|^2}{\langle \mathcal{O}_1^\dagger \mathcal{O}_1 \rangle_{G=1} \langle \mathcal{O}_2^\dagger \mathcal{O}_2 \rangle \langle \mathcal{O}_3^\dagger \mathcal{O}_3 \rangle} \quad (226)$$

The conditional probability of getting \mathcal{O}_2 given \mathcal{O}_3 is defined as

$$P(\mathcal{O}_2|\mathcal{O}_3) = \frac{P(\mathcal{O}_2, \mathcal{O}_3)}{P(\mathcal{O}_3)} \quad (227)$$

where the probability of getting \mathcal{O}_3 in the two outgoing states is given by

$$P(\mathcal{O}_3) = \sum_i P(\mathcal{O}_i, \mathcal{O}_3) = \sum_i \frac{|\langle \mathcal{O}_1^\dagger \mathcal{O}_i \mathcal{O}_3 \rangle|^2}{\langle \mathcal{O}_1^\dagger \mathcal{O}_1 \rangle_{G=1} \langle \mathcal{O}_i^\dagger \mathcal{O}_i \rangle \langle \mathcal{O}_3^\dagger \mathcal{O}_3 \rangle} \quad (228)$$

Similarly

$$P(\mathcal{O}_3|\mathcal{O}_2) = \frac{P(\mathcal{O}_2, \mathcal{O}_3)}{P(\mathcal{O}_2)} \quad (229)$$

From these it is clear that the Bayesian rule

$$\frac{P(\mathcal{O}_3|\mathcal{O}_2)}{P(\mathcal{O}_2|\mathcal{O}_3)} = \frac{P(\mathcal{O}_3)}{P(\mathcal{O}_2)} \quad (230)$$

is satisfied.

C The Metric, Euclidean time reversal and Orientation

Consider the effect of a change of coordinates $u = \bar{z}^{-1}$ on the operator $\partial_z Z(z)$. By the chain rule, we get

$$\partial_u Z(u) = -\bar{z}^2 \partial_{\bar{z}} Z(\bar{z}) \quad (231)$$

Note that the effect of this coordinate change is to reverse Euclidean time.

As in the general discussion of the Euclidean adjoint in [37] (see also section 3.1) we are supposed to follow the Euclidean time reversal with the usual operation of conjugation. In this case, where we are working with complex coordinates, we should also complex conjugate the coordinate. This leads to

$$-z^2 \partial_z Z^* \quad (232)$$

This is exactly what we need to get the desired metric. When Z is a matrix, the final complex conjugation on Z is accompanied by a matrix transposition.

Note that the $zw = 1$ relation we use in the gluing procedure is an orientation preserving map. In the 4d discussion, we use an orientation reversing map. The reason why both are acceptable ways of expressing the Hilbert space inner product is that the additional coordinate-conjugation of the 2d case is an orientation reversing map.

D Sphere Factorization

In this section, we will explicitly verify sphere factorization by gluing two S^2 correlators to give another S^2 correlator. This allows us to realize, in a very concrete way, CFT factorization. Denote the two Riemann spheres to be glued by M and N . M has puncture P located at $z_1 = 0$ with z_1 the local coordinate for a chart containing the puncture. N has puncture Q located at $z_2 = 0$ with z_2 the local coordinate for a chart containing the puncture. Choose an arbitrary constant $r > 1$. Assume z_1 and z_2 are well defined in the disks $|z_1| < r$ and $|z_2| < r$. The gluing then has two steps

- Cut the disks $|z_1| < \frac{1}{r}$ and $|z_2| < \frac{1}{r}$ from M and N .
- Sew M and N together by identifying points on the annulus $\frac{1}{r} < |z_1| < r$ that satisfy

$$z_1 z_2 = 1$$

To apply the CFT factorization equation, we need the inverse of the product on the space of local operators $\{\mathcal{A}_i(z, \bar{z})\}$

$$\mathcal{G}_{ij} = \langle i|j \rangle = \left\langle \mathcal{A}_i^\dagger(Q) \mathcal{A}_j(P) \right\rangle_{S^2}$$

which also gives the Hermitian inner product on the set of states, as described in section 4.2. Explicitly, we need to evaluate

$$\langle \partial^n Z(P) \partial^m Z^\dagger(Q) \rangle = \lim_{z_1, z_2 \rightarrow 0} \langle \partial^n Z(z_1) \partial^m Z^\dagger(z_2) \rangle$$

First, consider the case that $n \geq m$. We perform this calculation in the z_1 coordinate. $z_2 = 0$ corresponds to $z_1 = \infty$, so that the inner product that this correlator computes is the one discussed in section 3.4 of [36]. The simplest case is $m = n = 1$. Setting

$$z'_2 = \frac{1}{z_2}$$

we have the transformation

$$\partial Z^\dagger(z_2) \rightarrow -(z'_2)^2 \partial Z^\dagger(z'_2)$$

so that

$$\begin{aligned} \langle \partial Z(P) \partial Z^\dagger(Q) \rangle &= \lim_{z_1, z_2 \rightarrow 0} \langle \partial Z(z_1) \partial Z^\dagger(z_2) \rangle \\ &= - \lim_{z_1 \rightarrow 0} \lim_{z'_2 \rightarrow \infty} (z'_2)^2 \langle \partial Z(z_1) \partial Z^\dagger(z'_2) \rangle \\ &= \lim_{z_1 \rightarrow 0} \lim_{z'_2 \rightarrow \infty} (z'_2)^2 \frac{1}{|z_1 - z'_2|^2} \\ &= 1 \end{aligned} \tag{233}$$

Next, consider $n = 2$ and $m = 1$

$$\langle \partial^2 Z(P) \partial Z^\dagger(Q) \rangle = \lim_{z_1, z_2 \rightarrow 0} \langle \partial^2 Z(z_1) \partial Z^\dagger(z_2) \rangle$$

$$\begin{aligned}
&= - \lim_{z_1 \rightarrow 0} \lim_{z'_2 \rightarrow \infty} (z'_2)^2 \langle \partial^2 Z(z_1) \partial Z^\dagger(z'_2) \rangle \\
&= \lim_{z_1 \rightarrow 0} \lim_{z'_2 \rightarrow \infty} (z'_2)^2 \frac{1}{|z_1 - z'_2|^3} \\
&= 0
\end{aligned} \tag{234}$$

Now set $n = 2$ and $m = 2$. We have

$$\partial^2 Z^\dagger(z_2) \rightarrow \frac{\partial^2 z'_2}{\partial z_2^2} \partial Z^\dagger(z'_2) + \left(\frac{\partial z'_2}{\partial z_2} \right)^2 \partial^2 Z^\dagger(z'_2) = 2(z'_2)^3 \partial Z^\dagger(z'_2) + (z'_2)^4 \partial^2 Z^\dagger(z'_2)$$

so that

$$\begin{aligned}
\langle \partial^2 Z(P) \partial^2 Z^\dagger(Q) \rangle &= \lim_{z_1, z_2 \rightarrow 0} \langle \partial^2 Z(z) \partial^2 Z^\dagger(z_2) \rangle \\
&= \lim_{z_1 \rightarrow 0} \lim_{z'_2 \rightarrow \infty} [2(z'_2)^3 \langle \partial^2 Z(z_1) \partial Z^\dagger(z'_2) \rangle + (z'_2)^4 \langle \partial^2 Z(z_1) \partial^2 Z^\dagger(z'_2) \rangle] \\
&= 2
\end{aligned} \tag{235}$$

The general result is

$$\langle \partial^n Z(P) \partial^m Z^\dagger(Q) \rangle = m((m-1)!)^2 \delta_{m,n} \tag{236}$$

Consequently

$$[\langle \partial^n Z(P) \partial^m Z^\dagger(Q) \rangle]^{-1} = \frac{1}{m((m-1)!)^2} \delta_{m,n}$$

This result also follows from the state operator map: using

$$\begin{aligned}
\partial^k Z &\leftrightarrow -i(k-1)! \alpha_{-k} \\
\partial^k Z^\dagger &\leftrightarrow -i(k-1)! \alpha_{-k}^\dagger
\end{aligned}$$

our general result translates into the identity

$$\langle 0 | (i(p-1)! \alpha_p) (-i(k-1)! \alpha_{-k}^\dagger | 0 \rangle = k[(k-1)!]^2 \delta_{p,k} \tag{237}$$

We are now ready to explicitly verify the CFT factorization equation, which reads

$$\langle \partial Z(z_1) \partial Z^\dagger(w_1) \rangle = \sum_{m,n} \langle \partial Z(z_1) \partial^n Z^\dagger(P) \rangle [\langle \partial^n Z(P) \partial^m Z^\dagger(Q) \rangle]^{-1} \langle \partial^m Z(Q) \partial Z^\dagger(w_1) \rangle \tag{238}$$

Start with the RHS which gives

$$\begin{aligned}
&\sum_{m,n} \langle \partial Z(z_1) \partial^n Z^\dagger(P) \rangle [\langle \partial^n Z(P) \partial^m Z^\dagger(Q) \rangle]^{-1} \langle \partial^m Z(Q) \partial Z^\dagger(w_1) \rangle \\
&= \sum_m \langle \partial Z(z_1) \partial^m Z^\dagger(0) \rangle \frac{1}{m((m-1)!)^2} \langle \partial^m Z(0) \partial Z^\dagger(w_1) \rangle \\
&= \sum_m \frac{m!}{z_1^{m+1}} \frac{1}{m((m-1)!)^2} \frac{m!}{w_1^{m+1}} \\
&= \frac{1}{z_1 w_1} \sum_m \frac{m}{z_1^m w_1^m}
\end{aligned}$$

$$\begin{aligned}
&= -\frac{w_1}{z_1 w_1} \frac{\partial}{\partial w_1} \sum_m \frac{1}{z_1^m w_1^m} \\
&= -\frac{1}{(1 - z_1 w_1)^2}
\end{aligned} \tag{239}$$

Now, evaluating the LHS

$$\begin{aligned}
\langle \partial Z(z_1) \partial Z^\dagger(w_1) \rangle &= -\frac{(z')^2 \langle \partial Z(z_1) \partial Z^\dagger(z') \rangle}{(z')^2} \\
&= -\frac{1}{(z' - z_1)^2} \\
&= -\frac{1}{w_1^2 \left(\frac{1}{w_1} - z_1 \right)^2} \\
&= -\frac{1}{(1 - z_1 w_1)^2}
\end{aligned} \tag{240}$$

completing the demonstration.

E The Weierstrass elliptic function

E.1 Limits of the Weierstrass elliptic function

If $x \sim x + 2T_1 \sim x + 2iT_2$ where T_1 and T_2 are real then we can find some limits of the Weierstrass elliptic function.

If $T_2 \rightarrow \infty$ then we have

$$\wp(x) = \left(\frac{\pi}{2T_1} \right)^2 \left(\frac{1}{\sin^2(\pi x/2T_1)} - \frac{1}{3} \right) \tag{241}$$

which for $x = is$ gives

$$\wp(x) = \left(\frac{\pi}{2T_1} \right)^2 \left(-\frac{1}{\sinh^2(\pi s/2T_1)} - \frac{1}{3} \right) \tag{242}$$

If T_2 is now finite and $x = iT_2$ then we have

$$\wp(iT_2) = \frac{1}{(iT_2)^2} + \sum_{m,n \in \mathbb{Z} | (m,n) \neq (0,0)} \left\{ \frac{1}{(iT_2 + 2mT_1 + 2niT_2)^2} - \frac{1}{(2mT_1 + 2niT_2)^2} \right\} \tag{243}$$

Notice that the first term is the $(m,n) = (0,0)$ term of the first term in the sum. Then rewrite the sum for the second term in the sum

$$\sum_{m,n \in \mathbb{Z} | (m,n) \neq (0,0)} = \sum_{m,n \in \mathbb{Z} | n \neq 0} + \sum_{n=0, m \in \mathbb{Z} | m \neq 0} \tag{244}$$

so that we get

$$\begin{aligned}
\wp(iT_2) &= \sum_{m,n \in \mathbb{Z}} \frac{1}{(2mT_1 + (2n+1)iT_2)^2} - \sum_{m,n \in \mathbb{Z}|n \neq 0} \frac{1}{(2mT_1 + 2niT_2)^2} - \sum_{m \in \mathbb{Z}|m \neq 0} \frac{1}{(2mT_1)^2} \\
&= \sum_{m,n \in \mathbb{Z}|n \neq 0} \frac{1}{(2mT_1 + niT_2)^2} - 2 \sum_{m,n \in \mathbb{Z}|n \neq 0} \frac{1}{(2mT_1 + 2niT_2)^2} - \frac{\pi^2}{12T_1^2} \\
&= \left(\frac{\pi}{2T_1}\right)^2 \left(\sum_{n \in \mathbb{Z}|n \neq 0} \{-\operatorname{cosech}^2(n\pi T_2/2T_1) + 2\operatorname{cosech}^2(n\pi T_2/T_1)\} - \frac{1}{3} \right) \\
&= \left(\frac{\pi}{2T_1}\right)^2 \left(-4 \sum_{n>0} \{\coth(n\pi T_2/T_1)\operatorname{cosech}(n\pi T_2/T_1)\} - \frac{1}{3} \right) \tag{245}
\end{aligned}$$

which tends *up* to the correct limit (242) as $T_2 \rightarrow \infty$, i.e. $-\pi^2/(12T_1^2)$.

E.2 The method of images and the Weierstrass function

For a torus in x coordinates with $x \sim x+1 \sim x+\tau$ we might naïvely try to compute the correlator by the method of images (cf. [72] where they use this method for correlators on S^1). This would involve summing the correlators from x_1 to each of the images of x_2 on the entire x plane. If $x = x_1 - x_2$ we would have

$$Z_{T^2}^{-1} \langle \partial Z^\dagger(x_1) \partial Z(x_2) \rangle_{G=1, \tau} = -\frac{1}{x^2} - \sum_{m,n \in \mathbb{Z}|(m,n) \neq (0,0)} \frac{1}{(x+n+m\tau)^2} \tag{246}$$

Unfortunately this is divergent. In order to get a physical quantity we must regulate this sum by subtracting the divergent part to get the Weierstrass elliptic function

$$\begin{aligned}
Z_{T^2}^{-1} \langle \partial Z^\dagger(x_1) \partial Z(x_2) \rangle_{G=1, \tau} &= -\frac{1}{x^2} - \sum_{m,n \in \mathbb{Z}|(m,n) \neq (0,0)} \left\{ \frac{1}{(x+n+m\tau)^2} - \frac{1}{(n+m\tau)^2} \right\} \\
&\equiv -\wp(x; \tau). \tag{247}
\end{aligned}$$

In our conventions we have for a complex scalar field $Z(x, \bar{x})$

$$Z_{T^2}^{-1} \langle Z^\dagger(x_1, \bar{x}_1) Z(x_2, \bar{x}_2) \rangle_\tau = G(x_1, \bar{x}_1; x_2, \bar{x}_2) = -\ln \left| \theta_1 \left(x_1 - x_2 \middle| \tau \right) \right|^2 + \frac{2\pi}{\tau_2} [\operatorname{Im}(x_1 - x_2)]^2 \tag{248}$$

so that

$$\begin{aligned}
Z_{T^2}^{-1} \langle \partial_{x_1} Z^\dagger(x_1) \partial_{x_2} Z(x_2) \rangle_\tau &= -Z_{T^2}^{-1} \partial_{x_1}^2 \langle Z^\dagger(x_1) Z(x_2) \rangle_\tau \\
&= \partial_x^2 (\log \vartheta_{11}(x; \tau)) - \frac{2\pi}{\tau_2} \\
&= -\wp(x; \tau) \tag{249}
\end{aligned}$$

The divergences in the naïve method of images correlator (246) can be understood to arise because in the mode decomposition we have included the zero mode. Removing this zero mode is equivalent to the regulated correlator in (247).

F Windings from torus factorization sums

In what follows, we assume that the metric on the space of local operators has been diagonalized $\mathcal{G}_{ij} = \langle i|i\rangle\delta_{ij}$. According to factorization, the two point function of ∂Z on the torus is

$$\begin{aligned} \langle \partial Z^\dagger(p_1) \partial Z(p_2) \rangle_{T^2} &= (q\bar{q})^{-c/24} \sum_{ij} \sum_{kl} q^{h_j} \bar{q}^{\tilde{h}_j} \mathcal{G}^{ij} \mathcal{G}^{kl} \langle \partial Z^\dagger(p_1) \mathcal{A}'_j(z', \bar{z}' = 0) \mathcal{A}_l(z, \bar{z} = 0) \rangle_{S^2} \\ &\quad \times \langle \mathcal{A}_k^\dagger(w, \bar{w} = 0) \mathcal{A}_i^{\dagger'}(w', \bar{w}' = 0) \partial Z(p_2) \rangle_{S^2} \end{aligned} \quad (250)$$

To demonstrate how this sum gives the right correlation function on the torus, it is instructive to analyze a few terms explicitly.

For a correlation function to be non-zero in the free field theory, we need to consider the correlator of an even number of fields. One type of term which enters is when $\mathcal{A}'_j(z', \bar{z}' = 0) = \mathcal{A}_i^{\dagger'}(w', \bar{w}' = 0) = 1$ and $\mathcal{A}_l(z, \bar{z} = 0) = \partial^l Z(z, \bar{z} = 0)$, $\mathcal{A}_k^\dagger(w, \bar{w} = 0) = \partial^k Z^\dagger(w, \bar{w} = 0)$. Summing over operators of this type, we have (the double sum collapses since $\langle \partial^k Z^\dagger(w, \bar{w} = 0) \partial^l Z(z, \bar{z} = 0) \rangle_{S^2} \propto \delta^{lk}$)

$$(q\bar{q})^{-c/24} \sum_l \langle \partial Z^\dagger(p_1) \partial^l Z(z, \bar{z} = 0) \rangle_{S^2} \frac{1}{\langle l|l \rangle} \langle \partial^l Z^\dagger(w, \bar{w} = 0) \partial Z(p_2) \rangle_{S^2} \quad (251)$$

which, explicit evaluation shows, is the correlator to go from p_1 to p_2 passing through the point $z = \bar{z} = 0$. Another type of term which enters is when $\mathcal{A}_l(z, \bar{z} = 0) = \mathcal{A}_k^\dagger(w, \bar{w} = 0) = 1$ and $\mathcal{A}'_j(z', \bar{z}' = 0) = \partial^j Z'(z' = \bar{z}' = 0)$ and $\mathcal{A}_i^{\dagger'}(w', \bar{w}' = 0) = \partial^i Z'(w', \bar{w}' = 0)$. Summing over operators of this type, we have

$$(q\bar{q})^{-c/24} \sum_i q^{h_i} \bar{q}^{\tilde{h}_i} \langle \partial Z^\dagger(p_1) \partial^i Z'(z' = \bar{z}' = 0) \rangle \frac{1}{\langle i|i \rangle} \langle \partial^i Z'(w', \bar{w}' = 0) \partial Z(p_2) \rangle \quad (252)$$

which is the correlator to go from p_1 to p_2 passing through point $z' = \bar{z}' = 0$.

Next, consider the contribution when we sum over the terms $\mathcal{A}'_j(z', \bar{z}' = 0) = \partial^j Z'(z', \bar{z}' = 0)$, $\mathcal{A}_i^{\dagger'}(w', \bar{w}' = 0) = \partial^i Z'(w', \bar{w}' = 0)$ and $\mathcal{A}_l(z, \bar{z} = 0) =: \partial^{n_1} Z(z, \bar{z} = 0) \partial^{n_2} Z(z, \bar{z} = 0) :$, $\mathcal{A}_k^\dagger(w, \bar{w} = 0) =: \partial^{m_1} Z^\dagger(w, \bar{w} = 0) \partial^{m_2} Z^\dagger(w, \bar{w} = 0) :$ with $n_1 \geq n_2$ and $m_1 \geq m_2$ to avoid over counting. We make use of the fact that in the free field theory expectations of a product of $2n$ operators factorize into sums over n products of expectations of pairs of operators (Wick's theorem). Among the terms that appear, we obtain

$$\begin{aligned} &\frac{\langle \partial Z^\dagger(p_1) \partial^{n_1} Z(z, \bar{z} = 0) \rangle_{S^2} \langle \partial^{n_1} Z^\dagger(w, \bar{w} = 0) \partial^i Z'(w', \bar{w}' = 0) \rangle_{S^2}}{\langle \partial^{n_1} Z^\dagger(w, \bar{w} = 0) \partial^{n_1} Z(z, \bar{z} = 0) \rangle_{S^2}} \\ &\quad \times \frac{1}{\langle \partial^i Z'(z', \bar{z}' = 0) \partial^i Z'(w', \bar{w}' = 0) \rangle_{S^2}} \\ &\quad \times \frac{\langle \partial^i Z'(z', \bar{z}' = 0) \partial^{n_2} Z(z, \bar{z} = 0) \rangle_{S^2} \langle \partial^{n_2} Z^\dagger(w, \bar{w} = 0) \partial Z(p_2) \rangle_{S^2}}{\langle \partial^{n_2} Z^\dagger(w, \bar{w} = 0) \partial^{n_2} Z(z, \bar{z} = 0) \rangle_{S^2}} \end{aligned} \quad (253)$$

To interpret this expression note that the first factor (after summing on n_1) gives the amplitude to go from p_1 to $w' = \bar{w}' = 0$, passing through $z = \bar{z} = 0$; the last factor (after summing

on n_2) gives the amplitude to go from $z' = \bar{z}' = 0$ to p_2 passing through $z = \bar{z} = 0$. Finally, after summing on i we get the amplitude to go from p_1 to p_2 along a path with winding number 1.

Terms for which $\mathcal{A}'_j(z', \bar{z}' = 0)$ has n operators ∂Z^\dagger appearing and $\mathcal{A}_l(z, \bar{z} = 0)$ has $n + 1$ operators ∂Z appearing give the amplitudes with winding number n ; terms for which $\mathcal{A}'_j(z', \bar{z}' = 0)$ has $n + 1$ operators ∂Z appearing and $\mathcal{A}_l(z, \bar{z} = 0)$ has n operators ∂Z^\dagger appearing give the amplitudes with winding number $-n$.

G Some results with correct normalizations

Here we give the calculations for Section 6.

G.1 Sphere factorization

We want to work out

$$\begin{aligned} P(R_1(r = e^x, \Omega_i), R_2(r = e^x, \Omega_i) \rightarrow R(r = 0)) \\ = \frac{\left| \langle R_1^\dagger(r = e^x, \Omega_i) R_2^\dagger(r = e^x, \Omega_i) R(r = 0) \rangle \right|^2}{\langle R_2^\dagger(s = e^x, \Omega'_i) R_1^\dagger(s = e^x, \Omega'_i) R_1(r = e^x, \Omega_i) R_2(r = e^x, \Omega_i) \rangle \langle R^\dagger R \rangle} \end{aligned} \quad (254)$$

for sphere and AdS giants.

For two sphere giant $[1^{N/2}]$ combining into another sphere giant $[1^N]$

$$\begin{aligned} & \frac{\left| \langle [1^{N/2}]^\dagger(r = e^x) [1^{N/2}]^\dagger(r = e^x) [1^N](r = 0) \rangle \right|^2}{\langle [1^{N/2}]^\dagger(s = e^x) [1^{N/2}]^\dagger(s = e^x) [1^{N/2}](r = e^x) [1^{N/2}](r = e^x) \rangle \langle [1^N]^\dagger [1^N] \rangle} \\ & = \frac{g([1^{N/2}], [1^{N/2}]; [1^N])^2 f_{[1^N]}^2 e^{-4Nx}}{\sum_S g([1^{N/2}], [1^{N/2}]; S)^2 f_S e^{-2Nx} (e^x - e^{-x})^{-2N} f_{[1^N]}} \end{aligned} \quad (255)$$

where $g([1^{N/2}], [1^{N/2}]; S)$ is a Littlewood-Richardson coefficient. In the large x limit we get

$$P([1^{N/2}], [1^{N/2}] \rightarrow [1^N]) = \frac{f_{[1^N]}}{\sum_S g([1^{N/2}], [1^{N/2}]; S)^2 f_S} < 1 \quad (256)$$

The fusion of the two vertical Young diagrams gives a sum of representations, with column lengths $(N/2 + i, N/2 - i)$. Hence the denominator can be written as

$$\sum_{i=0}^{N/2} \frac{N!(N+1)!}{(N/2 - i)!(N/2 + i + 1)!} \quad (257)$$

The probability is less than one because $f_{[1^N]}$ is included in the sum. A similar formula can be written for two AdS giants $[N/2]$ combining into another AdS giant $[N]$. Now the denominator becomes

$$\sum_{i=0}^{N/2} \frac{(3N/2 + i - 1)!(3N/2 - i - 2)!}{(N - 1)!(N - 2)!} \quad (258)$$

G.2 $G = 1$ factorization

We want to work out

$$\begin{aligned}
P(R(r = e^x, \Omega_i) \rightarrow R'_1(r' = 0)R_2(r = 0)) \\
= e^{-2T\Delta_1} \frac{|\langle R^\dagger(r = e^x, \Omega_i)R'_1(r' = 0)R_2(r = 0) \rangle|^2}{\langle R^\dagger(s = e^x, \Omega_i)R(r = e^x, \Omega_i) \rangle_{G=1} \langle R_1^\dagger R_1 \rangle \langle R_2^\dagger R_2 \rangle}
\end{aligned} \tag{259}$$

in the large T limit. Here $\sum_{k \geq 1} k \text{cosech}(kT) \sim 2e^{-T}$. We will calculate the probability for R at $r = e^{T/2}$, which will maximize the distance of the insertion of R from the boundaries of the cut S^4 .

For the transition of an AdS giant $[N]$ into two smaller AdS giants $[N/2]$

$$\begin{aligned}
& e^{-2T\Delta_1} \frac{|\langle [N]^\dagger(r = e^{T/2})[N/2]'(r' = 0)[N/2](r = 0) \rangle|^2}{\langle [N]^\dagger(s = e^{T/2})[N](r = e^{T/2}) \rangle_{G=1} \langle [N/2]^\dagger[N/2] \rangle \langle [N/2]^\dagger[N/2] \rangle} \\
& \sim \frac{g([N/2], [N/2]; [N])^2 f_{[N]}^2 e^{-TN} e^{-2N(T/2)}}{e^{-2N(T/2)} (2e^{-T})^N f_{[N]} f_{[N/2]}^2} \\
& = \frac{1}{2^N} \frac{f_{[N]}}{f_{[N/2]}^2} = \frac{1}{2^N} \frac{(2N-1)!(N-1)!}{((3N/2-1)!)^2} \\
& = \frac{1}{2^N} \frac{9}{8} \frac{(2N)!N!}{((3N/2)!)^2} \sim \frac{1}{2^N} \frac{9}{8} \frac{\sqrt{4\pi N} (2N)^{2N} e^{-2N} \sqrt{2\pi N} N^N e^{-N}}{3\pi N (3N/2)^{3N} e^{-3N}} \\
& = \frac{3}{\sqrt{8}} \left(\frac{16}{27} \right)^N
\end{aligned} \tag{260}$$

For a sphere giant $[1^N]$ evolving into two smaller sphere giants $[1^{\frac{N}{2}}]$ we get

$$\begin{aligned}
& \sim \frac{1}{2^N} \frac{f_{[1^N]}}{f_{[1^{N/2}]}^2} = \frac{1}{2^N} \frac{((N/2)!)^2}{N!} \\
& \sim \frac{1}{2^N} \frac{\pi N (N/2)^N e^{-N}}{\sqrt{2\pi N} N^N e^{-N}} = \sqrt{\frac{\pi N}{2}} \frac{1}{2^{2N}}
\end{aligned} \tag{261}$$

G.2.1 Giants to KK gravitons

Here we must modify our factorization equations because the trace basis is not a diagonal basis. Fortunately there is a dual basis to the trace basis which we shall call the null basis in line with its use in [22]. A fuller explanation of this null basis will be given in a forthcoming paper.

To start with we will only be concerned with the index structure of the correlators. Define a set of elements σ_i in the permutation group S_n where each σ_i is an element of a different conjugacy class of S_n , $i = 1, \dots, p(n)$ where $p(n)$ is the number of partitions of n .

The *trace basis* is given by the $p(n)$ operators

$$\text{tr}(\sigma_i \Phi) = \sum_{R(n)} \chi_R(\sigma_i) \chi_R(\Phi) \tag{262}$$

Define the $p(n)$ elements of the *null basis* by

$$\xi_i(\Phi) := \frac{|[\sigma_i]|}{n!} \sum_{R(n)} \frac{1}{f_R} \chi_R(\sigma_i) \chi_R(\Phi) \quad (263)$$

where $|[\sigma_i]|$ is the size of the conjugacy class of σ_i . This basis is useful because it is dual to the trace basis. The matrix of correlators of the null basis is the inverse of the matrix of correlators of the trace basis. To prove this we work out

$$\langle \xi_i(\Phi^\dagger) \xi_j(\Phi) \rangle = \frac{|[\sigma_i]|}{n!} \frac{|[\sigma_j]|}{n!} \sum_{R(n)} \frac{1}{f_R} \chi_R(\sigma_i) \chi_R(\sigma_j) \quad (264)$$

and

$$\langle \text{tr}(\sigma_j \Phi^\dagger) \text{tr}(\sigma_k \Phi) \rangle = \sum_{S(n)} f_S \chi_S(\sigma_j) \chi_S(\sigma_k) \quad (265)$$

If we sum \sum_j over conjugacy classes of S_n we get

$$\begin{aligned} & \sum_j \langle \xi_i(\Phi^\dagger) \xi_j(\Phi) \rangle \langle \text{tr}(\sigma_j \Phi^\dagger) \text{tr}(\sigma_k \Phi) \rangle \\ &= \sum_j \sum_R \sum_S \frac{|[\sigma_i]|}{n!} \frac{|[\sigma_j]|}{n!} \frac{1}{f_R} \chi_R(\sigma_i) \chi_R(\sigma_j) f_S \chi_S(\sigma_j) \chi_S(\sigma_k) \\ &= \sum_R \frac{|[\sigma_i]|}{n!} \chi_R(\sigma_i) \chi_R(\sigma_k) \\ &= \delta_{ik} \end{aligned} \quad (266)$$

using the orthogonality properties of the characters of S_n (see Appendix J). The null basis is dual to the trace basis

$$\sum_j \langle \xi_i(\Phi^\dagger) \xi_j(\Phi) \rangle \text{tr}(\sigma_j \Phi) = \xi_i(\Phi) \quad (267)$$

Now schematically (dropping spacetime dependence and modular parameters) the genus 1 factorization we are interested in is

$$\begin{aligned} \langle R^\dagger R \rangle_{G=1} &= \sum_{ij} \sum_{kl} \mathcal{G}^{ij} \mathcal{G}^{kl} \langle R^\dagger \text{tr}(\sigma_j \Phi) \text{tr}(\sigma_l \Phi) \rangle \langle \text{tr}(\sigma_k \Phi^\dagger) \text{tr}(\sigma_i \Phi^\dagger) R \rangle \\ &= \sum_i \sum_k \langle R^\dagger \text{tr}(\sigma_i \Phi) \text{tr}(\sigma_k \Phi) \rangle \langle \xi_k(\Phi^\dagger) \xi_i(\Phi^\dagger) R \rangle \end{aligned} \quad (268)$$

using the fact that $\mathcal{G}^{ij} = \langle \xi_i^\dagger \xi_j \rangle$. Thus the probability of a transition to KK gravitons is given by

$$P(R \rightarrow \text{tr}(\sigma_i \Phi), \text{tr}(\sigma_k \Phi)) = \frac{\langle R^\dagger \text{tr}(\sigma_i \Phi) \text{tr}(\sigma_k \Phi) \rangle \langle \xi_k(\Phi^\dagger) \xi_i(\Phi^\dagger) R \rangle}{\langle R^\dagger R \rangle_{G=1}} \quad (269)$$

Now we shall do the computation for the transition of an AdS giant to two Kaluza-Klein gravitons. We will drop the spacetime dependencies and add them in at the end. First we must work out the two three point functions

$$\left\langle [N]^\dagger \text{tr}(\Phi^{\frac{N}{2}}) \text{tr}(\Phi^{\frac{N}{2}}) \right\rangle = \sum_{R_1, R_2} \chi_{R_1}(N/2) \chi_{R_2}(N/2) \langle [N]^\dagger R_1 R_2 \rangle \quad (270)$$

where $(N/2)$ is understood to be a cycle of length $N/2$. Since $[N]$ can only be made from other single-row representations, the only representations in the sum that contribute are the AdS giants. We get

$$\left\langle [N]^\dagger \text{tr}(\Phi^{\frac{N}{2}}) \text{tr}(\Phi^{\frac{N}{2}}) \right\rangle = f_{[N]} \quad (271)$$

Similarly

$$\begin{aligned} & \langle \xi_{(N/2)}(\Phi^\dagger) \xi_{(N/2)}(\Phi^\dagger) R \rangle \\ &= \sum_{R_1, R_2} \frac{|[(N/2)]|}{(N/2)!} \frac{|[(N/2)]|}{(N/2)!} \frac{1}{f_{R_1}} \frac{1}{f_{R_2}} \chi_{R_1}(N/2) \chi_{R_2}(N/2) \langle [N]^\dagger R_1 R_2 \rangle \\ &= \frac{4}{N^2} \frac{f_{[N]}}{f_{[N/2]}^2} \end{aligned} \quad (272)$$

where we have used $|[(N/2)]| = (N/2 - 1)!$. Thus, adding back in the spacetime dependencies, we have

$$P\left([N](r = e^x) \rightarrow \text{tr}(\Phi^{\frac{N}{2}})(r' = 0) \text{tr}(\Phi^{\frac{N}{2}})(r = 0)\right) \sim \frac{4}{N^2} \frac{3}{\sqrt{8}} \left(\frac{16}{27}\right)^N \quad (273)$$

and

$$P\left([1^N](r = e^x) \rightarrow \text{tr}(\Phi^{\frac{N}{2}})(r' = 0) \text{tr}(\Phi^{\frac{N}{2}})(r = 0)\right) \sim \frac{4}{N^2} \sqrt{\frac{\pi N}{2}} \left(\frac{1}{2}\right)^{2N} \quad (274)$$

G.3 Higher genus factorization

For the transition of an AdS giant into n smaller AdS giants, using the guess involving k_n from section 6, we have

$$\begin{aligned} P([N] \rightarrow n \times [N/n]) &= \frac{1}{k_n^N} \frac{f_{[N]}}{f_{[N/n]}^n} \\ &= \frac{1}{k_n^N} \frac{(2N-1)!}{(N-1)!} \left(\frac{(N-1)!}{(N+N/n-1)!} \right)^n \\ &\sim \frac{1}{k_n^N} \frac{1}{\sqrt{2}} \left[\frac{(n+1)}{n} \right]^{\frac{n}{2}} \frac{(2N)^{2N} e^{-2N} N^{N(n-1)} e^{-N(n-1)}}{\left[\frac{(n+1)}{n} \right]^{N(n+1)} N^{N(n+1)} e^{-N(n+1)}} \\ &= \frac{1}{\sqrt{2}} \left[\frac{(n+1)}{n} \right]^{\frac{n}{2}} \left[\frac{4n^{n+1}}{k_n(n+1)^{n+1}} \right]^N \end{aligned} \quad (275)$$

in the large N limit.

For the transition of a Schur polynomial operator to KK gravitons we find in general

$$\begin{aligned}
P(R \rightarrow \text{tr}(\sigma_{i_1} \Phi), \dots, \text{tr}(\sigma_{i_n} \Phi)) &= \frac{\langle R^\dagger \text{tr}(\sigma_{i_1} \Phi) \cdots \text{tr}(\sigma_{i_n} \Phi) \rangle \langle \xi_{i_n}(\Phi^\dagger) \xi_{i_1}(\Phi^\dagger) R \rangle}{\langle R^\dagger R \rangle_{G=n-1}} \\
&= \sum_{R_1, \dots, R_n} \chi_{R_1}(\sigma_{i_1}) \cdots \chi_{R_n}(\sigma_{i_n}) g(R_1, \dots, R_n; R) f_R \\
&\times \sum_{S_1, \dots, S_n} \chi_{S_1}(\sigma_{i_1}) \cdots \chi_{S_n}(\sigma_{i_n}) g(S_1, \dots, S_n; R) f_R \\
&\times \frac{1}{f_{S_1} \cdots f_{S_n}} \frac{|\sigma_{i_1}|}{\Delta_1!} \cdots \frac{|\sigma_{i_n}|}{\Delta_n!} \frac{1}{f_R k_n^{\Delta_R}} \quad (276)
\end{aligned}$$

Fortunately this simplifies dramatically if R is an AdS (or sphere) giant, since, by the Littlewood-Richardson rules, an AdS (or sphere) giant can only be made from other single row (or column) representations. Further if σ_{i_j} are single length Δ_j cycles for $j = 1, \dots, n$ we know that $\chi_{[\Delta_j]}(\Delta_j) = 1$ (± 1 for sphere) and also that $|\sigma_{i_j}| = (\Delta_j - 1)!$. Thus we get

$$\begin{aligned}
P([\Delta_R] \rightarrow \text{tr}(\Phi^{\Delta_1}), \dots, \text{tr}(\Phi^{\Delta_n})) &= \frac{1}{k_n^{\Delta_R}} \frac{1}{\Delta_1 \cdots \Delta_n} \frac{f_{[\Delta_R]}}{f_{[\Delta_1]} \cdots f_{[\Delta_n]}} \\
P([1^{\Delta_R}] \rightarrow \text{tr}(\Phi^{\Delta_1}), \dots, \text{tr}(\Phi^{\Delta_n})) &= \frac{1}{k_n^{\Delta_R}} \frac{1}{\Delta_1 \cdots \Delta_n} \frac{f_{[1^{\Delta_R}]}}{f_{[1^{\Delta_1}]} \cdots f_{[1^{\Delta_n}]}} \quad (277)
\end{aligned}$$

H Topology for 5D bulk and 4D boundary

H.1 Complements of graph neighborhoods in B^5 and wedge sum of spheres

Take a ball B^4 and remove n B^4_\circ balls from its interior. Call the resulting surface X . X is homotopic to an n -wedge of 3-spheres, $\vee_n S^3$, for which we know $H_3(\vee_n S^3) = \mathbb{Z}^n$ (page 126 of [73]).

Now quotient X by the outer S^3 boundary of the original B^4 . X/S^3 is an S^4 with n B^4_\circ balls removed, $\partial^{(i)} N(V_n, B^5)$, which is homotopic to the complement of a connected graph. There is an exact sequence (page 114 of [73])

$$\cdots \rightarrow H_4(X/S^3) \xrightarrow{\partial} H_3(S^3) \xrightarrow{i_\star} H_3(X) \xrightarrow{j_\star} H_3(X/S^3) \xrightarrow{\partial} H_2(S^3) \rightarrow \cdots \quad (278)$$

where i_\star is induced from the inclusion map on the chain group $C_3(S^3) \xrightarrow{i} C_3(X)$ and j_\star is induced from the quotient map $C_3(X) \xrightarrow{j} C_3(X/S^3)$.

We know that $H_4(X/S^3) = \{0\}$ since there are no boundaryless chains in $C_4(X/S^3)$. We also have $H_3(A) = H_3(S^3) = \mathbb{Z}$, $H_3(X) = H_3(\vee_n S^3) = \mathbb{Z}^n$ and $H_2(A) = H_2(S^3) = \{0\}$. Thus we get a short exact sequence

$$\cdots \rightarrow 0 \xrightarrow{\partial} \mathbb{Z} \xrightarrow{i_\star} \mathbb{Z}^n \xrightarrow{j_\star} H_3(\partial^{(i)} N(V_n, B^5)) \xrightarrow{\partial} 0 \rightarrow \cdots \quad (279)$$

Because this is a short exact sequence i_\star is an injection, j_\star is a surjection, and $\text{im } i_\star = \ker j_\star$. Hence, by the first isomorphism theorem on the map j_\star , $H_3(\partial^{(i)} N(V_n, B^5)) = \text{im } j_\star \cong \mathbb{Z}^n / \ker j_\star = \mathbb{Z}^n / \mathbb{Z} = \mathbb{Z}^{n-1}$.

H.2 Cell complexes

The easiest way to compute the homology groups of $\Sigma_4(n-1)$ is in terms of its cell complex decomposition. A k -cell is an *open* k -dimensional ball. We can build a manifold from cells by starting with 0-cells, i.e. a set of points, and inductively attaching cells of higher dimension. We attach the cells along the boundary of the cells. A k -cell has boundary S^{k-1} . An attaching map identifies this boundary with some submanifold of the manifold to which we are attaching the cell, even if that submanifold is of a lower dimension. For example, we can attach a 2-cell (an open disk) to a 0-cell by identifying the boundary of the 2-cell, a circle, with the 0-cell. This gives us a cell decomposition of the sphere S^2 . A more formal description follows.

A *cell complex* or *CW complex* is a space X constructed in the following way

1. Start with a discrete set X^0 , the 0-cells of X .
2. Inductively, form the k -skeleton X^k from X^{k-1} by attaching k -cells e_α^k . Do this via maps $\varphi_\alpha : S^{k-1} \rightarrow X^{k-1}$ where S^{k-1} is the boundary of the k -ball. This means that X^k is the quotient space of $X^{k-1} \sqcup B_\alpha^k$ (B_α^k is a closed k -ball here) under the identifications $x \sim \varphi_\alpha(x)$ for $x \in \partial B_\alpha^k$. The cell e_α^k is the homeomorphic image of the open disk $B_\alpha^k - \partial B_\alpha^k$ under the quotient map.

This is different to handlebody attachment because the boundary of the cell can be attached to any part of X^{k-1} , even one of dimension lower than $k-1$.

3. $X = X^d$ for some d if X is finite-dimensional.

The cell decomposition is virtually identical to the handlebody decomposition because a k -handle can be viewed as a thickening of a k -cell.

Once we have a cell decomposition of a manifold we can compute the homology using a boundary map on the cells. Let $\{e_\alpha^k\}$ be the k -cells that we are attaching to the lower-dimensional manifold X^{k-1} . The cellular boundary map d_k can be computed in terms of degrees. $d_k(e_\alpha^k) = \sum_\beta d_{\alpha\beta} e_\beta^{k-1}$ where $d_{\alpha\beta}$ is the degree of the map $S_\alpha^{k-1} \rightarrow X^{k-1} \rightarrow S_\beta^{k-1}$ that is the composition of the attaching map of e_α^k with the quotient map collapsing $X^{k-1} - e_\beta^{k-1}$ to a point. If the boundary of e_α^k is identified with a submanifold of dimension $k-2$ or lower then $d_k(e_\alpha^k) = 0$. Using this boundary map we can then compute the homology in the standard way.

We will give a cell decomposition of our spaces so that we can compute the homology groups.

H.3 Cell decomposition and homology for the complement of a connected graph

Since $\overline{B^5 \setminus N(V_n, B^5)}$ is homeomorphic to a thickening of the internal surface $\partial^{(i)} N(V_n, B^5) \times B^1$ it is also of the same homotopy type as the internal surface itself $\partial^{(i)} N(V_n, B^5)$. The internal surface is in fact a deformation retract of $\overline{B^5 \setminus N(V_n, B^5)}$ (a subspace R of a manifold X is a *retract* of X if there is a continuous map $f : X \rightarrow R$ such that $f|_R = \text{id}_R$; if id_X and f are homotopic then R is a *deformation retract* of X).

The cell decomposition of the 4-dimensional space $\partial^{(i)}N(V_n, B^5)$ is as follows.

- Take a single 0-cell.
- Attach to it n 3-cells, with a map which identifies the boundaries of the 3-cells (S^2 s) with the 0-cell. The space is now a *wedge sum* of n spheres S^3 , i.e. it is the disjoint union of n spheres S^3 with a point on each sphere identified to a single point. The wedge sum of n spheres is sometimes written $\vee_n S^3$.
- Now wrap a 4-cell around the n 3-cells. The 4-cell has a boundary of S^3 . To glue this to the n S^3 s divide it up into n pieces and glue each n th around each 3-sphere sequentially.

For example for a 3-dimensional bulk we obtain the pants diagram by taking a point and attaching three open intervals to it. We get three circles attached at a single point. Then we attach an open 2-ball with its S^1 boundary going around each of the three circles, pinching around the 0-cell. See Figure 27.

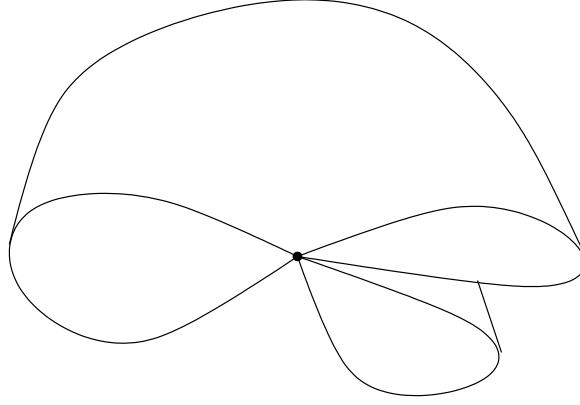


Figure 27: The cell decomposition of the pants diagram for $d = 3$, $n = 3$. It has a 0-cell at the center, 3 1-cells attached to the 0-cell to form the wedge sum of 3 circles S^1 and a 2-cell with S^1 boundary wrapping the 3 circles.

Note that for a connected Witten graph $\partial^{(i)}N(V_n, B^5)$ is the same as the n -punctured 4-sphere on which we do our CFT. The n spheres S^3 are the same as the boundaries of the 4-balls we cut out around each puncture.

For the set-up in general dimension see Appendix I.1.

Now that we have the cell decomposition of $\partial^{(i)}N(V_n, B^5)$ we can compute the homology groups using our cellular boundary map, $d_k(e_\alpha^k) = \sum_\beta d_{\alpha\beta} e_\beta^{k-1}$ where $d_{\alpha\beta}$ is the degree of the attaching map.

The homology groups for the complement of a connected Witten graph are

- $H_4(\partial^{(i)}N(V_n, B^5)) = \{0\}$ since the only 4-cell e^4 has a boundary, so $\ker d_4 = \{0\}$.
- $H_3(\partial^{(i)}N(V_n, B^5)) = \mathbb{Z}^{n-1}$. Let e_α^3 for $\alpha = 1, \dots, n$ be the n 3-cells. The image of d_4 is spanned by $d_4(e^4) = \sum_\alpha e_\alpha^3$ since the boundary of e^4 wraps the 3-cells sequentially.

The kernel of d_3 is spanned by the n 3-cells e_α^3 , since their boundaries are identified to a point. Thus $H_3 = \ker d_3 / \text{im } d_4 \cong \mathbb{Z}^{n-1}$.

- $H_2(\partial^{(i)}N(V_n, B^5)) = \{0\}$ since there are no 2-cells.
- $H_1(\partial^{(i)}N(V_n, B^5)) = \{0\}$ since there are no 1-cells.
- $H_0(\partial^{(i)}N(V_n, B^5)) = \mathbb{Z}$ since it is arcwise connected.

The only non-trivial homology group, $H_3(\partial^{(i)}N(V_n, B^5))$, can also be computed via a short exact sequence of homology groups (see Appendix H.1).

These homology groups satisfy the weak Morse inequalities. If c_k is the number of k -cells and b_k is the k th Betti number then

$$c_k \geq b_k \quad (280)$$

for all k .

H.4 Cell decomposition and homology for the complement of a disconnected graph

Suppose a Witten graph G is composed of m disconnected components $G = V_{n_1} \sqcup V_{n_2} \sqcup \dots \sqcup V_{n_m}$.

$B^5 \setminus N(G, B^5)$ is homotopic to the m connected spaces $\partial^{(i)}N(V_{n_i}, B^5)$ daisy-chained together in a line by 1-cells. For the cell decomposition

- Take m 0-cells.
- Link them in a line by $(m-1)$ 1-cells. The ends of each 1-cell attach to different 0-cells.
- Attach n_i 3-cells to each 0-cell for $1 \leq i \leq m$ as above. We have m wedge sums of 3-spheres linked together in a line by 1-cells.
- Now wrap a 4-cell around each collection of n_i 3-cells.

$\overline{B^5 \setminus N(G, B^5)}$ glued to itself is the same except we attach a further $(m-1)$ 1-cells, each of which has both ends attached to the same 0-cell.

$\overline{B^5 \setminus N(G, B^5)}$ has most of the same homology groups as $\overline{B^5 \setminus N(V_n, B^5)}$ except that now

$$H_3(\overline{B^5 \setminus N(G, B^5)}) = \mathbb{Z}^{\sum_j n_j - m} \quad (281)$$

The first homology group is unchanged because there are no closed loops from the 1-cells.

$\overline{B^5 \setminus N(G, B^5)}$ glued to itself is a different story. H_0 and H_i for $i > 1$ are the same as $\overline{B^5 \setminus N(G, B^5)}$.

Each of the $(m-1)$ 1-cell loops is a 1-cycle which is not the boundary of some 2-chain. Thus it increases the number of free Abelian generators of H_1 by $m-1$

$$H_1((\overline{B^5 \setminus N(G, B^5)}) \cup |_{\partial^{(i)}N}(\overline{B^5 \setminus N(G, B^5)})) = \mathbb{Z}^{m-1} \quad (282)$$

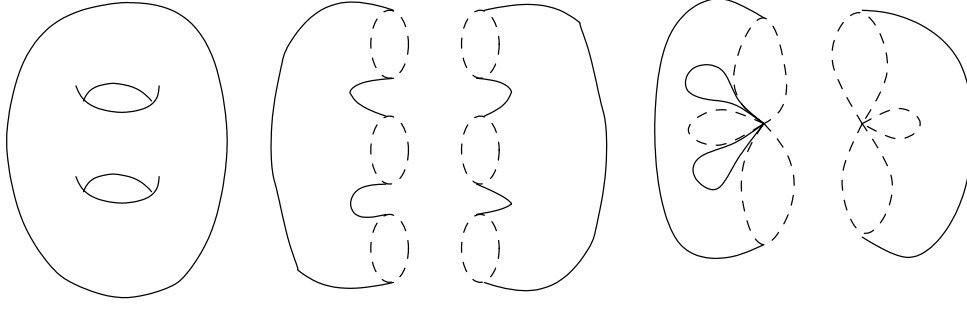


Figure 28: $\Sigma_4(G)$, the obvious way to cut it, and the easy way to cut it for the cell decomposition.

H.5 Cell decomposition and homology for $\Sigma_4(G)$

We want to find the cell decomposition of the 4-dimensional manifold with genus G , $\Sigma_4(G)$.

Figure 28 shows the 2-dimensional analogue of $\Sigma_4(2)$ and the different ways to cut it up in order to do the cell decomposition. The first way, in the middle of Figure 28, cuts $\Sigma_4(G)$ into two S^4 s with three holes each (these holes are represented with dotted lines; for $\Sigma_4(G)$ these holes will be S^3 -shaped). It turns out that this is a tricky way to do the cell decomposition. It is better to use the cutting in the final picture of Figure 28. This is homotopically different to the middle cutting because there are non-trivial 1-cycles in the left-hand piece of the final cutting.

The cell decomposition involves 1 0-cell, G 1-cells, $G + 1$ 3-cells e_α^3 and 2 4-cells, e_L^4 representing the left-hand piece of the last cutting in Figure 28 and e_R^4 representing the right-hand piece.

First attach all the ends of the G 1-cells to the 0-cell so that we get a wedge of G S^1 s.

Next attach the $G + 1$ 3-cells e_α^3 to the 0-cell. The boundary of the closure of each 3-cell, S^2 , is identified to the point of the 0-cell so that the 3-cell, an open 3-ball, is closed to become a sphere S^3 . We now have a wedge of G S^1 s and $G + 1$ S^3 s, i.e. G S^1 s and $G + 1$ S^3 s with a point on each of them identified to the same point. See Figure 29 for $G = 2$.

Next we need to describe how to attach the 2 4-cells, e_L^4 and e_R^4 .

e_L^4 attaches to the G 1-cells and the $G + 1$ 3-cells. We need to specify how the boundary of the closure of e_L^4 , i.e. an S^3 , is mapped to the lower-dimensional cells. To do this split the 3-sphere boundary up into $3G + 1$ segments. In terms of coordinates on the 3-sphere we let a $\phi \in [0, 2\pi]$ coordinate parameterize the $X_1 - X_2$ plane. Each segment is defined by $\phi \in [\frac{2(m-1)\pi}{3G+1}, \frac{2m\pi}{3G+1}]$ for $m = 1, \dots, 3G + 1$. Each segment is like a 3-ball (think segments of the circle or sphere). Each of the $G + 1$ 3-cells has a single segment attached to it and each of the G 1-cells has two segments attached to it on each side. The segments are attached in order as indicated in Figure 29, which generalizes to arbitrary genus.

When a segment is attached to an S^3 the boundary of the segment (an S^2) is identified to a point to give S^3 (just as when we attach the 3-cell to the 0-cell).

When we attach a segment to a 1-cell we identify the whole segment with the 1-ball intersection of the $X^1 - X^2$ plane with the segment.

e_R^4 attaches to the $G + 1$ 3-cells. We split the boundary of the closure of the e_R^4 into $G + 1$

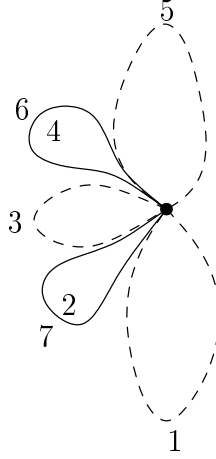


Figure 29: The 0-cell, 1-cells and 3-cells of $\Sigma_4(2)$, where the 0-cell is the blob in the middle, the 1-cells are the thick lines and the 3-cells are the dotted lines.

pieces and attach them to the 3-cells in order.

From this we can deduce the homology using the boundary operator $d_k(e_\alpha^k) = \sum_\beta d_{\alpha\beta} e_\beta^{k-1}$.

To find $H_4(\Sigma_4(G))$ we use $d_4(e_L^4) = \sum_\alpha e_\alpha^3$ and $d_4(e_R^4) = -\sum_\alpha e_\alpha^3$ so that $H_4(\Sigma_4(G))$ is generated by $\Sigma_4(G) = e_L^4 + e_R^4$, which has no boundary. Thus $H_4(\Sigma_4(G)) = \mathbb{Z}$.

All the 3-cells e_α^3 are annihilated by d_3 so that $\ker d_3$ is spanned by $\{e_\alpha^3\}$. The image of d_4 is spanned by $\sum_\alpha e_\alpha^3$, so $H_3(\Sigma_4(G)) = \mathbb{Z}^{G+1}/\mathbb{Z} = \mathbb{Z}^G$. Roughly, the S^3 cross-sections near the different G holes are not homologous.

There are no 2-cells so $H_2(\Sigma_4(G)) = \{0\}$.

By well-known results about the homology of genus G graphs, $H_1(\Sigma_4(G)) = \mathbb{Z}^G$.

$H_0(\Sigma_4(G)) = \mathbb{Z}$ because the manifold is arcwise-connected.

As expected, Poincaré duality holds. For a general $(d-1)$ -dimensional boundary constructed this way see Appendix I.3.

The homology groups above can also be obtained by using the Mayer-Vietoris sequence which follows from the construction of $\Sigma_4(G)$ as a union of two copies of $S^4 \setminus \sqcup_{\alpha=1}^{G+1} (B_\alpha^4)_\circ$ intersecting over $\sqcup_{\alpha=1}^{G+1} (S^3)_\alpha$.

H.6 Handlebody decompositions

As another way to visualize the topologies involved in our discussion, we give their handlebody decompositions.

H.6.1 Handlebody decomposition for the complement of a connected graph

Consider the n -valent connected Witten graph V_n with a single n -fold vertex. To start with we will work with a three-dimensional bulk because it is easy to visualize.

The handlebody decomposition of $\overline{B^3 \setminus N(V_n, B^3)}$ is as follows.

- Start with a 0-handle.

- Attach n 1-handles to the ball (taking care that the different 1-handles do not wind around each other). We now have a filled pretzel with n holes, each generated by an S^1 .
- Attach a single 2-handle. Glue it along $S^1 \times B^1$ so that the S^1 encircles each of the n -holes of the donut once (see Figure 30).

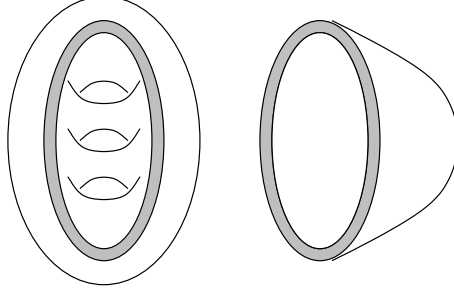


Figure 30: The gluing of the 2-handle

This lifts directly to five dimensions for $\overline{B^5 \setminus N(V_n, B^5)}$.

- Start with a 0-handle.
- Attach n 3-handles to the ball (taking care to avoid non-trivial windings). The resulting manifold has n holes, each generated by an S^3 .
- Attach a single 4-handle. Glue it along $S^3 \times B^1$ so that the S^3 encircles each of the n holes once.

For the set-up in a general dimension see Appendix I.4.1.

H.6.2 Handlebody decomposition for the complement of a disconnected graph

We will describe two ways of providing the handle decomposition of $\overline{B^5 \setminus N(G, B^5)}$ where $G = V_{n_1} \sqcup V_{n_2} \sqcup \dots V_{n_m}$. The first is the one described above: take the m connected $\overline{B^5 \setminus N(V_{n_i}, B^5)}$ and glue them together with $(m - 1)$ 1-handles.

The second way is similar to that for the connected cases.

- Start with a 0-handle.
- Attach $\sum_i n_i$ 3-handles to the ball (taking care to avoid non-trivial windings).
- For each connected component V_{n_i} attach a 4-handle. Glue it along $S^3 \times B^1$ so that the S^3 encircles n_i holes. Make sure that the 4-handles encircle different holes.

For $\overline{B^5 \setminus N(G, B^5)}$ glued to a copy of itself use the same decomposition but add $(m - 1)$ 1-handles at the end.

I Topology for gluings in general dimensions

Here we have a d -dimensional bulk and a $(d - 1)$ -dimensional boundary.

I.1 Cell decomposition and homology for the complement of a connected graph

The cell decomposition of the $(d - 1)$ -dimensional space $\partial^{(i)}(N(V_n, B^d))$ is as follows.

- Take a single 0-cell.
- Attach to it n $(d - 2)$ -cells, with a map which sends the boundaries of the $(d - 2)$ -cells (S^{d-3}) to the point of the 0-cell. The space is now a *wedge sum* of n spheres S^{d-2} , i.e. it is the disjoint union of n spheres S^{d-2} with a point on each sphere identified to a single point.
- Now wrap a $(d - 1)$ -cell around the n $(d - 2)$ -cells. The $(d - 1)$ -cell has a boundary of S^{d-2} . To glue this to the n S^{d-2} s divide it up into n pieces and glue each n th around each $(d - 2)$ -sphere.

Note that for a connected Witten graph $\partial^{(i)}(N(V_n, B^d))$ is the same as the n -punctured $(d - 1)$ -sphere on which we do our CFT. The n spheres S^{d-2} are the same as the boundaries of the $(d - 1)$ -balls we cut out around each puncture.

The homology groups for a connected Witten graph are

- $H_0(\partial^{(i)}(N(V_n, B^d))) = \mathbb{Z}$ since it is arcwise connected.
- $H_i(\partial^{(i)}(N(V_n, B^d))) = \{0\}$ for $1 \leq i \leq d - 3$ since there are no i -cells.
- $H_{d-2}(\partial^{(i)}(N(V_n, B^d))) = \mathbb{Z}^{n-1}$ by the same reasoning as for $d = 5$.
- $H_{d-1}(\partial^{(i)}(N(V_n, B^d))) = \{0\}$ since there are no boundaryless $(d - 1)$ -chains.

This gives the Euler character formula

$$\begin{aligned} \chi(\partial^{(i)}(N(V_n, B^d))) &= \sum_j (-1)^j b_j \\ &= 1 + (-1)^{d-2}(n - 1) \end{aligned} \tag{283}$$

I.2 Cell decomposition and homology for the complement of a disconnected graph

Suppose a Witten graph G is composed of m disconnected components $G = V_{n_1} \sqcup V_{n_2} \sqcup \dots \sqcup V_{n_m}$.

$B^d \setminus N(G, B^d)$ is homotopic to the m connected spaces $\partial^{(i)}(N(V_{n_i}, B^d))$ daisy-chained together in a line by 1-cells. For the cell decomposition

- Take m 0-cells.
- Link them in a line by $(m - 1)$ 1-cells. The ends of each 1-cell attach to different 0-cells.

- Attach n_i $(d - 2)$ -cells to each 0-cell for $1 \leq i \leq m$ as above. We have m wedge sums of $(d - 2)$ -spheres linked together in a line by 1-cells.
- Now wrap a $(d - 1)$ -cell around each collection of n_i $(d - 2)$ -cells.

$\overline{B^d \setminus N(G, B^d)}$ glued to itself is the same except we attach a further $(m - 1)$ 1-cells, each of which has both ends attached to the same 0-cell.

$\overline{B^d \setminus N(G, B^d)}$ has most of the same homology groups except that

$$H_{d-2}(\overline{B^d \setminus N(G, B^d)}) = \mathbb{Z}^{\sum_j n_j - m} \quad (284)$$

For $d > 3$ the first homology group is unchanged because there are no closed loops from the 1-cells.

$\overline{B^d \setminus N(G, B^d)}$ glued to itself is a different story. H_0 and H_i for $i > 1$ are the same as $\overline{B^d \setminus N(G, B^d)}$.

Each of the $(m - 1)$ 1-cell loops is a 1-cycle which is not the boundary of some 2-chain. Thus it increases the number of free Abelian generators of H_1 by $m - 1$. So for $d > 3$ we have

$$H_1((\overline{B^d \setminus N(G, B^d)}) \cup |_{\partial^{(i)}N}(\overline{B^d \setminus N(G, B^d)})) = \mathbb{Z}^{m-1} \quad (285)$$

and for $d = 3$

$$H_1((\overline{B^3 \setminus N(G, B^3)}) \cup |_{\partial^{(i)}N}(\overline{B^3 \setminus N(G, B^3)})) = \mathbb{Z}^{\sum_j n_j - 1} \quad (286)$$

I.3 General genus boundaries

Here we work with a bulk of dimension d and a boundary of dimension $d - 1$.

The homology groups for a boundary of genus $n - 1$ for $d > 3$ are

- $H_0(\Sigma_{d-1}(n - 1)) = \mathbb{Z}$ since the manifold is arcwise-connected.
- $H_1(\Sigma_{d-1}(n - 1)) = \mathbb{Z}^{n-1}$ from the topology of the graph.
- $H_i(\Sigma_{d-1}(n - 1)) = \{0\}$ for $2 \leq i \leq d - 3$.
- $H_{d-2}(\Sigma_{d-1}(n - 1)) = \mathbb{Z}^{n-1}$ because the S^{d-2} cross-sections near the different $(n - 1)$ holes are not homologous. This also follows from Poincaré duality for a closed, compact, oriented surface.
- $H_{d-1}(\Sigma_{d-1}(n - 1)) = \mathbb{Z}$ since the manifold itself has no boundary and is arcwise-connected.

I.4 Handlebody decompositions

I.4.1 Handlebody decomposition for the complement of a connected graph

Here we do a handlebody decomposition of $\overline{B^d \setminus N(V_n, B^d)}$.

- Start with a 0-handle.

- Attach n $(d-2)$ -handles to the ball (taking care to avoid non-trivial windings). The resulting manifold has n holes, each generated by an S^{d-2} .
- Attach a single $(d-1)$ -handle. Glue it along $S^{d-2} \times B^1$ so that the S^{d-2} encircles each of the n holes once.

From the CFT point of view this set-up corresponds to an S^{d-1} with n operator insertions. To perform the gluing we cut out from the S^{d-1} a B^{d-1}_o hole around each operator insertion. This gives us n disconnected S^{d-2} boundaries. Each S^{d-2} boundary corresponds to the S^{d-2} that generates each hole in the handlebody decomposition above of the $\overline{B^d \setminus N(V_n, B^d)}$ bulk. The $(d-1)$ -handle above then makes sure that the n holes meet up inside the bulk.

I.4.2 Handlebody decomposition for the complement of a disconnected graph

We will describe two ways of providing the handle decomposition of $\overline{B^d \setminus N(G, B^d)}$ where $G = V_{n_1} \sqcup V_{n_2} \sqcup \dots V_{n_m}$. The first is the one described above: take the m connected $\overline{B^d \setminus N(V_{n_i}, B^d)}$ and glue them together with $(m-1)$ 1-handles.

The second way is similar to that for the connected cases.

- Start with a 0-handle.
- Attach $\sum_i n_i$ $(d-2)$ -handles to the ball (taking care to avoid non-trivial windings).
- For each connected component V_{n_i} attach a $(d-1)$ -handle. Glue it along $S^{d-2} \times B^1$ so that the S^{d-2} encircles n_i holes. Make sure that the $(d-1)$ -handles encircle different holes.

For $\overline{B^d \setminus N(G, B^d)}$ glued to a copy of itself use the same decomposition but add $(m-1)$ 1-handles at the end.

J Identities, notation and conventions

We define

$$\text{tr}(\sigma\Phi) = \sum_{i_1, i_2, \dots, i_n} \Phi_{i_{\sigma(1)}}^{i_1} \Phi_{i_{\sigma(2)}}^{i_2} \dots \Phi_{i_{\sigma(n)}}^{i_n} \quad (287)$$

The Schur polynomials are defined as a sum of these trace operators over the elements σ of S_n , weighted by the characters of σ in the representation R of S_n ,

$$\chi_R(\Phi) = \frac{1}{n!} \sum_{\sigma \in S_n} \chi_R(\sigma) \text{tr}(\sigma\Phi) \quad (288)$$

A representation R of S_n can be written as a Young diagram with n boxes, with which we also associate a representation R of the unitary group¹³. We can reverse the relation between

¹³This arises because $U(N)$ and S_n have a commuting action on $V^{\otimes n}$ where V is the fundamental representation of $U(N)$. If the Schur polynomial takes an element of $U(N)$ as its argument it is the character of that element in the irreducible representation R .

traces and Schur polynomials

$$\text{tr}(\sigma\Phi) = \sum_{R(n)} \chi_R(\sigma)\chi_R(\Phi) \quad (289)$$

where we sum over representations R of S_n with Young diagrams of n boxes. To do this we have used the orthogonality relation for two elements $\sigma, \tau \in S_n$

$$\sum_{R(n)} \chi_R(\sigma)\chi_R(\tau) = \frac{n!}{|[\sigma]|} \delta_{\tau \in [\sigma]} \quad (290)$$

where we have summed over representations of S_n . We also have another orthogonality relation for two representations R, S of S_n

$$\sum_{\sigma \in S_n} \chi_R(\sigma)\chi_S(\sigma) = n! \delta_{RS} \quad (291)$$

R	a representation of the symmetric group and the unitary group; as an operator we mean $\chi_R(\partial Z)$ for the 2d theory and $\chi_R(\Phi)$ for the 4d theory
R^\dagger	as an operator $\chi_R(\partial Z^\dagger)$ for the 2d theory and $\chi_R(\Phi^\dagger)$ for the 4d theory
$[L]$	the Young diagram with a single row of length L ; for $L \sim N$, $[L]$ corresponds to the AdS giant graviton
$[1^L]$	the Young diagram with a single column of length L ; for $L \sim N$, $[1^L]$ corresponds to the sphere giant graviton
f_R	the combinatorial coefficient that appears in the two-point function of the Schur polynomials. It is computed by $f_R = \frac{\text{Dim}_R \Delta_R!}{d_R!}$ where Dim_R is the dimension of the $U(N)$ representation R and d_R is the dimension of the symmetric group S_{Δ_R} representation R . A useful identity is $f_R = \prod_{i,j} (N - i + j)$ where we sum over the boxes of the Young diagram for R , i labeling the rows and j the columns.
$g(R_1, R_2, \dots, R_n; R)$	the Littlewood-Richardson (LR) coefficient, which counts the number of times the representation R appears in the tensor product of R_1, \dots, R_n
$ [\sigma] $	the size of the conjugacy class $[\sigma]$ of σ , an element of the symmetric group

Table 1: representation theory notation

B^k	the closed k -ball
B_o^k	the open k -ball
V_n	the Witten graph obtained by joining n points on the boundary to a single vertex in the bulk
$\sqcup V_{n_i}$	a disjoint union of graphs V_{n_i}
$N(G, B^5)$	the neighborhood of the graph G in B^5 . Formally $N(G, B^5) = \{x \in B^5 : \ G - x\ \leq \epsilon\}$ where we are using the metric of \mathbb{R}^5 , not Euclidean AdS .
$\partial^{(i)} N(G, B^5)$	the interior boundary of the neighborhood of the graph G . Formally $\partial^{(i)} N(G, B^5) = \{x \in B^5 : \ G - x\ = \epsilon\}$.
$\Sigma_4(G)$	the 4-dimensional analog of a genus G surface in two dimensions. It can be obtained by taking two copies of S^4 with $G+1$ non-intersecting balls removed, and gluing the two along the S^3 boundaries.
$\vee_n S^k$	the wedge sum of n k -spheres. It is the disjoint union of n spheres S^k with a point on each sphere identified to a single point.

Table 2: topology notation

References

- [1] J. M. Maldacena, “The large N limit of superconformal field theories and supergravity,” Adv. Theor. Math. Phys. **2** (1998) 231 [Int. J. Theor. Phys. **38** (1999) 1113] [arXiv:hep-th/9711200].
- [2] S. S. Gubser, I. R. Klebanov and A. M. Polyakov, “Gauge theory correlators from non-critical string theory,” Phys. Lett. B **428** (1998) 105 [arXiv:hep-th/9802109].
- [3] E. Witten, “Anti-de Sitter space and holography,” Adv. Theor. Math. Phys. **2** (1998) 253 [arXiv:hep-th/9802150].
- [4] J. McGreevy, L. Susskind and N. Toumbas, “Invasion of the giant gravitons from anti-de Sitter space,” JHEP **0006** (2000) 008 [arXiv:hep-th/0003075].
- [5] M. T. Grisaru, R. C. Myers and O. Tafjord, “SUSY and Goliath,” JHEP **0008**, 040 (2000) [arXiv:hep-th/0008015].
- [6] A. Hashimoto, S. Hirano and N. Itzhaki, “Large branes in AdS and their field theory dual,” JHEP **0008**, 051 (2000) [arXiv:hep-th/0008016].
- [7] V. Balasubramanian, M. Berkooz, A. Naqvi and M. J. Strassler, “Giant gravitons in conformal field theory,” JHEP **0204** (2002) 034 [arXiv:hep-th/0107119].
- [8] S. Corley, A. Jevicki and S. Ramgoolam, “Exact correlators of giant gravitons from dual $N = 4$ SYM theory,” Adv. Theor. Math. Phys. **5** (2002) 809 [arXiv:hep-th/0111222].

- [9] A. Dhar, G. Mandal and M. Smedback, “From gravitons to giants,” JHEP **0603** (2006) 031 [arXiv:hep-th/0512312].
- [10] H. Lin, O. Lunin and J. M. Maldacena, “Bubbling AdS space and 1/2 BPS geometries,” JHEP **0410** (2004) 025 [arXiv:hep-th/0409174].
- [11] D. Z. Freedman, S. D. Mathur, A. Matusis and L. Rastelli, “Correlation functions in the CFT(d)/AdS($d + 1$) correspondence,” Nucl. Phys. B **546** (1999) 96 [arXiv:hep-th/9804058].
- [12] S. M. Lee, S. Minwalla, M. Rangamani and N. Seiberg, “Three-point functions of chiral operators in $D = 4$, $N = 4$ SYM at large N ,” Adv. Theor. Math. Phys. **2** (1998) 697 [arXiv:hep-th/9806074].
- [13] D. Berenstein, J. M. Maldacena and H. Nastase, “Strings in flat space and pp waves from $N=4$ Super Yang Mills,” AIP Conf. Proc. **646**, 3 (2003).
- [14] N. R. Constable, D. Z. Freedman, M. Headrick, S. Minwalla, L. Motl, A. Postnikov and W. Skiba, “PP-wave string interactions from perturbative Yang-Mills theory,” JHEP **0207**, 017 (2002) [arXiv:hep-th/0205089].
- [15] C. Kristjansen, J. Plefka, G. W. Semenoff and M. Staudacher, “A new double-scaling limit of $N = 4$ super Yang-Mills theory and PP-wave strings,” Nucl. Phys. B **643**, 3 (2002) [arXiv:hep-th/0205033].
- [16] M. Spradlin and A. Volovich, “Superstring interactions in a pp-wave background,” Phys. Rev. D **66**, 086004 (2002) [arXiv:hep-th/0204146].
- [17] S. Corley and S. Ramgoolam, “Finite factorization equations and sum rules for BPS correlators in $N = 4$ SYM theory,” Nucl. Phys. B **641** (2002) 131 [arXiv:hep-th/0205221].
- [18] T. Banks, M. R. Douglas, G. T. Horowitz and E. J. Martinec, “AdS dynamics from conformal field theory,” arXiv:hep-th/9808016.
- [19] D. Berenstein, D. H. Correa and S. E. Vazquez, “Quantizing open spin chains with variable length: An example from giant gravitons,” Phys. Rev. Lett. **95**, 191601 (2005) [arXiv:hep-th/0502172].
- [20] D. Berenstein, D. H. Correa and S. E. Vazquez, “A study of open strings ending on giant gravitons, spin chains and integrability,” JHEP **0609**, 065 (2006) [arXiv:hep-th/0604123].
- [21] D. Berenstein, “A toy model for the AdS/CFT correspondence,” JHEP **0407**, 018 (2004) [arXiv:hep-th/0403110].
- [22] R. de Mello Koch and R. Gwyn, “Giant graviton correlators from dual $SU(N)$ super Yang-Mills theory,” JHEP **0411** (2004) 081 [arXiv:hep-th/0410236].
- [23] H. Takayanagi and T. Takayanagi, “Notes on giant gravitons on pp-waves,” JHEP **0212** (2002) 018 [arXiv:hep-th/0209160].

- [24] K. Okuyama, “1/2 BPS correlator and free fermion,” JHEP **0601** (2006) 021 [arXiv:hep-th/0511064].
- [25] Y. Takayama and A. Tsuchiya, “Complex matrix model and fermion phase space for bubbling AdS geometries,” JHEP **0510** (2005) 004 [arXiv:hep-th/0507070].
- [26] K. A. Intriligator, Nucl. Phys. B **551** (1999) 575 [arXiv:hep-th/9811047].
- [27] B. U. Eden, P. S. Howe, A. Pickering, E. Sokatchev and P. C. West, “Four-point functions in $N = 2$ superconformal field theories,” Nucl. Phys. B **581** (2000) 523 [arXiv:hep-th/0001138].
- [28] B. U. Eden, P. S. Howe, E. Sokatchev and P. C. West, “Extremal and next-to-extremal n-point correlators in four-dimensional SCFT,” Phys. Lett. B **494** (2000) 141 [arXiv:hep-th/0004102].
- [29] V. Balasubramanian, V. Jejjala and J. Simon, “The library of Babel,” Int. J. Mod. Phys. D **14**, 2181 (2005) [arXiv:hep-th/0505123].
- [30] V. Balasubramanian, J. de Boer, V. Jejjala and J. Simon, “The library of Babel: On the origin of gravitational thermodynamics,” JHEP **0512**, 006 (2005) [arXiv:hep-th/0508023].
- [31] K. Osterwalder and R. Schrader, Commun. Math. Phys. **31** (1973) 83.
- [32] J. Polchinski, L. Susskind and N. Toumbas, “Negative energy, superluminosity and holography,” Phys. Rev. D **60** (1999) 084006 [arXiv:hep-th/9903228].
- [33] L. Susskind, “Holography in the flat space limit,” arXiv:hep-th/9901079.
- [34] J. Polchinski, “S-matrices from AdS spacetime,” arXiv:hep-th/9901076.
- [35] S. B. Giddings, “The boundary S-matrix and the AdS to CFT dictionary,” Phys. Rev. Lett. **83**, 2707 (1999) [arXiv:hep-th/9903048].
- [36] P. H. Ginsparg, “Applied Conformal Field Theory,” arXiv:hep-th/9108028.
- [37] J. Polchinski, “String theory. Vol. 1: An introduction to the bosonic string, ” CUP (1998).
- [38] C. Vafa, “Conformal Theories and Punctured Surfaces,” Phys. Lett. B **199** (1987) 195.
- [39] H. Sonoda, “Sewing Conformal Field Theories,” Nucl. Phys. B **311** (1988) 401.
- [40] H. Sonoda, “Sewing Conformal Field Theories. 2,” Nucl. Phys. B **311** (1988) 417.
- [41] H. Sonoda, “Functional Determinants on Punctured Riemann Surfaces and their Applications to String Theory,” Nucl. Phys. B **294**, 157 (1987).
- [42] P. H. Ginsparg and G. W. Moore, “Lectures on 2-D gravity and 2-D string theory,” arXiv:hep-th/9304011.

- [43] E. Witten, “On the Structure of the Topological Phase of Two-Dimensional Gravity,” Nucl. Phys. B **340** (1990) 281.
- [44] R. Dijkgraaf, “Fields, strings and duality,” arXiv:hep-th/9703136.
- [45] M. Brigante, G. Festuccia and H. Liu, “Inheritance principle and non-renormalization theorems at finite temperature,” Phys. Lett. B **638** (2006) 538 [arXiv:hep-th/0509117].
- [46] N. D. Birrell and P. C. W. Davies, “Quantum Fields In Curved Space,” CUP (1982).
- [47] O. Aharony, J. Marsano, S. Minwalla, K. Papadodimas and M. Van Raamsdonk, “The Hagedorn / deconfinement phase transition in weakly coupled large N gauge theories,” Adv. Theor. Math. Phys. **8**, 603 (2004) [arXiv:hep-th/0310285].
- [48] J. Kinney, J. M. Maldacena, S. Minwalla and S. Raju, “An index for 4 dimensional super conformal theories,” arXiv:hep-th/0510251.
- [49] G. Gibbons, “Euclidean quantum gravity: the view from 2002” in “The Future of Theoretical Physics and Cosmology,” edited by G.Gibbons, E.Shellard, S.Rankin CUP (2003)
- [50] E. Witten, “Anti-de Sitter space, thermal phase transition, and confinement in gauge theories,” Adv. Theor. Math. Phys. **2**, 505 (1998) [arXiv:hep-th/9803131].
- [51] R. Gompf, A. Stipsicz, “4-manifolds and Kirby calculus,” Graduate Studies in Mathematics, Volume 20. AMS, Providence, Rhode Island.
- [52] H. F. Dowker and R. S. Garcia, “A handlebody calculus for topology change,” Class. Quant. Grav. **15** (1998) 1859 [arXiv:gr-qc/9711042].
- [53] S. A. Hartnoll, “Compactification, topology change and surgery theory,” Class. Quant. Grav. **20** (2003) 3093 [arXiv:hep-th/0302072].
- [54] G. T. Horowitz, “Topology change in classical and quantum gravity,” Class. Quant. Grav. **8**, 587 (1991).
- [55] J. M. Maldacena, “Non-Gaussian features of primordial fluctuations in single field inflationary models,” JHEP **0305** (2003) 013 [arXiv:astro-ph/0210603].
- [56] J. B. Hartle and S. W. Hawking, “Wave Function Of The Universe,” Phys. Rev. D **28** (1983) 2960.
- [57] B. Freivogel and L. Susskind, “A framework for the landscape,” Phys. Rev. D **70** (2004) 126007 [arXiv:hep-th/0408133].
- [58] R. Bousso, “Holographic probabilities in eternal inflation,” arXiv:hep-th/0605263.
- [59] D. N. Page, “Predictions and tests of multiverse theories,” arXiv:hep-th/0610101.
- [60] J. Garriga, D. Schwartz-Perlov, A. Vilenkin and S. Winitzki, “Probabilities in the inflationary multiverse,” JCAP **0601** (2006) 017 [arXiv:hep-th/0509184].

- [61] B. Freivogel, Y. Sekino, L. Susskind and C. P. Yeh, “A holographic framework for eternal inflation,” *Phys. Rev. D* **74** (2006) 086003 [arXiv:hep-th/0606204].
- [62] P. Horava and P. G. Shepard, “Topology changing transitions in bubbling geometries,” *JHEP* **0502** (2005) 063 [arXiv:hep-th/0502127].
- [63] D. A. Lowe, J. Polchinski, L. Susskind, L. Thorlacius and J. Uglum, “Black hole complementarity versus locality,” *Phys. Rev. D* **52** (1995) 6997 [arXiv:hep-th/9506138].
- [64] S. B. Giddings, D. Marolf and J. B. Hartle, “Observables in effective gravity,” *Phys. Rev. D* **74** (2006) 064018 [arXiv:hep-th/0512200].
- [65] A. Baratin and L. Freidel, “Hidden quantum gravity in 3d Feynman diagrams,” arXiv:gr-qc/0604016.
- [66] J. M. Maldacena, “Wilson loops in large N field theories,” *Phys. Rev. Lett.* **80** (1998) 4859 [arXiv:hep-th/9803002].
- [67] N. Drukker, D. J. Gross and H. Ooguri, “Wilson loops and minimal surfaces,” *Phys. Rev. D* **60** (1999) 125006 [arXiv:hep-th/9904191].
- [68] K. Okuyama and G. W. Semenoff, “Wilson loops in $N = 4$ SYM and fermion droplets,” *JHEP* **0606** (2006) 057 [arXiv:hep-th/0604209].
- [69] J.Q. Chen, *Group Representation theory for Physicists*, World Scientific, 1987, Chapter 7.
- [70] A. Partensky, *J. Math. Phys.* **13** , 1972 , 1503.
- [71] S. Ramgoolam, Thesis, Yale 1995.
- [72] R. Rabadan and F. Zamora, “Dilaton tadpoles and D-brane interactions in compact spaces,” *JHEP* **0212** (2002) 052 [arXiv:hep-th/0207178].
- [73] Allen Hatcher, “Algebraic Topology”, CUP (2002).
<http://www.math.cornell.edu/~hatcher/>